Domain of Attraction Estimation and Optimization-Based Control : Application to Tumor Growth Models

Kaouther Moussa

Université Grenoble Alpes

THÈSE

Pour obtenir le grade de

DOCTEUR DE L'UNIVERSITE GRENOBLE ALPES

Spécialité : **Automatique-Productique**

Arrêté ministériel : 25 mai 2016

Présentée par

Kaouther MOUSSA

Thèse dirigée par **Mazen ALAMIR, Directeur de recherche, CNRS**, et
codirigée par **Mirko FIACCHINI, Chargé de recherche, CNRS**

préparée au sein du **Laboratoire Gipsa-Lab**
dans **l'École Doctorale EEATS**

Estimation de domaines d'attraction et contrôle basé sur l'optimisation : application à des modèles de croissance tumorale

Thèse soutenue publiquement le **16 décembre 2020**,
devant le jury composé de :

M. Christophe PRIEUR
Directeur de recherche CNRS à Gipsa-Lab, Examinateur (Président du jury)
Mme. Cristina STOICA MANIU
Professeure à CentraleSupélec, Examinatrice
M. Teodoro ÁLAMO CANTARERO
Professeur à Université de Séville, Rapporteur
M. Franco BLANCHINI
Professeur à Université de Udine, Rapporteur
M. Mirko FIACCHINI
Chargé de recherche CNRS à Gipsa-Lab, Co-Encadrant de thèse (invité)
M. Mazen ALAMIR
Directeur de recherche CNRS à Gipsa-Lab, Directeur de thèse

To my lovely husband,

Abstract

The main objective of this thesis is to propose frameworks and algorithms that are based on advanced control approaches, in order to guide cancer treatments scheduling. It also aims at pointing out the importance of taking into account the problem of stochastic uncertainties handling in the drug scheduling design, since cancer dynamical systems are considered to be highly uncertain phenomena.

Cancer dynamical interactions are still an open research topic which is not fully understood yet. The complexity of such dynamics comes from their partially unknown behavior and their uncertain nature. Additionally, they are often described by nonlinear complex dynamics and require taking into consideration many constraints related to physiology as well as biology.

In terms of control design, this topic gathers many complexity ingredients such as nonlinear dynamics, constraints handling and optimality issues. Therefore, in this thesis, we propose to use a recent optimal control approach that is based on moment optimization. This framework has the advantage of considering all the state and input variables as probability densities, allowing therefore to explicitly consider parametric as well as initial state uncertainties in the optimal control problem. We use this framework in Part II, in order to design robust optimal control schedules that represent cancer drugs injection profiles.

The second problem that we address in Part III consists in the estimation of regions of attraction for cancer interactions models. This problem is interesting in the context of cancer treatment design, since it provides the set of all possible initial conditions (tumor and patient health indicators), that can be driven to a desired targeted safe region, where the patient is considered to be healed. Furthermore, we focus on the assessment of methodologies that take into consideration the parametric uncertainties that can affect the dynamical model.

Keywords: Optimal control, Uncertain systems, Stochastic parametric uncertainties, Moment optimization, Domain of attraction estimation, Probabilistic certification, Cancer dynamics, Immunotherapy, Chemotherapy.

Résumé

L'objectif de cette thèse consiste à proposer des algorithmes ainsi que des approches, basés sur des méthodes avancées de l'automatique, afin de guider la synthèse des traitements de cancer. Cette thèse a également pour but de relever l'importance de la considération des différentes incertitudes stochastiques qui peuvent affecter ce genre de systèmes.

Le phénomène de croissance tumorale et ses différentes dynamiques sont encore à nos jours un sujet de recherche ouvert. La complexité de ce type de systèmes vient de leur nature incertaine ainsi que de la méconnaissance de leurs comportements. Par ailleurs, ces systèmes sont souvent décrits par des dynamiques non-linéaires complexes et requièrent la prise en compte de différentes contraintes liées à la physiologie ainsi que la biologie de l'être humain.

Ce sujet regroupe plusieurs ingrédients de complexité en termes de synthèse de contrôle, tels que les dynamiques non-linéaires, la prise en considération des contraintes ainsi que des problèmes d'optimalité. Pour cela, nous proposons dans cette thèse d'utiliser une méthode récente de contrôle optimal basée sur l'optimisation par les moments. Cette approche a pour avantage de considérer les différentes variables d'état et de contrôle comme étant des densités de probabilité, rendant la prise en considération d'incertitudes décrites par des distributions de probabilité directe dans le problème de contrôle optimal. Nous utilisons cette méthodologie dans la Partie II afin de synthétiser des contrôles optimaux et robustes, représentant des profils d'injection de médicaments.

Le second problème qu'on considère dans la Partie III consiste en l'estimation de régions d'attraction pour des modèles dynamiques de cancer. Ce problème est intéressant dans le contexte de traitements de cancer, car ces régions caractérisent l'ensemble des conditions initiales (volume tumoral et indicateurs de santé), qui peuvent être amenées à une région saine, où le patient est considéré comme guéri. Par ailleurs, on analyse des méthodologies permettant de prendre en considération des modèles dynamiques présentant des incertitudes paramétriques.

Mots-clés: Contrôle optimal, Systèmes incertains, Incertitudes paramétriques stochastiques, Optimisation par les moments, Estimation de domaines d'attraction, Certification probabiliste, Dynamiques de cancer, Immunothérapie, Chimiothérapie.

Acknowledgments

Working as a PhD student has been a long journey with an immersion into the life of a young researcher. During this period of time, I have met many nice people who definitely made this experience special.

First of all, I would like to thank my supervisors Mirko and Mazen, for their kindness, availability and support all along the thesis duration. I am grateful for the opportunity that I had to work with them and to learn from their insights.

I would like also to thank the jury members of my thesis, for reading and assessing the manuscript as well as for their highly interesting and valuable comments.

Finally, I thank the source of happiness in my life, family & friends, for their continuous support during the hardest times, but also for sharing the best unforgettable moments, I love you all!

Kaouther Moussa
Grenoble
December 16, 2020

Contents

List of Symbols

$\mathbb{R}$	Set of real numbers
$\mathbb{N}$	Set of natural numbers
$\mathbb{R}_+$	Set of non-negative real numbers
$\times$	Vector product
M^T	Transpose of a matrix M
i	Unit imaginary number
$\succeq 0$	Positive semidefinite matrix
$\succ 0$	Positive definite matrix
$\nabla_x v = \left[\frac{\partial v}{\partial x_1}, ..., \frac{\partial v}{\partial x_n}\right]$	The gradient of v with respect to x
$\bigcup_{k\in\mathbb{N}} X_k$	Union of the sets X_k
$\langle \cdot, \cdot \rangle$	Inner product
deg=(F)	the degree of a polynomial F
$\bigcap_{k\in\mathbb{N}} X_k$	Intersection of the sets X_k
$\mathcal{U}(X)$	Uniform probability distribution supported on X
$\mathcal{N}(\mu, V)$	Normal probability distribution with mean μ and variance V
$\mathbf{E}_p[J(p)]$	The expectation of J with respect to the random variable p
$p \sim \mathcal{P}$	p is a random variable following the probability distribution $\mathcal{P}$
$\Pr_{\mathcal{P}}\{e(p)\}$	Probability of occurrence of an event e that depends on a random variable p following the distribution $\mathcal{P}$

Acronyms

OCP	Optimal Control Problem
RoA	Region of Attraction
LP	Linear Programming
ODE	Ordinary Differential Equation
PDE	Partial Differential Equation
MPC	Model Predictive Control
SDP	Semidefinite Programming
LMI	Linear Matrix Inequality
SOS	Sum-Of-Squares
HJB	Hamilton-Jacobi-Bellman
ROCP	Robust Optimal Control Problem
CDI	Convex Difference Inclusion
MC	Monte-Carlo

VEGF	Vascular Endothelial Growth Factors
DNA	Deoxyribonucleic Acid
CAR T cells	Chimeric Antigen Receptor T cells
CL	Circulating Lymphocytes
CTLs	Cytotoxic T Lymphocytes
CD8+ T cells	Cytotoxic T Lymphocytes
NK cells	Natural Killer cells
IL-2	Interleukin 2
TNF	Tumor Necrosis Factors
CSF	Colony-Stimulating Factors
TIL	Tumor Infiltrating Lymphocytes
PK	Pharmacokinetics
ECs	Effector immune Cells

Chapter 1

General Introduction

Control design for biological systems has a long history dating back to many decades. It is a wide research field that deals with the different mechanisms related to living organisms. This research field raised a lot of interest due to its wide range of applications and their importance from several aspects. Control theory provides a large collection of mathematical tools that one can use to change the system behavior and achieve specific objectives of stability, optimality and robustness. Furthermore, simulation has served recently as a powerful tool in order to study the biological systems behavior in general.

The particular problem of tumor growth phenomenon is not fully understood yet in the medical and biological fields. Many research and investigations are still going on to understand the different mechanisms related to this phenomenon. Few decades ago, researchers started modeling the phenomenon of tumor growth and its different interactions with the human body organs as well as the existing treatments. These models help to analyze the different dynamics that are involved in the process of tumor growth. Furthermore, they can be used in order to provide more systematic approaches for cancer drug scheduling. It also helps to validate some well known drugs injection protocols, since tumor progression is difficult to approach by experimental methods alone.

The availability of many models describing cancer dynamics motivated researchers to apply different control strategies in order to propose frameworks for designing cancer treatment profiles. This topic gathers many complexity ingredients in terms of control design. Cancer drug scheduling requires taking into account many constraints such as health and toxicity constraints, as well as optimality considerations.

There exists a rich literature regarding control for cancer dynamics, with a focus on optimal control methods. Usually, optimal control problems are defined, where the cost describes the optimal desired behavior. These problems can be solved using different methods. In Chapter 2, we present a literature review on different control design methods that have been applied to cancer dynamics.

1.1 Thesis context

Modeling cancer dynamics can be achieved using different types of equations. In this thesis, we are interested particularly in investigating models described by a set of ODEs. These systems involve many parameters that describe the interaction between the different compartments of the human body. In the literature regarding the control of cancer dynamics, the parameters involved in the models are usually considered to be deterministic, and estimated to some degree of precision. However, in the medical field, cancer dynamics are known to be highly uncertain by nature, since they involve many complex and only partially known mechanisms. Furthermore, the effects of the treatment and the evolution of the cancer depend highly on the patient.

The aim of this thesis is to analyze and investigate dynamical systems describing cancer interactions dynamics, which are subject to stochastic parametric uncertainties. It is commonly known that achieving optimal recovery performances under uncertainties is a complex task. Therefore, in this thesis we will investigate some approaches that allow to handle uncertainties in the context of optimal control design.

This thesis addresses two main problems in terms of control for cancer dynamics:

– The first problem is addressed in Part II and consists of drug injection schedules design for cancer treatment, in the presence of model parametric uncertainties. The problem of optimal control under parametric uncertainties, that are described by probability distributions, is not straightforward, since we have in this case a flow of trajectories generated by the probability distributions of the different parameters. Therefore, we need to define a cost from a statistical point of view. Furthermore, the satisfaction of the constraints is not easy to guarantee when having uncertain parameters described by probability distributions. This problem is stated and explained in details in Chapter 2.

  We propose to use a recent optimal control computation approach that is based on moment optimization. This framework has the advantage of defining all the state and input variables as probability densities, allowing therefore to explicitly consider parametric uncertainties in the optimal control problem. In Chapters 4 and 5 we use this framework in order to design robust optimal control schedules for a specific cancer dynamical model.

– The second problem is addressed in Part III and consists in the estimation of domains of attraction for cancer interactions models. The problem of estimating regions of attraction in the context of cancer treatment is interesting, since it provides the set of all possible initial conditions (tumor and patient health indicators), that can be driven to a desired targeted benign region. We propose a methodology to estimate the robust region of attraction of cancer immune interaction model. Furthermore, we suggest a framework for the estimation of probabilistically certified regions of attraction for a cancer model.

1.2 Manuscript outline

This thesis consists of six main chapters divided into three different parts. Part I is intended to review the literature of cancer dynamics modeling and control, as well as the different theoretical concepts that are necessary to understand the subsequent chapters.

- In Chapter 2, the different mechanisms related to the tumor growth phenomenon are explained. We also present the different therapies that are used for cancer treatment with a focus on immune dynamics and immunotherapy. Furthermore, we present a brief review on the different models that describe cancer dynamics and some control strategies that have been applied in order to schedule cancer treatments. Moreover, in this chapter, we highlight the importance of taking into account parametric uncertainties in drug cancer scheduling. Finally, we state the problems of optimal control as well as domain of attraction estimation under parametric uncertainties.

- Chapter 3 recalls the main theoretical aspects of optimal control via moment optimization. We explain in this chapter how optimal control problems can be reformulated in terms of measures and thereby moments. Furthermore, we highlight the main advantage of this approach which consists in describing the different variables as probability distributions, allowing to explicitly consider parametric uncertainties in optimal control problems.

Part II revolves around optimal control for cancer treatment scheduling in presence of uncertainties. It contains the two following chapters:

- In Chapter 4, a dynamical model that describes the interaction dynamics between cancer and the immune system is investigated. This model considers a combined treatment of chemotherapy and immunotherapy and does not include the effects of chemotherapy on immune cells. In this chapter, we explain how to use the moment optimization framework in order to reformulate optimal control problems involving uncertainties. Furthermore, some numerical simulations are presented in order to highlight the importance of taking into account parametric uncertainties in drug schedules design.

- In Chapter 5, the model used in Chapter 4 is further investigated, a new term is added to this model, this term counts for the detrimental effects of chemotherapy on immune cells. Furthermore, we add a new constraint on the minimal allowed density of immune cells in the optimal control problem, in order to solve a realistic problem. The parameter standing for the detrimental effects of chemotherapy is considered to be uncertain and described by a probability distribution. Finally, we present the optimal schedules for cancer drugs, and we highlight the importance of adding this new term in the model.

Part III deals with the problem of estimating the domain of attraction, it contains the two following chapters.

- In Chapter 6, we provide a parametric analysis of a cancer growth model. Furthermore, we propose a methodology to estimate the region of attraction of this model using bang-bang control strategies. Finally, we use this approach to provide a heuristic-estimate of the robust region of attraction of the same model.

- In Chapter 7, we propose to enhance the model used in Chapter 6 by considering the pharmacokinetics of chemotherapy. Furthermore, we suggest a framework for the estimation of probabilistically certified regions of attraction of a cancer dynamics model. This framework is based on the randomized algorithms and allows to derive the certified control strategies corresponding to the estimated domains of attraction.

1.3 List of publications

1. Maria Dassow, Seddik Djouadi, Kaouther Moussa, "Optimal Control of a Tumor-Immune System with a Modified Stepanova Cancer Model", 2021, (submitted to The 11th IFAC Symposium on Biological and Medical Systems).

2. Kaouther Moussa, Mirko Fiacchini, Mazen Alamir, "Robust Domain of Attraction Estimation for a Tumor Growth Model", 2020, (submitted to the Journal of Applied Mathematics and Computation).

3. Kaouther Moussa, Mirko Fiacchini, Mazen Alamir, "Probabilistically Certified Region of Attraction of a Tumor Growth Model with Combined Chemo- and Immunotherapy", 2020, (submitted to the International Journal of Robust and Nonlinear Control).

4. Kaouther Moussa, Mirko Fiacchini, Mazen Alamir, "Robust Optimal Scheduling of Combined Chemo- and Immunotherapy: Considerations on Chemotherapy Detrimental Effects", The 2020 American Control Conference, July 2020, Denver, USA.

5. Kaouther Moussa, Mirko Fiacchini, Mazen Alamir,"Robust Optimal Control-based Design of Combined Chemo- and Immunotherapy Delivery Profiles", The 8th IFAC Conference on Foundations of Systems Biology in Engineering, October 2019, Valencia, Spain.

Part I

State of the art and theoretical background

Chapter 2

Modeling cancer therapies dynamics

Cancer is one of the first leading causes to death in the world. According to the worldwide medical statistics, in 2018, 9.6 million people are estimated to have died from the various forms of cancer. Therefore, a great deal of research had been carried out since many decades, in order to bring out useful solutions in terms of cancer treatment. This wide area of research involves many scientific fields such as oncology, experimental and theoretical biology, but also computational methods and tools allowing to schedule cancer treatment.

In this chapter, we will present some biological aspects regarding the tumor growth phenomenon and explain how the existing therapies are intended to induce tumor growth inhibition. Furthermore, we will specifically focus on how the different phenomena related to cancer dynamics are modeled in the literature. Finally, we will provide some insights on how control helps to address cancer treatment scheduling problems.

2.1 Tumor growth and cancer therapies

2.1.1 Cancer growth phenomenon

The tumor microenvironment is a dynamical structure with highly varying composition and distribution. Therefore, the tumor growth phenomenon involves very complex mechanisms resulting from highly uncertain nonlinear dynamics. In this section, we present the main mechanisms which are important to the understanding of the modeling of cancer dynamics.

The complex phenomenon of cancer growth consists in an abnormal proliferation of cells in the human body. The cancer cells grow and divide rapidly to create new cells and form thereby a tumor which can contain millions of cancer cells. These cells are huge consumers of oxygen and nutrients, they divide very fast at the early stages, then, they slow down due to a lack of nutrients. Thereafter, the cancer cells secrete vascular endothelial growth factors (VEGF) which allow to develop new blood vessels. This process helps to induce a tumor regrowth, resulting from the tumor cells feeding via the new blood vessels. This mechanism is called tumor angiogenesis and is illustrated in Figure 2.1.

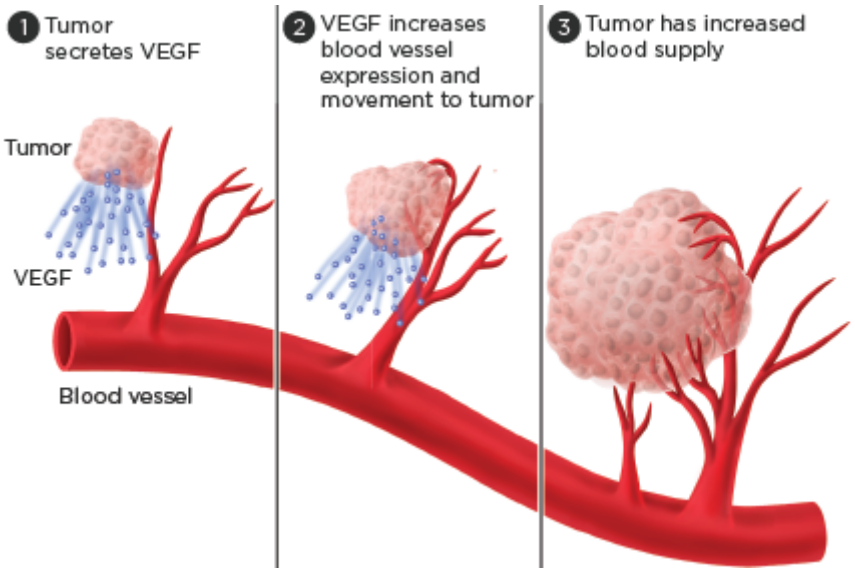

Figure 2.1: Tumor angiogenesis process [1].

As shown in Figure 2.1, when the tumor gets bigger, its centre becomes further away from the area where blood vessels are concentrated. Therefore, the cancer cells situated in the center of the tumor start lacking oxygen and nutrients as the tumor grows. Similarly to the healthy cells in the human body, cancer cells are not able to live without nutrients and oxygen. Thus, they send out angiogenic factors (VEGF signals) which induce angiogenesis, these signals encourage new blood vessels to grow into the tumor. Furthermore, the fact that a tumor cannot keep up growing without a blood supply is a very relevant observation, we will see in the sequel that one of the therapies that researchers developed consists in inhibiting the vascularisation formation using anti-angiogenic substances.

Once a tumor starts stimulating the growth of hundreds of new small blood vessels called capillaries, in order to bring in nutrients and oxygen, it grows very fast and gets bigger, taking up therefore more and more space in the human body. At this stage, the tumor burden resulting from this uncontrolled growing behavior can cause a high pressure on the surrounding body structures. Furthermore, It can invade the nearby body organs, this process is called local invasion.

The tumor cells compete with healthy cells as well as the physical microenviornment for space and resources. In fact, the difference between normal and cancer cells is that the latter can move more easily, making therefore the spread of cancer through the different nearby tissues easier. In spite of the considerable progress in cancer biology, the way that cancer evolves through the surrounding tissues is not fully understood yet.

Cancer cells appear first in a primary site, these cells can break away and spread to other surrounding parts of the body, through the bloodstream or lymphatic system, forming thereby new tumors known as secondary cancers. This process is called metastasis which is the fundamental definition of malignancy.

Tumors can be classified into three types, benign, premalignant and malignant tumors. Benign tumors are not cancerous, in general, they do not have the ability to spread or

grow, whereas the premalignant ones have the potential to become malignant. Although the benign tumors are harmful, their presence near to vessels or nerves can induce some pains and health problems. Furthermore, due to some mutations, benign tumors can become in some cases cancerous, therefore it is very important to be able to monitor such uncontrolled growths. Finally, malignant tumors are cancerous and characterized by the metastasis process, they develop and spread very quickly to other parts of the human body. Such tumors are highly threatening to the life of the patient.

Nowadays, cancer has still a high death rate despite the considerable advances in understanding its genomic changes. In the next section we will present some of the advances of cancer therapies techniques that researchers have been investigating lately.

2.1.2 Cancer therapies

The last decades witnessed a noticeable progress in the cancer treatment research field, many therapies and techniques for cancer treatment have been developed. In this section, we will present some of these therapies that are relevant in terms of cancer dynamics modeling and control.

Conventional cancer treatment covers many procedures, all having the same basic objectives which consist of directly killing the tumor cells and preventing their eventual proliferation [42]. However, one of the most important thing to highlight in cancer therapies, is that staging (determination of the stage of the cancer) is crucial to the choice of the treatment that patients need. Indeed, the choice of an appropriate therapy depends on many criteria, for example, the size of the tumor, its location, its stage and the general health of the patient.

One of the commonly used therapies that doctors may recommend as a local treatment for cancer is surgery. This therapy can be advantageous when the cancer is fully contained in one area. Otherwise, in the case of metastasis, a treatment that can reach all body parts might be more convenient. Radiotherapy is also a local treatment allowing to shrink the tumor burden and control some symptoms. This therapy consists in using radiation (usually X-rays) in order to target cancer cells, it can be used either internally or externally. The ionising radiation used in radiotherapy allows to destroy cancer cells in the targeted area by inducing a damage in the DNA of these cells. However, this therapy has also the ability to damage the nearby healthy cells, causing thereby some side effects. Therefore, it can be combined in some cases with other treatments such as surgery or immunotherapy in order to increase the chances to meet treatment objectives.

In addition to local therapies, there exist treatments that are able to circulate throughout the whole human body, which make them more appropriate for treating widespread cancers. These therapies are called systemic treatments and include chemotherapy, hormone therapy, immunotherapy and targeted cancer therapies, those different treatments will be defined briefly in the sequel.

Chemotherapy is a type of anti-cancer drug treatments that allow to damage cells while they divide. There exist several chemotherapeutic agents characterized by different

mechanisms, some of them are able to damage cells at the point of splitting and others allow to target cells while they make copies of their genes, before they start splitting. This explains why chemotherapy drugs cause side effects by affecting the healthy tissues where cells are continually growing and dividing such as the hair, the skin and the bone marrow. Doctors might recommend using a combination of several chemotherapeutic drugs allowing to target cells at different division stages in order to increase the killing effect on cancer cells. In addition to the several side effects that chemotherapy has on the normal healthy cells, this treatment is subject to drug resistance problems, due to the fast evolution of cancer cells towards new resistant phenotypes [74].

Furthermore, it has been proven that some cancers are sensitive to hormones, in fact, cancers might use hormones in order to grow and develop. Therefore, hormone therapy consists of drugs allowing to reduce the quantity of hormones in the body, in order to stop or slow down the cancer growth, it is used to treat some specific types of cancer such as breast and prostate cancers. However, this therapy might induce some side effects.

The immune system is a powerful barrier allowing the human body to protect itself against illnesses and infections, it also helps to protect the body from any potential cancer development. The immune system includes the white blood cells, the spleen and the lymph glands (specific human body organs). Therefore, it is a collection of many organs, cells and substances collaborating to recognize and attack cancer cells. Immunotherapy helps to enhance the immune response of the body against cancer cells, it gathers many treatments such as monoclonal antibodies, cytokines, vaccines and CAR T-cell therapy which all have different stimulation mechanisms. Immunotherapy is considered as a standard treatment for some types of cancer such as widespread melanoma, while it is still in trials for other types of cancer. The next section is dedicated to explain further details about the dynamics of immune system and immunotherapy, since the context of this thesis revolves around combined chemotherapy and immunotherapy for cancer treatment.

Cancer cells are different from the healthy ones because of the changes that they have in their DNA, which make them behave differently in the human body. Targeted cancer drugs is a wide collection of treatments whose main objective is to target the differences that a cancer cell has. There exist several types of targeted treatments having different effects and dynamics, for example, some types of immunotherapy such as monoclonal antibodies are considered as targeted treatments, they allow to trigger the immune system to damage cancer cells. Another example is targeted drugs allowing to prevent cancers from developing new blood vessels. This type of drugs is called anti-angiogenic treatments.

In 1971, Folkman showed that the inhibition of the tumor vascular network helps to reduce the tumor burden, by starving it of oxygen and nutrients. According to [16], these therapies had been consolidated along the nineties by different discoveries, important research efforts are still going on into angiogenesis. Some of the interesting information that researchers discovered is that the amount of angiogenic factors is very high at the outer edges of a cancer. Although this type of therapy is known to have limited side effects

compared to conventional chemotherapies and radiotherapies, anti-angiogenic drugs are most often not able to eliminate a cancer completely, it can rather shrink it or stop its growing in some cases.

Furthermore, according to [60], there exist other therapies that are less used due to a lack of monitoring or efficiency such as gene therapy, which consists in introducing DNA molecules that are able to interfere with cancer cells in order to eliminate them. Gene therapy is still in the early stages of clinical trials and research.

The growth mechanisms of a cancer are very complex processes, involving many biological interactions. This makes the response of a cancerous tumor to treatment also complex, and depending on many factors such as the severity of the disease and the general health of the patient [26]. Therefore, understanding the various aspects related to cancer growth and how it interacts with treatments is of key importance. Indeed, a good treatment protocol is intended to effectively eliminate the tumor without damaging the healthy cells. According to [60], doctors usually combine many therapies in order to compensate the side effects of some treatments (in particular chemotherapy and radiotherapy) and to increase the chances to reduce the cancer effectively and safely.

One of the questions that the recent developments in the cancer research field led to, is how to effectively combine different cancer treatments, in particular for the case of combined chemotherapy and immunotherapy [24]. The answer to this question is definitely not straightforward, due to the complexity and the ambiguous nature of the involved interactions. Furthermore, the existence of various therapies for cancer might make this task more complicated. Therefore, it is highly interesting to consider mathematical models and computational tools that can help to explain the experimental and clinical observations in order to design effective cancer treatment strategies.

2.2 Immune dynamics and immunotherapy

The role of the immune system consists in defending the human body from intruders such as pathogens (infectious agents). According to [90], the defense systems that the body is characterized by, are able to limit the growth of cancer cells by specifically recognizing proteins that are not derived from the organism, considered therefore as foreign proteins. This section will briefly review some basic immunological principles which are important for the modeling of immune dynamics.

2.2.1 Immune system mechanisms

The involvement of the immune system in all stages of the tumor life cycle, including prevention, maintenance and response to therapy is recognized as central to understanding cancer development.

We can distinguish between two basic types of immune responses:

- Innate immune responses

- Adapted immune responses

These two types of immune responses are connected via the action of various cells such as dendritic cells, cytokines and antibodies [33]. They generally cooperate to ensure the protection of the human body.

The innate immune system focuses on the physical and chemical barriers formed by cells and molecules that recognize foreign pathogens. It provides a first line of defense which does not recognize foreign proteins specifically, it rather supplies environments which generally inhibit the spread of intruders. Although these responses are important to limit a potential initial pathogen growth, they are usually not sufficient to heal diseases.

The adaptive immune system focuses on the lymphocytes actions to clear pathogens. In contrast to the innate immune responses, the adaptive ones are considered to be very specific, allowing cells to recognize and respond to a large variety of antigens (foreign proteins). The cytotoxic T lymphocytes (CTLs), which are called more commonly *killer cells*, are the most important branch of the immune system in fighting cancers [90]. They can distinguish the cells that potentially display a foreign protein by mean of a specific receptor, which triggers the release of particular molecules that induce apoptosis (cell death) in the cells displaying foreign proteins. They can also be referred to as CD8+ T cells, since they are characterized by the expression of the CD8 molecule on the surface of the cell.

According to [33], the notion of immune memory has been for a long while directly related to the different adaptive immune responses. Nonetheless, according to recent experimental results, there might exist a type of innate immune memory associated with macrophages or natural killer (NK) cells.

It is important to underline the fact that the role of the immune system in fighting cancers is not fully understood yet [23]. Indeed, experimental data showed that cancer cells present different characteristics which prevent the immune system from recognizing the potential mutated proteins and successfully killing the corresponding cells [90].

According to [23], there is not an agreement on the underlying dynamics taking place in the immune response process. Figure 2.2 presents a non-exhaustive scheme for these dynamics from a modeling point of view, this scheme is based on the works presented in [20] and [79].

Figure 2.2 shows the main interactions between tumor, innate and adapted immune responses and circulating lymphocytes. The NK cells allowing to attack cancer cells, represent the innate immune response, they are a specific type of circulating lymphocytes that are stimulated by the presence of a tumor in the human body. In order to simplify the complex mechanisms related to the NK cells stimulation, a population of circulating lymphocytes is considered as a source of these cells.

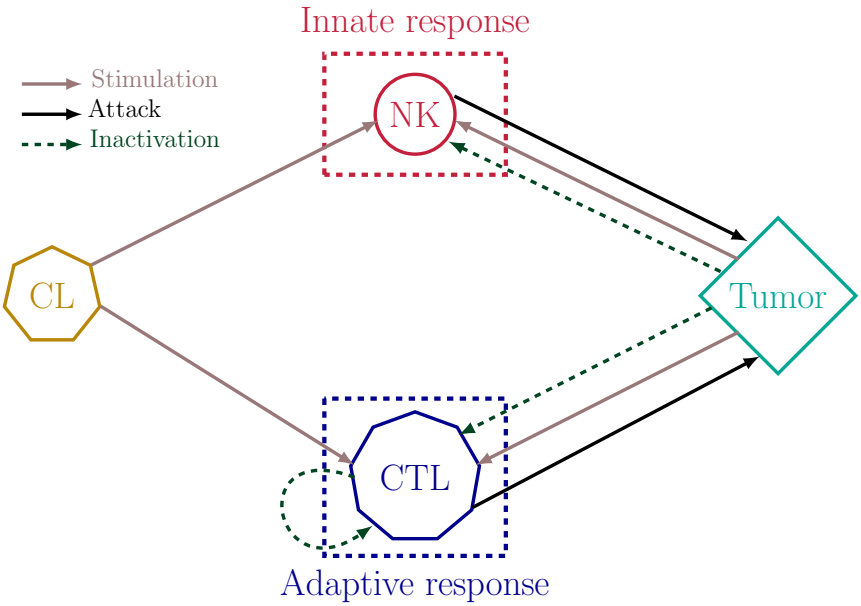

Figure 2.2: A non-exhaustive scheme of immune interactions, CL stands for circulating lymphocytes, NK for natural killer cells and CTL for cytotoxic T lymphocytes.

Furthermore, the adaptive immune response is represented by a population of T cells which are cytotoxic T lymphocytes allowing to kill tumor cells by direct contact. According to [79], the repertoire of T cells receptors present in the organism is rich of about 10^7 different types of cells, which are able to identify several antigens. Once a tumor-specific T cell is activated, it proliferates rapidly producing cells with the same receptor.

As a part of the adapted immune system, T-suppressor cells allow to regulate the cytotoxic activity of CTLs in order to prevent autoimmune diseases. This process occurs when there are very high levels of activated CTL cells. Moreover, both CTL and NK cells are inactivated after several interactions with tumor cells.

In the next section, a specific focus will be given on how immunotherapy is intended to induce a tumor growth inhibition and the different mechanisms related to this process.

2.2.2 Immunotherapy as a cancer treatment

The noticeable progress in genetics and biochemistry that has taken place lately led to significant advances in experimental and clinical immunology [33]. Therefore, due to their abilities to boost the body's immune system in targeting the cancer, immunotherapies are becoming an important treatment for different forms of cancer. According to [21], the importance of the immune system in combating cancers has been proven in the laboratory as well as with clinical experiments. Indeed, conventional treatments such as chemotherapy, deplete the patient's immune system, which makes the human body prone to dangerous infections. Therefore, it is crucial to strengthen the immune system after an immune-depleting.

Moreover, through the mathematical modeling of tumor growth, the presence of an immune component has been shown to be indispensable for inducing clinically observed phenomena such as tumor dormancy, oscillations in tumor size, and spontaneous tumor regression.

The clinical evidence for the ability of immune system in controlling certain malignancies has motivated new research aiming at the development of immunotherapies and vaccine therapies for cancers.

According to [21], immunotherapy falls into three main categories :

- Immune response modifiers: they consist of substances that affect the immune response, such as interleukins (including IL-2), interferons, tumor necrosis factors (TNF), colony-stimulating factors (CSF), B-cell growth factors, and tumor infiltrating lymphocyte (TIL) injections.

- Monoclonal antibodies: they are able to distinguish between normal and cancer cells, and are currently being developed to target specific cancer antigens.

- Vaccines: they are generally used for a therapeutic purpose, and are created from cancer cells in order to help the immune system to recognize and attack specific cancer cells.

One of the immune responses modifiers that is used as an immunotherapy is the cytokine interleukin 2 (IL-2). This cytokine is naturally produced by the body and known to stimulate CD8+T cells (a type of CTL cells) recruitment and proliferation [21]. IL-2 can be administered to the body in order to boost the immune system function. Furthermore, CD8+T cells might undergo an inactivation due to its high quantity in the body, therefore, the cytokine IL-2 helps in the resistance of the CD8+T cells population to this inactivation.

Moreover, TIL injections is another type of immune responses modifiers that is used as an immunotherapy, in which a large number of highly activated CD8+T cells are injected to the human body.

The design of an effective immunotherapy might be complicated due to various factors, including a potentially immunosuppressive tumor micro-environment, immune modulating effects of conventional treatments and therapy related toxicities. Therefore, it is important to incorporate these complexities into mathematical and computational models of cancer immunotherapy, in order to create a pragmatic tool allowing to assess the different drug protocols that are widely used.

Furthermore, in the case of combined therapies, such as chemotherapy and immunotherapy, it is necessary to have such tools in order to effectively combine many therapies, to guarantee the protection of the patient from opportunistic infections as well as the cancer

growth inhibition [24]. In [21], many illustrative situations in which neither chemotherapy nor immunotherapy alone are sufficient to control tumor growth, however, combining these two therapies allowed to eliminate the entire cancer.

2.3 Modeling tumor growth and drugs interactions

In the last decades, researchers had been interested in modeling the interaction dynamics between cancer and the human body in order to better understand and analyse the behavior of these phenomena. As mentioned in the previous sections, the dynamics of cancer growth are extremely complex, therefore, we can find many different models in the literature, depending on the therapies that are used, for example, or the different phenomena that occur in the human body. According to [22], these models try to focus on the most important elements related to the tumor growth process and its response to therapies. Therefore, it is crucial that the modeling process includes the essential behavior in order to answer specific questions about this system.

Accordingly, modeling techniques are diverse, multifaceted and highly dependent on the elements that one wants to describe. Usually, these models include different cells populations or compartments and try to characterize the main interactions between them, as well as with the different therapies. In some works, tumor behaviors are described by several variables and partial/ordinary differential equations (PDEs/ODEs). Although these models lose the microscopic individual cell dynamics and microenvironment, they allow to catch the global properties of the tumor growth mechanisms. In this section, we will give a specific focus on cancer modeling through ODEs, since the literature regarding other modeling techniques is very wide and rich.

Several works had been done on modeling the interaction of chemotherapy with the tumor growth process, for example, [64], [72], [2] and [66]. Moreover, there are some models considering specific phenomena, for instance [14], where authors took into account the influence of nutrients on the drug effect or [36], where authors considered the common phenomenon of cancer cells resistance to chemotherapy. Furthermore, with the development of new cancer therapies such as immunotherapy and anti-angiogenic therapy, other recent models describing the interaction of these drugs with the tumor growth have been developed. In particular, the recent advances in genetics led to considerable progress in experimental and clinical immunology [33] and many researches on modeling the immune system dynamics had been carried out.

We can also find some stochastic models involving uncertainties. For instance, [29] considered an uncertainty on the time which is necessary to the eradication of endothelial cells while [15] modeled the effect of drugs on the different compartments as a stochastic process.

Finally, the challenge of modeling biological systems in general is to focus on the

elements which are known to be significant in terms of control design in order to have a simplified and reliable model. In this section, a brief overview on tumor growth modeling will be presented.

2.3.1 Cancer growth modeling

According to [90], the mathematical modeling of tumor cells growth is one of the oldest and best developed topics in biomathematics. One of the commonly basic models for cancer growth is the exponential term described by the following ODE:

$$\dot{x} = r_x x, \quad x(0) = x_0, \tag{2.1}$$

where $x = x(t)$ is the quantity of cancer cells at time t, it can be either the volume or the number of tumor cells, r_x is the growth rate and x_0 is the initial quantity of tumor cells. Equation (2.1) allows to model the cancer growth with an exponential term without taking into account the potential carrying capacity of a tumor. Therefore, other terms that are more realistic and allow to consider a limited carrying capacity for the cancer, have been proposed in the literature:

$$\dot{x} = r_x x \left(1 - \frac{x}{x_\infty}\right), \quad x(0) = x_0. \tag{2.2}$$

$$\dot{x} = -r_x x \ln\left(\frac{x}{x_\infty}\right), \quad x(0) = x_0. \tag{2.3}$$

Equation (2.2) models a logistic growth while equation (2.3) models a Gompertzian growth, they both consider a limited cancer carrying capacity represented by x_∞, since for $x = x_\infty$, we have $\dot{x} = 0$ for both equations, meaning that the variation of cancer cells quantity with respect to time becomes null once the quantity of tumor cells reaches x_∞.

Chemotherapy is a conventional treatment that targets tumor cells using cytotoxic or cytostatic molecules. It is usually delivered intravenously in order to limit cells division [60]. This therapy might undergo a resistance from cancer cells when the cell division process is stopped. Therefore, we can find many works in the literature regarding the modeling of cancer chemotherapy interactions, for example [64], [72], [2], [66] and [67].

In [64], authors proposed the following model in order to describe tumor chemotherapy interactions:

$$\dot{x} = r_x f(x, x_\infty) - \Lambda_x(x, u), \quad x(0) = x_0, \tag{2.4}$$

where $u = u(t)$ stands for the concentration of a chemotherapeutic agent at time t, Λ_x denotes the decrease of tumor cells that is induced by the effect of chemotherapy and f represents the tumor growth term which can be either exponential, logistic or Gompertzian.

This drug effect term is usually considered to be proportional to the tumor cells population, *i.e*: $\Lambda_x(x,u) = \kappa x u$. In some works such as [66], the authors considered that the drug spreads within the body instantaneously so that the drug infusion rate, that we denote $c = c(t)$, is approximately proportional to the drug concentration u. However, this consideration might be an oversimplification especially in the case of chemotherapy [57]. Therefore, it is important to take into account the drug pharmacokinetic dynamics (PK) allowing to model the concentration of the chemotherapeutic agent in the body, for example in [57], the following term was considered:

$$\dot{u} = -a_c u + b_c c, \quad u(0) = 0. \tag{2.5}$$

In equation (2.5), the drug infusion rate c and its corresponding concentration in the human body u are linked through a simple first order dynamics, allowing to model the drug concentration with an exponential growth/decay dynamical model.

As mentioned in the previous sections, chemotherapy might induce critical side effects to the cells that are constantly dividing in the human body. Therefore, it is highly important to consider these secondary effects in the modeling process. The authors in [72] proposed a model that takes into account the detrimental effects of chemotherapy on the normal healthy cells of the human body:

$$\begin{aligned} \dot{x} &= r_x f(x, x_\infty) - \Lambda_x(x,u), \quad x(0) = x_0, \\ \dot{n} &= r_n h(n, n_\infty) - \Upsilon(n,u), \quad n(0) = n_0. \end{aligned} \tag{2.6}$$

The model (2.6) describes the dynamics of two populations, cancer cells population x and normal healthy cells population n, where r_n stands for the growth rate of normal cells and $h(n, n_\infty)$ represents its corresponding growth function. Furthermore, $\Upsilon(n,u)$ models the side effects of chemotherapy on normal healthy cells and n_0 stands for the initial quantity of normal cells.

In addition to the chemotherapy secondary effects, [2] proposed to add a term describing the detrimental effects of the tumor on the normal healthy cells:

$$\begin{aligned} \dot{x} &= r_x f(x, x_\infty) - \Lambda_x(x,u), \quad x(0) = x_0, \\ \dot{n} &= r_n h(n, n_\infty) - \Upsilon(n,u) - \Xi(x,n), \quad n(0) = n_0. \end{aligned} \tag{2.7}$$

The term $\Xi(x,n)$, in the equation of normal cells dynamics, stands for the normal cells loss induced by the presence of the tumor, it is considered to be proportional to the normal cells, *i.e*: $\Xi(x,n) = \varrho x n$.

As a recent improvement for these classical models, [14] proposed to multiply the growth terms for both cancer and normal cells populations with a function $G(g)$, standing for the effect of nutrients on the populations growth. The dynamics of nutrients is represented by g which is modeled through an ODE. Furthermore, [36] proposed to split the population of tumor cells into two categories, non-resistant and resistant tumor cells, in order to model the phenomenon of tumor cells resistance to chemotherapy. Therefore,

it is assumed that the injected chemotherapeutic agent can only kill the non-resistant cancer cells and has no effect on resistant cancer cells. Furthermore, it is considered that a sub-population of non-resistant cancer cells can mutate and become resistant to chemotherapy.

2.3.2 Angiogenesis dynamics modeling

As mentioned in the previous sections, the angiogenesis phenomenon consists in the development of a vascularization by the tumor, in order to increase its supply in oxygen and nutrients. The main biologically validated model of the angiogenesis phenomenon was presented in [42] and consists of the following equations:

$$\begin{aligned} \dot{x} &= r_x f(x,q), \\ \dot{q} &= S(x,q) - I(x,q) - \eta_q q, \end{aligned} \tag{2.8}$$

where :

- x is the tumor volume and q is the vascular capacity.
- $f(x,q)$ stands for the tumor growth, it can be either logistic (equation (2.9)) or Gompertzian (equation (2.10)):

$$\dot{x} = r_x x \left(1 - \frac{x}{q}\right). \tag{2.9}$$

$$\dot{x} = -r_x x \ln\left(\frac{x}{q}\right). \tag{2.10}$$

- $I(x,q)$ stands for the tumor inhibition effect and is chosen to be proportional to the tumor surface as follows :

$$I(x,q) = bqx^{\frac{2}{3}}.$$

- $S(x,q)$ stands for the tumor stimulation effect. The term $I(x,q)$ tends to grow at a rate $q^\alpha x^\beta$ faster than $S(x,q)$ with $\alpha + \beta = \frac{2}{3}$, which gives the following ODE :

$$\dot{q} = bx - \left(\varrho + dx^{\frac{2}{3}}\right) q. \tag{2.11}$$

- r_x is the tumor growth rate, b is the vessels birth rate (stimulated by the tumor) while d is the vessels death rate (inhibited by the tumor) and ϱ is the natural loss of vessels.

The assumption $\alpha + \beta = \frac{2}{3}$, considered in [42], led researchers to suggest some modifications to the original model presented in [42]. These modifications are summarized in Table 2.1.

Models	$I(x,q)$	$S(x,q)$	References
H_0	$dx^{2/3}q$	bx	[42]
H_1	$dq^{5/3}$	bq	H_0 modified by [34]
E	$dq^{4/3}$	$bx^{2/3}$	[34]
O	$dx^{2/3}q$	bq	[31]
S_c	$dx^{1/3}q$	$bx^{2/3}$	[81]

Table 2.1: The several versions of the model presented by Hahnfeldt in [42].

If we take a look at the evolution of x and q with respect to time in Figure 2.3, we notice that changing the model parameters (α and β) affects mainly the speed with which the variables x and q reach their maximal capacity. It is interesting to notice that without any drugs injections, the tumor and its vascularization keep on growing, even when the initial quantity of tumor cells is very small.

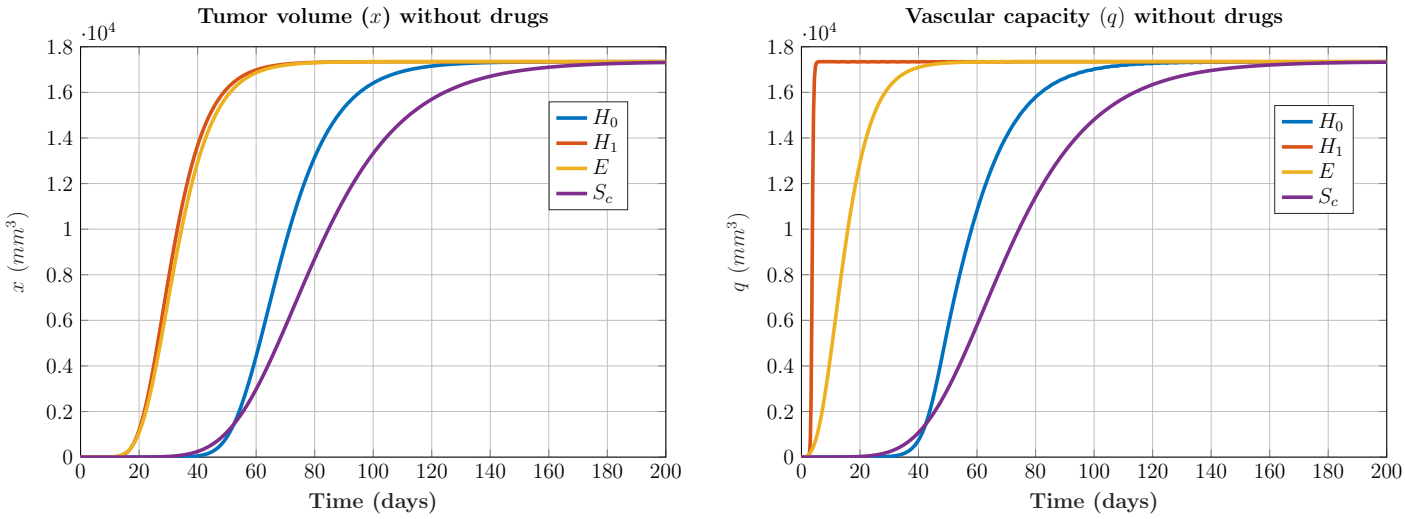

Figure 2.3: Comparison between the models H_0,H_1, E and S_c. The simulations are carried out using the following parameters values: r_x=0.084 with a Gompertzian growth, d=0.00873, b=5.85, η_q=0 [58], $x(0)$=10^{-4} and $q(0)$=0.

Anti-angiogenic therapy has been developed in order to inhibit the vascular growth, preventing thereby the tumor to proliferate. Similarly to chemotherapy, anti-angiogenic therapy induced loss on tumor cells is usually considered to be proportional to the tumor volume x and the vascular capacity q. Thus, the dynamical system (2.8) with drugs interactions consideration is the following:

$$\begin{aligned} \dot{x} &= r_x f(x,q) - \lambda x u, \\ \dot{q} &= S(x,q) - I(x,q) - \eta_q q - \gamma q v, \end{aligned} \tag{2.12}$$

where u and v are respectively the injection rates of chemotherapeutic and anti-angiogenic agents, with λ and γ standing for their respective effects factors on the two compartments

(the tumor and its vascularization).

As a recent modification for the system presented in [42], [9] proposed to split the vascularization compartment into two categories, the first sub-compartment consists of unstable vessels which are developed thanks to the tumor stimulation, these vessels are sensitive to anti-angiogenic treatment and their volume can be reduced. The second category consists of stable vessels which result from the maturity of some unstable vessels, they provide the tumor with nutrients and oxygen and are not sensitive to anti-angiogenic agents. Furthermore, a variable standing for the quality of the vascularization is introduced and affects the treatments effects.

2.3.3 On modeling immune system dynamics

Immunotherapy consists in stimulating some specific immune cells in the body in order to inhibit the cancer growth. According to [79], constructing an accurate mathematical model for cancer immune interactions requires taking into account the most important mechanisms that occur between the different cell populations, using existing knowledges from cell biology, molecular biology, biochemistry and immunology. Indeed, the mathematical modeling of the entire immune system can be a very complex task, that is one of the reasons that researchers focus on the elements of the immune system that are known to be significant in controlling the tumor growth [20].

Mathematical models can provide a relevant framework helping to systematically organize immunological concepts, and to show the range of outcomes of various immunological hypotheses that cannot be tested experimentally yet [33]. The literature of cancer immune interactions modeling covers many different models, from simple ODE systems to more complex and large models of ODEs, as well as, hybrid systems, multi-scale models that combine ODEs with PDEs and agent-based approaches [33], [63]. However, it is relevant to underline the fact that increasing model complexity leads to difficulties in the calibration of the model and its use for quantitative predictions, as well as difficulties to analytically investigate these models [33].

According to [55], mathematical models for tumor immune interactions have a long history dating back to Stepanova's model [84]. The latter gives the advantage of a minimally parametrized model that nevertheless includes the main aspects of cancer-immune interactions.

The models considered in this thesis are based on the model proposed by [84] that has been generalized in [32], the original model describes the interactions between two populations, tumor cells and immune effector cells. This second population gathers different types of immune cells (NK cells, CTLs,...). Therefore, it aggregates both the innate and adaptive immune reponses. This model includes also explicitly two therapies delivery, cytotoxic chemotherapy and immunostimulation. Furthermore, it takes into account the chemotherapy-induced loss on tumor cells and incorporates the beneficial effects of the

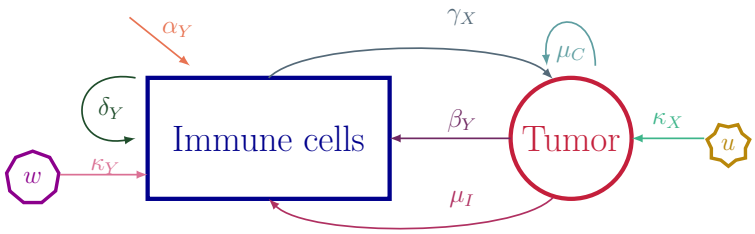

Figure 2.4: A scheme showing the interactions in model (2.13), between the tumor and the immune system.

immune system in controlling the tumor growth. According to [55], the immune system can be effective in controlling small cancer burdens, but for large volumes, the cancer dynamics overwhelms the immune system. Therefore, using a combined therapy is important to achieve patient recovery.

The model proposed by [84] and generalized by [32] is the following:

$$\begin{aligned} \dot{x} =& \mu_C f\left(x, x_\infty\right) - \gamma_X xy - \kappa_X xu, \\ \dot{y} =& \mu_I xy - \beta_Y \mu_I x^2 y - \delta_Y y + \kappa_Y yw + \alpha_Y, \end{aligned} \tag{2.13}$$

where x and y denote, respectively, the number of tumor cells and the density of effector immune cells (ECs), u and w are, respectively, the delivery rates of a cytotoxic agent and an immunostimulator, and f denotes the tumor growth term that has been defined previously, it can be either exponential, logistic or Gompertzian. Figure 2.4 presents a scheme describing the different interactions between the tumor and the immune system according to this model. Table 2.2 summarizes the definitions of the other model parameters and their numerical values.

Table 2.2: Numerical values and definitions of the parameters used in model (2.13) and taken from[32].

Parameter	Definition	Numerical value
μ_C	tumor growth rate	$0.5599 \cdot 10^7$ cells/day
μ_I	tumor stimulated proliferation rate	0.00484 day^{-1}
α_Y	rate of immune cells influx	0.1181 day^{-1}
β_Y	inverse threshold	0.00264
γ_X	interaction rate	$1 \cdot 10^7$ cells/day
δ_Y	death rate	0.37451 day^{-1}
κ_X	chemotherapeutic killing parameter	$1 \cdot 10^7$ cells/day
κ_Y	immunotherapy injection parameter	$1 \cdot 10^7$ cells/day
x_∞	fixed carrying capacity	$780 \cdot 10^6$ cells

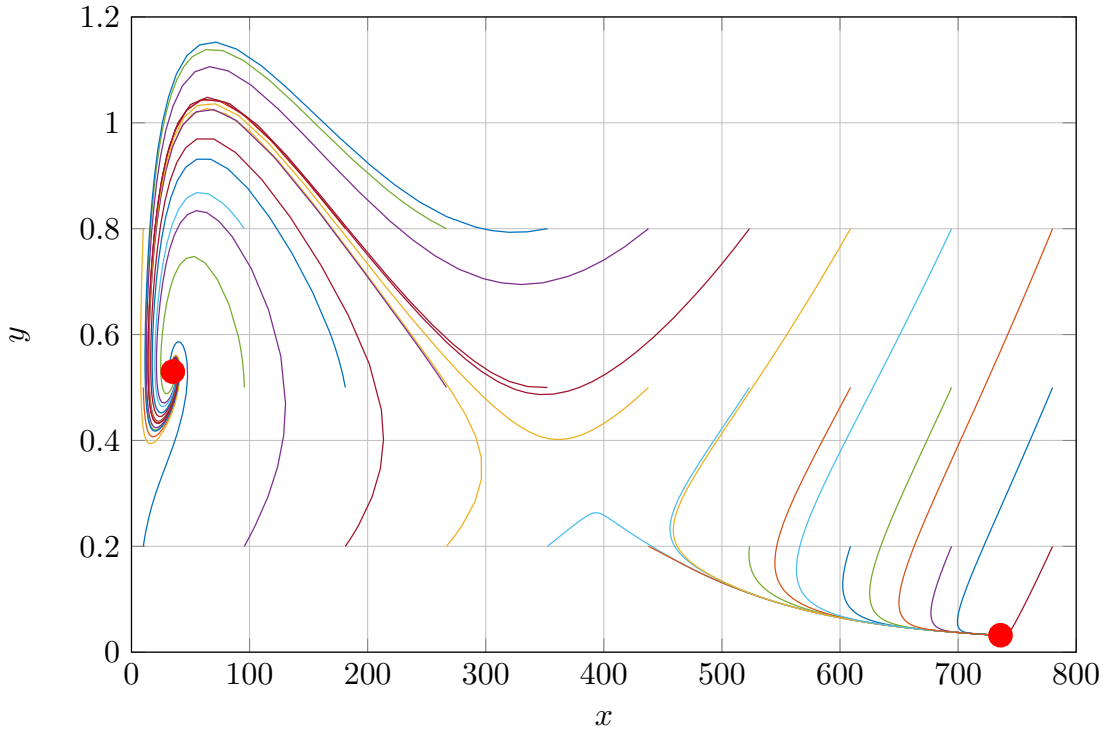

Figure 2.5: The phase portrait of system (2.13) with a logistic growth, in red the benign and malignant equilibrium points.

As shown in Figure 2.5, the uncontrolled model (2.13) has two locally asymptotically stable equilibrium points. The macroscopic malignant equilibrium is $(x_m, y_m) = (735.9, 0.032)$ and the benign one is $(x_b, y_b) \simeq (34.98, 0.53)$. It is relevant to underline the fact that the treatment performance highly depends on the initial conditions, since there is coexistence of macro- and microscopic equilibriums. The initial states of system (2.13) can be estimated with some uncertainties, before designing the drug injection schedules. The objective of cancer treatment can be formulated as to drive the state initial conditions from the region of attraction of the malignant equilibrium to the region of attraction of the benign equilibrium.

We can find in the literature a wide range of cancer immune interactions models. Some of them are biologically validated with mice and human data, such as [27] where the authors considered three populations, tumor cells, circulating lymphocytes and effector immune cells, whereas in [21] the authors splitted the population of effector immune cells into two populations, NK cells and CTLs in order to separate the innate and adaptive immune responses. Furthermore, the authors considered three treatments, a chemotherapeutic agent, IL-2 and TIL injections.

Since the objective of this thesis is to provide a qualitative assessment of some tools and methodologies in terms of cancer dynamics control, and does not intend to focus on a particular cancer type, we chose to base our work on a relatively simple model (based on the one presented in [84]) in order to push further the analysis and investigation of the tools that we develop.

2.4 Control for cancer therapies scheduling

In real cancer treatment cases, the doctors use standard injection protocols with predetermined treatment dosages, depending on the type of the cancer. These protocols are defined based on the results of many clinical trials. Therefore, the control theory related approaches allow to provide a pragmatic tool to design cancer treatment protocols that are based on biologically validated models, by specifying how to combine the different therapies, their respective frequencies and dose administration, which allows to avoid the laborious process of clinical trials as well as its high cost.

The main problem in cancer treatment is to provide a guarantee or a certification that the designed drug injection protocol reduces the tumor burden while keeping the patient in healthy conditions. Therefore, it requires balancing the benefits of treating the cancer with the detrimental side effects of some treatments such as chemotherapy and radiotherapy.

Let's consider the following general ODE model of cancer growth with drugs interactions :

$$\dot{x} = F(x, u), \tag{2.14}$$

where the state x gathers many variables representing information about some compartments in the human body or quantities of specific cell populations, while the control inputs represented by u stand for the drug rates that are injected in the body. The function F models the dynamical interactions between the different variables.

Cancer treatment scheduling requires taking into account state and input constraints, system non-linearities and optimality issues. Furthermore, since the biological systems are in general highly uncertain, it is crucial to handle the uncertainties in terms of cancer protocols scheduling. This is definitely the collection of all complexity ingredients in the context of control design.

In the last decades there has been a new wave of methods for addressing different cancer therapies scheduling problems, they are mainly based on mathematical modeling and control, in order to help biologists to predict the behavior of the cancerous tumors and establish adequate drug administration strategies. According to [57], the application of optimal control to the cancer treatment scheduling problems started by the mid-1970s in order to investigate drug regimens effects in reducing the tumor burden. Since then, this topic generated a lot of attention and researchers started applying different control approaches in order to schedule cancer treatments.

Usually, researchers focus on studying the theoretical effects of the control inputs and analyzing the state trajectories, in order to prove the feasibility or the unfeasibility of the designed therapeutic strategies, under specific biological assumptions. Another interesting application is to design multi-targeted therapies profiles that are optimized according to the oncologists specifications.

The progress in cancer dynamics modeling motivated researchers to apply control approaches in order to schedule cancer treatments using different control strategies. We can cite for instance, optimal control in [56], [58], [73] and [29]. There exist also other works where feedback control schemes are considered such as [3], [89], [48] and [61]. Furthermore, we can find model predictive control (MPC) applications such as [82] and [17].

Although the literature of control for cancer treatment is very rich, only few works addressed the problem of handling parametric uncertainties in drugs schedules design. One can cite for example, [3] where a robust feedback scheme is proposed to schedule anti-angiogenic treatment combined with chemotherapy, [50] where an H_∞ based robust control was applied to the same model and [4] where a general framework for probabilistic certification of cancer therapies was proposed. We will explain in the subsequent section why it is important to consider parametric uncertainties in the control design process.

2.4.1 Parametric uncertainties

Due to the empirical nature of cancer dynamics modeling, this branch of biomathematics suffers from parameters estimation problems [90]. The complexity of this process comes not only from the unavoidable inaccuracy of the parameters estimation but mainly from their intrinsic changing and uncertain behavior.

According to [23], one of the most challenging tasks in modeling cancer therapies dynamics is the computation of biological parameters from empirical data. The complexity of this task might increase with the number of the cell populations considered in the dynamical model.

In mathematical and computational immunology, usually, researchers consider parameters that are published in the literature in order to assess their methodologies. However, this might be misleading since in addition to their dependence on the case study only few laboratories measure and estimate these parameters [33].

Therefore, it is crucial to include the different uncertainties, that the model is subject to, in the drug scheduling design, in order to provide a strong guarantee on the efficiency of the treatment profile in presence of uncertainties. Moreover, one can estimate the probability of achieving the treatment objectives from a statistical point of view in order to assess the performance of the considered methodology.

The context of this thesis revolves around the investigation of optimal control approaches that are able to consider parametric uncertainties for the purpose of cancer treatment scheduling. The next sections will briefly present the context of the main contributions of this thesis that will be detailed further in the following chapters.

2.4.2 Optimal control under uncertainties for cancer treatment

Since the design of cancer treatment protocols requires the consideration of state and input constraint and many optimization issues, the different optimal control approaches turn out to be adequate to this challenge.

We can find in the literature many works regarding the application of optimal control methods on cancer treatment problems. For instance, [58], [81] and [30], where optimal protocols for anti-angiogenic treatment were investigated, or [25] where authors designed linear controls for a tumor-immune interactions model with chemotherapy delivery.

In order to properly state an optimal control problem, one needs to define some ingredients, namely the cost function to be minimized or maximized and the constraints that need to be fulfilled:

- The cost function: which gathers the different treatment objectives that one seeks to achieve, such as reducing the tumor burden, enhancing the patient health, etc.
- State constraints: they represent the restrictions on the values of the different physiological indicators.
- Control input constraints: they stand for the limitations on the drug dosages or duration.

Let's consider the general model for cancer therapies interactions (2.14):

$$\dot{x} = F(x, u).$$

A typical optimal control problem (OCP) to be solved is:

$$\begin{aligned} \min_{u(\cdot)} \quad & J\left(x(t), x(T), u(t)\right) \\ \text{s.t.} \quad & \dot{x}(t) = F(x(t), u(t)), \\ & x(t) \in X, \;\; u(t) \in U, \;\; t \in [0, T], \\ & x(0) \in X_0, \;\; x(T) \in X_T, \end{aligned} \tag{2.15}$$

where t stands for time and belongs to the interval $[0, T]$ with T being the therapy duration, J stands for the cost to be minimized, it is chosen according to the objectives that one seeks to achieve. It can contain many terms such as the states at the end of the treatment duration denoted by $x(T)$, integrals of the state trajectories and the control inputs, with different penalties in order to achieve a trade-off between the different control objectives. $x(0)$ stands for the initial state which represents the quantities of the different considered cell populations at the beginning of the treatment. X_0, X_T, X and U stand respectively for the sets of admissible values of the initial states, the final states, the state trajectories and the control inputs.

Solving the optimal control problem in (2.15) provides the optimal profile $u(\cdot)$ that minimizes the cost J and satisfies all the specified constraints. The solution of this problem might require some specific computational methods.

The challenge arises when the dynamics of the cancer model incorporate uncertain parameters that are described by probability distributions for example. The solution of the problem in this case is definitely not straightforward since one needs to define a new cost from a statistical point of view. Furthermore, we need to guarantee the satisfaction of the constraints given the nature of the parametric uncertainties. In Part II, we will address the problem of drug injection schedules design for cancer treatment, in the presence of model parametric uncertainties, by investigating the use of a recent optimal control approach, based on the moment optimization framework. This method allows to formulate and solve robust optimal control problems by taking into account uncertain parameters and initial states, modeled as probability distributions.

In the same Part we will analyse a two dimensional model that describes the interaction dynamics between tumor and immune cells. Furthermore, we derive statistically optimal combined strategies of chemo- and immunotherapy treatments, assuming the knowledge of probability distributions of some uncertain model parameters, namely, the tumor growth rate and the rate of immune cells influx. Numerical simulations will be presented in order to illustrate the effects of parametric uncertainties on dynamics, when using a nominal injection profile (considering a nominal value for model parameters). Finally, we compare the recovery performance of nominal and robust schedules.

2.4.3 Domain of attraction estimation under parametric uncertainties

The estimation of the region of attraction (RoA) for cancer models is an interesting problem since it provides the set of possible initial conditions (tumor and patient health indicators) that can be driven to a desired targeted benign region.

This problem becomes complex when dealing with nonlinear systems and even more challenging for uncertain systems. There are some works which dealt with the problem of estimating the RoA for cancer models but only few of them considered model uncertainties. In particular, in [78], an iterative method to estimate the robust RoA was presented. However, robust RoA estimation is based on the worst-case scenario analysis leading to a very pessimistic design. This is because the worst case is considered no matter how small its probability of occurrence is.

In Part III, we propose a framework to probabilistically certify the existence of a control structure that drives the states, corresponding to quantities of specific cells populations in the human body, from an initial state set to a certified target set. This probabilistic certification framework is based on the randomized methods proposed in [7] and [8], which, unlike the robust classical design, avoids focusing on few unlikely very bad

scenarios allowing to overcome the conservatism of the robust RoA design.

The methodology that we propose consists mainly of two steps. Firstly, we derive an ordered sequence of sets and a control strategy over each of them, such that the states can be driven from one set to a previous one with a certain probabilistic guarantee. The second step consists of providing a global certification on the probability of convergence to the initial certified target set, providing therefore a global estimation of the patient recovery probability under parametric uncertainties.

2.5 Conclusion

In this chapter, we presented firstly a general introduction about the different biological mechanisms that are involved in the cancer growth phenomenon, in addition to a brief summary of the existing cancer therapies and the different related dynamics.

Furthermore, we explained in a more detailed way the different mechanisms of the immune system in defending the human body and the role of immunotherapy in fighting the cancer growth. Thereafter, we presented an overview on the literature of tumor growth modeling and some related topics, such as modeling angiogenesis and immune dynamics.

Finally, we introduced the problem of cancer therapies scheduling in terms of control design, and presented the main challenges that one has to face. This led us to present briefly the main contributions and the context of this thesis, which consists mainly in parametric uncertainties considerations in the optimal control for cancer therapies as well as in the estimation of probabilistically certified regions of attraction.

In Chapter 3, we will present brief recalls of the theoretical notions that will be used in the sequel, namely moments optimization for optimal control. Furthermore, a recall of randomized methods for probabilistic certification will be presented in Chapter 7.

Chapter 3

Overview on moment optimization for optimal control

The moment approach for solving polynomial optimal control problems (OCPs) was presented in [54] as an extension of the work presented in [51] and [52], where the author proved that nonconvex polynomial optimization problems can be addressed by solving a hierarchy of convex semidefinite programming (SDP) problems.

This approach, developed by Lasserre [53] and summarized in Figure 3.1, is based on the fact that polynomial optimization problems (a class of nonconvex finite dimensional problems) are equivalent, in the space of measures, to infinite dimensional problems, under mild assumptions. These infinite dimensional problems are nevertheless linear and can be reformulated in terms of moments since the latter are linked to measures. Approximations of the global optimal solutions can be obtained by solving relaxations of the infinite dimensional LP problems [53], providing therefore a converging sequence of lower bounds on the global minima, under some compactness assumptions. Therefore, generating and solving these relaxations allow to approach the exact solution of the original polynomial optimization problem with arbitrary precision.

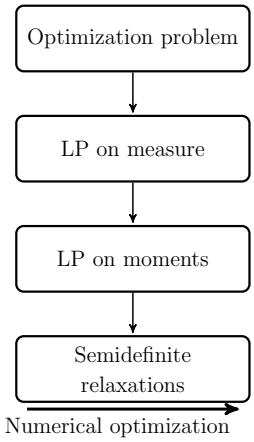

Figure 3.1: A scheme presenting the main steps of the moment optimization approach.

Recently, this approach has been extended to optimal control problems with a polynomial structure and bounded constraints [54], for which one can obtain sub-optimal solutions converging to the exact optimal control as the relaxation order increases, by solving sequences of convex problems. Furthermore, a finite convergence certificate can be provided in order to check the global optimum recovery. Moreover, as the linear infinite dimensional problems are defined in the space of measures, this approach allows to address optimal control problems with uncertain variables (states and parameters) described by probability distributions.

The idea of using moments to solve optimization and optimal control problems has been extensively studied. For instance in [44], where the authors used the moments approach and its dual to derive outer approximations of the region of attraction for polynomial dynamical systems. We can cite also the work presented in [80] that proposes to reformulate the discrete-time stochastic optimal control problem in terms of occupation measures and to solve it using moments relaxations. Furthermore, the authors in [85] presented a framework of estimation and model invalidation based on the moment optimization framework, using probabilistically uncertain data.

In this chapter, we will present an overview on the main key points of the generalized moment problem, which are necessary to the understanding of the reformulation of optimal control problems in terms of moments. These tools will be used in Part II in order to provide a framework of optimal control under uncertainties for a dynamical model representing the dynamics of tumor in interaction with appropriate therapies.

3.1 Definitions

Firstly, we provide some basic definitions and mathematical tools that are necessary for the next sections.

Definition 3.1 (Closed basic semi-algebraic set) *A closed basic semi-algebraic set is an intersection of finitely many closed polynomial superlevel sets, it is defined as follows:*

$$X = \{x \in \mathbb{R}^n : \quad h_i(x) \geq 0, \;\; h_i(x) \in \mathbb{R}[x], \;\; i = 1, ..., n_X\},$$

where $h_1, ..., h_{n_X}$ are polynomials and $\mathbb{R}[x]$ stands for the ring of polynomials of the variable $x \in \mathbb{R}^n$ with real coefficients.

Definition 3.2 (Signed measure [53]) *Let's denote by $\mathcal{B}(X)$ the Borel σ-algebra of X, which is a particular set of subsets of X containing all the open subsets of X. A signed measure is a function $\mu : \mathcal{B}(X) \to \mathbb{R} \cup \{\infty\}$ such that $\mu(\emptyset) = 0$ and $\mu(\cup_{k\in\mathbb{N}} X_k) = \Sigma_{k\in\mathbb{N}} \mu(X_k)$, where $X_k \in \mathcal{B}(X)$ are disjoint sets. Therefore, it is a function that assigns a real number to any subset of X.*

It's is important to precise that measures can be defined as the space of linear functionals that acts on the space of continuous functions on X [43], *i.e.* with the action that measures have on the elements of the dual space $l \in \mathcal{C}(X)$ through integration:

$$\langle l, \mu \rangle = \int_X l(x)\mu(dx).$$

Definition 3.3 (Probability measure) *It is a signed measure taking only real non-negative values (positive measure) such that $\mu(X) = 1$. This measure can be also interpreted as the probability distribution of the elements on a given set X.*

Example: Given the following set X with subsets X_1 and X_2:

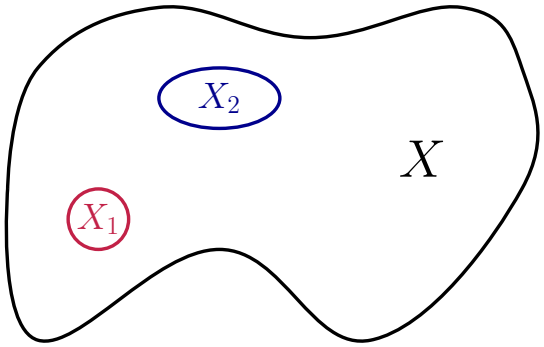

Let's consider that μ_p is a probability measure defined on the set X such that $\mu_p(X) = 1$, if $\mu_p(X_1) = 0.95$, this means that if x is a random variable whose distribution is given by the measure μ_p, then the probability for x to be in X_1 is 95%, *i.e.* $P(x \in X_1) = 95\%$

Definition 3.4 (Dirac measure) *We denote by $\delta_\vartheta(X)$ the Dirac measure at ϑ is defined as follows:*

$$\delta_\vartheta(X) = \begin{cases} 1 & \text{if } \vartheta \in X \\ 0 & \text{otherwise} \end{cases}$$

Note that the Dirac measure $\delta_\vartheta(X)$ is an example of a positive measure since it returns two possible non-negative values (either 0 or 1).

Definition 3.5 (Moments) *Considering a compact set $X \in \mathbb{R}^n$, $\mathcal{M}(X)$ denotes the space of signed measures supported on X [43]. Given $x \in X$ and an integer vector $\sigma \in \mathbb{N}^n$, the moment of order σ of $\mu \in \mathcal{M}(X)$ is defined as:*

$$y_\sigma = \int_X x^\sigma \mu(dx), \tag{3.1}$$

where $x^\sigma = \prod_{k=1}^n x_k^{\sigma_k}$ with σ being a multi-index.

Definition 3.6 (Riesz functional [43]) *Given a sequence of moments denoted $y = (y_\sigma)_{\sigma \in \mathbb{N}^n}$, the Riesz functional $\mathcal{R}_y : \mathbb{R}[x] \to \mathbb{R}$ acting on polynomials $p(x)$ is defined as follows:*

$$\mathcal{R}_y(p) = \Sigma_\sigma p_\sigma y_\sigma, \tag{3.2}$$

where p_σ stands for the σ-order coefficient of $p(x)$ with $p(x) = \Sigma_\sigma p_\sigma x^\sigma$.

Definition 3.7 (Moment matrix) *The moment matrix of order d denoted $M_d(y)$ is the Gram matrix of the quadratic form $p(x) \to \mathcal{R}_y(p^2)$, such that $\mathcal{R}_y(p^2) = p^\top M_d(y)p$, where $p(x)$ is a polynomial with degree d, and $p = (p_\sigma)_{|\sigma|\leq d}$ (p is the vector of coefficients corresponding to the polynomial $p(x)$ up to degree d). The moment matrix is symmetric and linear in y by construction.*

Note that with a slight abuse of notation, we use $p(x)$ in order to emphasize the fact that the polynomial is considered as a function, whereas the notation p represents the vector of coefficients related to this polynomial.

Definition 3.8 (Localizing matrix) *Considering a polynomial $w(x)$, its localizing matrix of order d is the Gram matrix of the form $w(x) \to \mathcal{R}_y(wp^2)$, such that $\mathcal{R}_y(wp^2) = p^\top M_d(wy)p$ with w being the coefficient vector corresponding to the polynomial $w(x)$.*

Note that the localizing matrix can be interpreted as a linear combination of different moment matrices.

Given an infinite sequence of moments y corresponding to a measure μ, we denote by $M(y) = M_\infty(y)$ and $M(wy) = M_\infty(wy)$, respectively, the infinite-dimensional moment and localizing matrices. Furthermore, we denote by $\mathcal{M}_+(X)$ the space of positive measures supported on X and by $\mathcal{P}(X)$ the set of probability measures supported on X.

3.2 Linking moments to measures

Given a measure μ defined on a compact set, this measure is uniquely defined by the infinite sequence of its corresponding moments [53]. This is very useful since, in practice, instead of manipulating abstract objects such as measures, one manipulates their moments [43]. In this section, we recall the theoretical notions allowing to link moments to measures. These notions will help us, in the sequel, to explain how to reformulate optimal control problems in terms of moments.

Definition 3.9 (representing measure) *Given an infinite sequence of moments $y = (y_\sigma)_{\sigma\in\mathbb{N}^n}$, the measure μ satisfying*

$$y_\sigma = \int_X x^\sigma \mu(dx), \qquad \forall \sigma \in \mathbb{N}^n, \tag{3.3}$$

*is said to be a **representing** measure of the sequence y.*

Note that Definition 3.9 holds also for the case of truncated moments vectors, see [53].

The infinite dimensional moment and localizing matrices allow to explicitly model the constraint that a sequence of moments y has a representing measure μ on a compact basic semi-algebraic set X, under a mild assumption on the representation of X. These constraints are infinite dimensional LMIs (Linear Matrix Inequalities).

Assumption 3.1 *Given a closed basic semi-algebraic set X defined as follows:*

$$X = \{x \in \mathbb{R}^n : \quad h_i(x) \geq 0, \;\; h_i(x) \in \mathbb{R}[x], \;\; i = 1, ..., n_X\}. \tag{3.4}$$

We assume that one of the polynomial inequalities $h_i(x)$ is of the form $r - \Sigma_{j=1}^{n} x_i^2 \geq 0$, with $r \in \mathbb{R}_+$ being a sufficiently large positive real number (such that $X \subset \{x \in \mathbb{R}^n : \Sigma_{j=1}^{n} x_i^2 \leq r\}$).

As mentioned in [43], although Assumption 3.1 is stronger than the compactness property of the set X (which requires closeness and boundedness), assuming the compactness of X and adding a supplementary constraint to its description in (3.4), allows to ensure the satisfaction of Assumption 3.1 without loss of generality.

Proposition 3.1 (Putinar's Theorem [76]) *Consider that the set X satisfies Assumption 3.1. The infinite sequence y has a representing measure in $\mathcal{M}_+(X)$ if and only if $M(y) \succeq 0$ and $M(h_i y) \succeq 0$ for all $i = 1, ..., n_X$.*

Therefore, the moment and localizing matrices defined in Definition 3.7 and 3.8 allow to reformulate infinite-dimensional problems that are written in terms of measures into infinite-dimensional problems on moments. The latter problems can be relaxed by truncating the moments vectors up to some degrees using a specific hierarchy that we will detail in the sequel.

Although Proposition 3.1 provides a powerful tool to state if a sequence of moments has a representing measure or not, this result concerns infinite dimensional vectors that cannot be manipulated in practice. Therefore, in order to avoid manipulating infinite dimensional vectors of moments, one can deal with their finite truncations. The question that arises is: given a truncated sequence of moments (a finite sequence) denoted $y^{(\leq d)} = (y_\sigma)_{|\sigma| \leq d}$ (the vector of moments up to order d) such that $\sigma \in \Delta \subset \mathbb{N}^n$, does there exist a measure μ supported on X, such that:

$$y_\sigma = \int_X x^\sigma \mu(dx), \qquad \forall \sigma \in \Delta? \tag{3.5}$$

In Chapter 3 of [53], the author provides an important sufficient condition for the truncated moment problem (formulated in the previous question). Therefore, in addition to the condition required in Proposition 3.1 (regarding the moment and localizing matrices), one needs to check additional conditions on the rank of these matrices for some relaxation degrees, for more details see [53]. Note that this rank condition can be numerically checked using standard linear algebra techniques.

3.3 Optimal control problem reformulation

The approach that we recall in this chapter provides a powerful tool allowing to solve optimal control problems where uncertainties are considered. In Part II, we will investigate

this approach in order to design optimal control profiles that are drug injection schedules, using a dynamical model describing the interaction between a tumor and some specific therapies. In this section we explain how a specific class of nonlinear OCPs (polynomial OCPs) can be reformulated in terms of moments.

First, let's consider the following polynomial optimal control problem:

$$\begin{aligned} \inf_{u(\cdot)} \quad & \int_0^T L(x(t),u(t))\,dt + \Phi\left(x(T)\right) \\ \text{s.t.} \quad & \dot{x}(t) = F(x(t),u(t)), \\ & x(t) \in X,\ u(t) \in U,\ t \in [0,T], \\ & x(0) \in X_0,\ x(T) \in X_T, \end{aligned} \tag{3.6}$$

where $x \in \mathbb{R}^n$ is the state, $u \in \mathbb{R}^m$ is the input, the functions $F : \times\mathbb{R}^n \times \mathbb{R}^m \to \mathbb{R}$, $L : \times\mathbb{R}^n \times \mathbb{R}^m \to \mathbb{R}$ and $\Phi : \mathbb{R}^n \to \mathbb{R}$ are polynomials allowing to define the cost to be minimized. X_0, X, X_T and U stand for the constraints sets and are defined as follows:

$$\begin{aligned} X_0 &= \{x_0 \in \mathbb{R}^n : h_{0_i}(x_0) \geq 0; i = 1,...,n_{X_0}\}, \\ X &= \{x \in \mathbb{R}^n : h_i(x) \geq 0; i = 1,...,n_X\}, \\ X_T &= \{x_T \in \mathbb{R}^n : h_{T_i}(x_T) \geq 0; i = 1,...,n_{X_T}\}, \\ U &= \{u \in \mathbb{R}^m : h_{u_i}(u) \geq 0; i = 1,...,n_U\}. \end{aligned} \tag{3.7}$$

Note that F and L can also be functions of time. Furthermore, several OCPs can be formulated from problem (3.6). We can think for instance of the case where X_0 and X_T contain respectively only one element, which is a classical optimal control problem, where we want to drive the dynamical system in (3.6) from one point (initial condition) to a final point $x(T)$ while minimizing a given cost function.

Assumption 3.2 *X_0, X, X_T and U are compact basic semi-algebraic sets.*

Note that compactness is posed to satisfy standard assumptions for ensuring desirable properties of measures and moments.

Assumption 3.3 *The polynomial dynamical system $\dot{x}(t) = F(x(t),u(t))$ with $u(t) \in U$ can be interpreted as a differential inclusion $\dot{x}(t) \in F\left(x(t),U\right) := \{F(x(t),u(t)) \ : \ u(t) \in U\}$. The set $F\left(x(t),U\right)$ is assumed to be convex.*

Provided that Assumptions 3.2 and 3.3 hold, a linear infinite dimensional optimization problem can be defined over the space of probability measures, which has the same optimum as problem (3.6). Therefore, we need to provide some definitions allowing to achieve the reformulation of the OCP presented in (3.6).

Definition 3.10 (Indicator function) *The indicator function of a set X is defined by:*

$$I_X(x) = \begin{cases} 1 & \text{if } x \in X \\ 0 & \text{otherwise} \end{cases}$$

Definition 3.11 (Controlled occupation measure) *Considering the following dynamical system:*

$$\dot{x} = F(x,u), \qquad x(0) = x_0. \tag{3.8}$$

If the function F in (3.8) is polynomial, therefore it is smooth and there exists a unique trajectory which is solution of (3.8), given an initial condition x_0 and a control law $u(t)$, this trajectory is denoted $x(t|x_0,u)$. The controlled occupation measure of the trajectory $x(t|x_0,u)$ is defined as follows:

$$\mu\left(A \times B \times C | x_0, u\right) := \int_A I_B(x(t|x_0,u))dt,$$

for all $A \in \mathcal{B}\left([0,T]\right)$, $B \in \mathcal{B}\left(X\right)$ and $C \in \mathcal{B}\left(U\right)$ with $t \in [0,T]$, T can be either fixed of free.

Therefore, the occupation measure allows to measure the time that the trajectory $(t, x(t|x_0,u), u(t))$ spends on a subset $A \times B \times C$ of $[0,T] \times X \times U$.

Furthermore, if we consider that the initial state x_0 is a random variable in X instead of being a deterministic vector, the distribution of x_0 can be interpreted as a probability measure $\xi_0 \in \mathcal{P}(X)$, such that the expected value of the random variable x_0, denoted $\mathbf{E}\left[x_0\right]$ is the first order moment of ξ_0, *i.e.* $\mathbf{E}\left[x_0\right] = \int_X x\xi_0(dx)$. Furthermore, the other higher order moments of the random variable x_0 are defined through the measure ξ_0 as: $y_\sigma = \int_X x^\sigma \xi_0(dx)$, with σ being the corresponding moment order. Therefore, in this case the solution of the ODE in (3.8) is interpreted as a flow of trajectories generated by the distribution of the random initial condition. Furthermore, the state trajectories at each time t are also interpreted as random variables.

Definition 3.12 (Average controlled occupation measure) *The average controlled occupation measure of the flow of trajectories is defined as :*

$$\mu\left(A \times B \times C | u\right) = \int_{X_0} \mu\left(A \times B \times C | x_0, u\right) \xi_0\left(dx_0\right).$$

Moreover, the *initial occupation measure* $\mu_0 \in \mathcal{P}\left(\{0\} \times X_0\right)$ captures the information on the initial condition and is defined as : $\mu_0(dt,dx) = \delta_0(dt)\xi_0(dx)$. The *terminal occupation measure* $\mu_T \in \mathcal{P}\left(\{T\} \times X_T\right)$ captures the information on the state a time T and is defined as : $\mu_T(dt,dx) = \delta_T(dt)\xi_T(dx)$ where ξ_T is the probability measure that rules the distribution of the terminal condition $x(T)$.

3.4 Infinite-dimensional measure problem

Studying the evolution of test functions $v \in \mathcal{C}^1([0,T] \times X)$ along the trajectories alows to characterize the flow of the system trajectories [46]. As explained in [54] and [53], by defining the Liouville operator $\mathcal{L} : \mathcal{C}^1([0,T] \times X) \to \mathcal{C}([0,T] \times X \times U)$ as $v \to \mathcal{L}v = -\frac{\partial v}{\partial t} + (\nabla_x v)' F$, the dynamics in (3.8) can be reformulated as follows :

$$\int_0^T \int_X \int_U \left(\frac{\partial v}{\partial t} + (\nabla_x v)' F \right) d\mu = \int_{X_T} v \, d\mu_T - \int_{X_0} v \, d\mu_0, \tag{3.9}$$

where $\nabla_x v = \left[\frac{\partial v}{\partial x_1}, ..., \frac{\partial v}{\partial x_n} \right]$ stands for the gradient of v with respect to x. Equation (3.9) is called the controlled Liouville equation, it describes the time evolution of the density transported by the flow of a nonlinear dynamical system. It will be used in the sequel to express the moments constraints characterizing the system dynamics.

The following linear problem in the space of measures

$$\begin{aligned} \inf_{\mu_0,\mu,\mu_T} \quad & \langle L, \mu \rangle + \langle \Phi, \mu_T \rangle \\ \text{s.t.} \quad & \int_{[0,T]\times X \times U} \left(\frac{\partial v(t,x)}{\partial t} + \nabla_x (v(t,x))' F(t,x,u) \right) d\mu \\ & \qquad = \langle v, \mu_T \rangle - \langle v, \mu_0 \rangle, \quad \forall v \in \mathcal{C}^1([0,T] \times X) \\ & \mu_0 \in \mathcal{M}_+(\{0\} \times X_0), \ \mu_T \in \mathcal{M}_+(\{T\} \times X_T) \\ & \mu \in \mathcal{M}_+([0,T] \times X \times U), \\ & \langle 1, \mu_0 \rangle = 1, \end{aligned} \tag{3.10}$$

is infinite dimensional and has the same optimum value as the original optimal control problem (3.6), under mild assumptions [54], this problem remains highly complex. However, Lasserre hierarchy [53] of relaxed LMI problems can be determined to obtain sub-optimal solutions, that converge to the optimal solution of the original optimal control problem, under some compactness and convexity assumptions. In order to obtain the relaxations, one has first to consider the relation between the measure μ_0, μ and μ_T and their moments that has been presented in Section 3.2.

Given a constraint of the type $\mu \in \mathcal{M}(X)$, it can be expressed in terms of LMI constraints involving infinite dimensional matrices that contain the infinite dimensional vector of moments y, as a consequence of the Putinar's theorem. Nevetheless, relaxations can be obtained by considering the matrix structures obtained, by appropriately truncating the vector of moments to a finite maximal degree (d) and imposing in (3.10) constraints over polynomials of a finite maximal degree in spite of all $v \in \mathcal{C}^1([0,T] \times X)$. In the sequel, we will give more details on the choice of the test functions v. This leads to a hierarchy of finite-dimensional SDP problems whose solutions converge to the solution of the optimal control problem as the relaxation degree grows.

The interesting feature of this approach is the fact that, even in the case of deterministic dynamical systems, the initial state as well as the final one and the state along trajectories, are dealt with by defining measures on the state space, see (3.10). The same holds for the input. For instance, if $x_0 = x(0) \in X_0$ is a singleton, then the initial measure μ_0 in (3.10) should be imposed by fixing, for all $\sigma \in \mathbb{N}^n$, its moments given as:

$$\langle t^\tau x^\sigma, \mu_0 \rangle = \begin{cases} x_0^\sigma & \text{if } \tau = 0 \\ 0 & \text{if } \tau \in \mathbb{N}^+ \backslash \{0\} \end{cases}$$

Therefore, no additional complexity is induced by considering states and inputs that are random variables of a deterministic point in the state and input spaces, since in both cases they are modeled by their measures.

3.5 Moment LP and relaxations

According to [53], every measure defined on a compact support is determinate (representing and unique), because the space of polynomials is dense (with respect to the supremum norm) in the space of continuous functions in $\mathbb{R}$. For a particular choice of monomial test functions of the form $v(t,x) = t^\alpha x^\beta$ (the choice of this basis is mainly motivated by the simplicity of notation [43]), notice that the integral of v with respect to a given measure $\mu(dt, dx)$, *i.e.* $\int v d\mu = \int t^\alpha x^\beta d\mu$, is the moment of order γ of μ, where $\gamma = (\alpha, \beta) \in \mathbb{N} \times \mathbb{N}^n$. Therefore, using monomial test functions allows to manipulate the measures with their respective moment vectors.

$\mathbf{z}_0$,$\mathbf{z}_T$ and $\mathbf{z}$ are compact notations of $\mathbf{z}_0^{(\leq d_1)}$,$\mathbf{z}_T^{(\leq d_1)}$ and $\mathbf{z}^{(\leq d_2)}$, standing for the moment vectors (up to degrees d_1 and d_2), corresponding to μ_0, μ_T and μ, respectively. The cost function in (3.6) can be rephrased in terms of moments for some degrees d_1 and d_2 as follows:

$$\int_0^T L(x(t), u(t))\, dt + \Phi\left(x(T)\right) = c_L' \, \mathbf{z} + c_\Phi' \, \mathbf{z}_T, \tag{3.11}$$

where c_L' and c_Φ' are vectors containing the coefficients of the polynomial costs L and Φ introduced in (3.6).

In addition to the cost, the dynamical constraints in (3.10) can also be rephrased in terms of moments. By replacing the test function $v(t,x)$ with its monomial form $t^\alpha x^\beta$ in (3.9), one can obtain a matrix equality in terms of the truncated moments vectors $\mathbf{z}_0$,$\mathbf{z}_T$ and $\mathbf{z}$. Furthermore, as explained previously, Putinar's theorem allows to express constraints of the type $\mu \in \mathcal{M}(X)$ in terms of LMI constraints, allowing therefore to rephrase the constraints of this form that (3.10) involve.

Thereby, problem (3.10) can be relaxed into a truncated convex moment problem as

follows:

$$\begin{aligned} \min_{\mathbf{z},\mathbf{z}_0,\mathbf{z}_T} \quad & c'_L\,\mathbf{z} + c'_\Phi\,\mathbf{z}_T \\ \text{s.t.} \quad & A_T\mathbf{z}_T = A_0\mathbf{z}_0 + A\mathbf{z}, \\ & M\left(\mathbf{z}_T\right) \succeq 0, L_{h_{T_i}}\left(\mathbf{z}_T\right) \succeq 0, \forall i = 1, ..., n_{X_T}, \\ & M\left(\mathbf{z}_0\right) \succeq 0, L_{h_{0_i}}\left(\mathbf{z}_0\right) \succeq 0, \forall i = 1, ..., n_{X_0}, \\ & M\left(\mathbf{z}\right) \succeq 0,\ L_{h_i}\left(\mathbf{z}\right) \succeq 0\ ,\ \forall i = 1, ..., n_X, \end{aligned} \tag{3.12}$$

where A,A_0 and A_T are some coefficient matrices related to the dynamics and resulting from (3.9), for further details see [54], [53] and [46]. The minimum is with respect to the moment vectors $\mathbf{z}$,$\mathbf{z}_0$ and $\mathbf{z}_T$, meaning that the measures μ,μ_0 and μ_T are all unknown. Therefore, semi-definite constraints are imposed on the moment and the localizing matrices, in order to guarantee the positivity and the support of the measures μ,μ_0 and μ_T.

In order to construct the convex relaxations, the truncation degrees d_1 and d_2 has to satisfy some specific conditions, see [46] and [53]. In the case where d_1 and d_2 are even numbers the conditions are the following:

$$\begin{aligned} & d_1 \geq \deg(\Phi), \\ & d_2 \geq \deg(L), \\ & d_2 \geq d_1 + \deg(F). \end{aligned} \tag{3.13}$$

Finally, increasing the relaxation orders (d_1 and d_2) provides a monotonically non-decreasing sequence of lower bounds converging to the optimal value. The LMI relaxations defined in problem (3.12) can be solved with Gloptipoly [45], using an SDP solver.

3.6 Optimal control reconstruction

After solving the LMI relaxations defined in problem (3.12), the vectors $\mathbf{z}_0$,$\mathbf{z}_T$ and $\mathbf{z}$ provide approximations of the moment vectors corresponding to the different occupation measures. Therefore, one needs to reconstruct the optimal trajectories based on the approximated moments. According to [19], this problem turns out to be a typical inverse problem, which is well mastered in the case of polynomial finite-dimensional optimization problems. However, this problem is more challenging in the case of optimal control problems, since we can only have a finite number of approximated moments, which prevents the reconstruction of exact measures. Therefore, we can use some numerical methods in order to derive an approximate of the optimal trajectories and their corresponding control law.

In [46], the authors proposed to solve the dual of the LMI moment problem which is the LMI sum-of-squares (SOS) formulation, that can be interpreted as the search of a smooth sub-solution of the Hamilton-Jacobi-Bellman (HJB) equation. However, this method is computationally expensive, since one needs to impose bounds on the discretization grid in order to avoid numerical instability. Furthermore, in [47], a polynomial densities based

method was presented in order to approximate occupation measures. In this method, one has to consider only a part of the approximated moments, which leads to a simple linear problem to solve. However, the main inconvenient of this method is that it fails in approximating discontinuous as well as non-smooth functions such as bang bang controls. Furthermore, approximating the state trajectories and the controls with polynomials can lead to inadmissible approximations.

Moreover, in [19], the authors proposed a framework for approximating occupation measures by atomic measures, meaning that they consider only measures supported on a finite number of points. Therefore, they propose to set a time-space grid of Dirac measures, in order to obtain a finite dimensional LP. Thereby, the decision variables are the mass of the Dirac measures (moments of order 0), which enter linearly in the problem. This method provides good admissible approximations and allows to deal with the different possible control structures. Furthermore, the authors proposed in this approach to consider a family of moments, containing only time and one of the states or control variables, in order to solve a lower dimensional linear problem, making thereby the approach more computationally effective.

More recently, the authors of [65] proposed a method based on Christoffel-Darboux kernels in order to approximate functions that are possibly discontinuous. The sequence of Christoffel-Darboux polynomials related to a measure provides an adequate tool to accurately approximate the support of a measure. This method is based on the spectral decomposition of the moment matrix, providing a semi-algebraic approximation, and allows to take into consideration all the moments up to some degree. Furthermore, with this approach, the computation process can be performed in polynomial time.

3.7 Conclusion

We presented in this chapter a brief overview on how to solve optimal control problems using moments relaxations. This theory gathers many other theoretical aspects, the readers interested in further details should refer to the book [53].

An appealing feature of this approach is that, since the optimal control problems are reformulated in terms of moments, this method is suitable for dealing with states and inputs that are characterized by probability distributions, simply by managing the moments of the related probability distribution functions. Furthermore, one can consider uncertain model parameters and initial states that are described by probability distributions, in the control design.

In Part II, we will use this relevant feature in order to propose a framework for designing robust optimal controls, that represent cancer drug injection profiles, using a dynamical model describing the interaction between the cancer and the immune system, with parametric uncertainties.

Part II

Optimal control under uncertainties for cancer drugs scheduling

Chapter 4

Robust optimal control-based design for combined cancer therapies without chemotherapy detrimental effects on immune cells

Control design for biological systems is a very promising research topic. It allows to make profit from the different mathematical tools related to control theory, in order to control biological phenomena in general. For the specific case of control for cancer dynamics, a very rich literature dating back to many decades is available. This topic raised a real interest in the research community, since control provides systematic and generic tools allowing to manage systems and meet particular specifications. We cited in Chapter 2 many works that have been done on optimal control for cancer dynamical systems.

As pointed out in Chapter 2, the different phenomena related to cancer growth are modeled in the literature through different forms such as ODEs. These models involve many parameters that help to describe the interaction between the different organs and compartments of the human body. In the literature of control for cancer dynamics, usually deterministic parameters are considered.

In the medical field, it is commonly known that cancer mechanisms are highly uncertain by nature. Both cancer evolution and the induced treatment effects are patient-dependent. We pointed out in Chapter 2 the importance of taking into account the different uncertainties that are likely to affect the cancer growth phenomenon. Therefore, in this thesis, we are interested in investigating optimal control methods allowing to take into consideration the possible parametric uncertainties.

This chapter addresses the problem of drug injection schedules design for a combined cancer treatment, in the presence of model parametric uncertainties. It is commonly accepted that achieving optimal recovery performances under uncertainties is a complex task. Therefore, we propose to use a recent optimal control approach, based on the moment optimization framework presented in Chapter 3. This method allows to formulate

and solve robust optimal control problems by taking into account uncertain parameters and initial states, modeled as random variables through their probability distributions. Furthermore, we will explain how to derive statistically optimal combined strategies of chemo- and immunotherapy treatments, assuming the knowledge of probability distributions of some uncertain model parameters.

In Section 4.1, we present the dynamical model describing the interactions between the tumor, the immune system and combined therapies. In Section 4.2, we state the problem of solving optimal control problems that involve parametric uncertainties. In Section 4.3, we explain how to reformulate robust optimal control problems into moment optimization problems. Some technical aspects related to the implementation are presented in Section 4.4 and the simulation results of a given case study are presented in Section 4.5. Finally, in Section 4.6, we present a brief summary of this chapter and we discuss the main advantages and limitations of the proposed approach.

4.1 Dynamical model

In this chapter, we will consider the two dimensional model presented in (2.13), which describes the interaction dynamics between the tumor and the immune system. According to [55] the advantage of this model is the fact that it is minimally parameterized, however, it still describes the main aspects of tumor-immune interactions. Furthermore, this model had been intensively used in the literature in order to investigate its equilibriums and propose some optimal control strategies. For instance [59], where the authors investigated the existence and the optimality of singular arcs for this model. Furthermore, [82] proposed a multiple model predictive control scheme to design chemo- and immunotherapy injection schedules.

Moreover, in [83], the authors proposed a robust multiple model predictive control scheme for this model, in order to consider direct drug targeting pharmacokinetic uncertainties as well as system model mismatches. This approach consists in using a bank of models that are linear approximations of the nonlinear process around several operating points, then an adaptive controller switching is performed in order to make the output error converge to 0. Although this method allows to reduce the model mismatches that are due to linearization, it doesn't allow to rigorously consider parametric uncertainties in the design of optimal control.

As pointed out in Chapter 2, a realistic tumor growth should consider a limited carrying capacity for the cancer cells population. Therefore, we consider in this chapter a logistic growth function for the tumor dynamics $f(x_1, x_\infty) = \mu_C x_1 \left(1 - \frac{x_1}{x_\infty}\right)$, which leads to the following polynomial dynamics :

$$\begin{aligned} \dot{x}_1 =& \mu_C x_1 - \frac{\mu_C}{x_\infty} {x_1}^2 - \gamma_X x_1 x_2 - \kappa_X x_1 u_1, \\ \dot{x}_2 =& \mu_I \left(x_1 - \beta_Y {x_1}^2\right) x_2 - \delta_Y x_2 + \kappa_Y x_2 u_2 + \alpha_Y, \end{aligned} \tag{4.1}$$

where x_1 and x_2 denote, respectively, the number of tumor cells and the density of effector immune cells (ECs), u_1 and u_2 are respectively, the delivery profiles of a cytotoxic agent and an immunostimulator. Table 4.1 recalls the definitions of the model parameters and their numerical values.

Table 4.1: Numerical values and definitions of the parameters used in model (4.1) and taken from[32].

Parameter	Definition	Numerical value
μ_C	tumor growth rate	$0.5599 \cdot 10^7$ cells/day
μ_I	tumor stimulated proliferation rate	0.00484 day^{-1}
α_Y	rate of immune cells influx	0.1181 day^{-1}
β_Y	inverse threshold	0.00264
γ_X	interaction rate	$1 \cdot 10^7$ cells/day
δ_Y	death rate	0.37451 day^{-1}
κ_X	chemotherapeutic killing parameter	$1 \cdot 10^7$ cells/day
κ_Y	immunotherapy injection parameter	$1 \cdot 10^7$ cells/day
x_∞	fixed carrying capacity	$780 \cdot 10^6$ cells

As explained in Chapter 2, the model (4.1) has two locally asymptotically stable equilibrium points. The macroscopic malignant equilibrium is $(x_m, y_m) \simeq (735.9, 0.032)$ and the benign one is $(x_b, y_b) \simeq (34.98, 0.53)$. The objective of cancer treatment can be formulated as to drive the state initial conditions from the region of attraction of the malignant equilibrium to the region of attraction of the benign equilibrium. It is important to notice that the treatment performance depends highly on the initial conditions, since there is a coexistence of multiple equilibriums (benign and malignant). These initial conditions can be approximated beforehand with some degree of precision.

4.2 Robust optimal control for cancer treatments

Let's consider the following continuous-time dynamical system:

$$\dot{x}(t) = F\left(x(t), u(t), p\right), \; x(0) = x_0, \tag{4.2}$$

where $x(t) \in \mathbb{R}^n$ and $u(t) \in \mathbb{R}^m$ denote respectively the state and the input vectors and $p \in \mathbb{P} \subset \mathbb{R}_+^{n_p}$ stands for a vector whose elements can represent some unknown parameters in the model.

In order to use the moment optimization framework presented in Chapter 3, we consider that F is polynomial. Note that in the case where system (4.2) is uncontrolled (*i.e.*

$u = 0$), for every pair of values of the initial state $x(0) = x_0$ and the vector p, system (4.2) admits a unique solution that we denote $x(t|x_0, p)$ for all $t \in \mathbb{R}_+$. Thus, considering x_0 and p as uncertain variables described by probability distributions means that the state is interpreted as a flow of trajectories generated by the distributions of x_0 and p.

In standard optimal control problems (OCPs), we consider nominal parameters values that we denotes p_{nom}. These nominal values are the most representative for the model parameters. In this case, the aim is to design a control function $u(\cdot)$ that minimizes an objective function, which is in general a combination of a stage integral cost L and a final cost Φ, under some constraints. The OCP can be formulated as follows:

$$\begin{aligned} \min_{u(\cdot)} \quad & \int_0^T L(x(t), u(t))\, dt + \Phi\left(x(T)\right) \\ \text{s.t.} \quad & \dot{x}(t) = F\left(x(t), u(t), p_{nom}\right), \\ & x(t) \in X,\ u(t) \in U,\ t \in [0, T], \\ & x(T) \in X_T, x(0) \in X_0, \end{aligned} \tag{4.3}$$

with $X_0, X, X_T \subset \mathbb{R}^n$ and $U \subset \mathbb{R}^m$.

As pointed out in Chapter 2, in the context of cancer treatment, the cost function to be minimized can include the tumor burden and the amount of injected drugs for example. Whereas the constraints can represent health constraints that consist in keeping the body immunity above a certain level, or prevent drug toxicity consequences.

Cancer dynamics are known to be highly uncertain, therefore it is important to consider the different uncertainties that can affect this kind of systems. In this chapter, we investigate an optimal control approach that allows to explicitly consider uncertainties on parameters and initial states.

In the case where uncertainties are considered, the cost to be minimized depends on the uncertain initial state and parameters vector, since both p and x_0 affect the behavior of the state trajectory $x(t)$. Therefore, solving an OCP in the context of uncertainties, aims at obtaining $u(\cdot)$ which minimizes some statistics of a given cost function $J(x_0, u(\cdot), p)$ that we denote $\Psi(u)$.

In stochastic nonlinear MPC literature, Ψ is usually the expectation of the cost J with respect to the time invariant uncertainties p, denoted $\Psi(x_0, u) = \mathbf{E}_p\left[J(x_0, u, p)\right]$, where x_0 is a fixed initial condition, see [68]. It can also be considered as a function of the moments of J, as in [13] where the authors included the variance in the objective statistics Ψ.

We will see in the sequel that using the moment approach allows to solve optimal control problems that explicitly involve uncertainties in the parameters and initial states. According to [46], when the initial state is uncertain and modeled via a probability distribution, the cost to be minimized in the moment optimization framework, is the average

of the defined cost with respect to the distribution of the uncertain initial states. In the next section, we will explain how one can explicitly include the parametric uncertainties, such that the cost to be minimized is the expectation with respect to the uncertainties on both the initial state and model parameters.

Therefore, the robust optimal control problem that we seek to solve can be formulated as follows:

$$\begin{aligned} \min_{u(\cdot)} \quad & \Psi(u) = \mathbf{E}_{x_0,p}\left[J(x_0,u,p)\right] \\ \text{s.t.} \quad & \dot{x}(t) = F(x(t),u(t),p), \\ & x(t) \in X,\ u(t) \in U,\ t \in [0,T], \\ & x(T) \in X_T, x(0) \sim \mathcal{P}_{X_0}, p \sim \mathcal{P}, \end{aligned} \tag{4.4}$$

where x_0 and p are uncertain variables following the probability distributions $\mathcal{P}_{X_0}$ and $\mathcal{P}$, supported on X_0 and $\mathbb{P}$ respectively. Furthermore, $\mathbf{E}_{x_0,p}$ stands for the expectation with respect to the uncertain initial states and model parameters. As explained previously, since x_0 and p are uncertain, the state at time t is also interpreted as a random variable, that we denote, with a slight abuse of notation, simply by $x(t)$.

Our main objective in this chapter is to solve optimal control problems involving uncertainties, in order to design drug injection schedules for cancer. Therefore, in the next section, we will explain how to use the moment optimization framework to reach this objective. Furthermore, we will explain the different technical aspects related to implementation. Finally, we will highlight the importance of considering uncertainties in optimal control design for cancer dynamics through a case study.

4.3 Optimal control under uncertainties via moment optimization framework

In this section we will explain how to use the moment optimization framework, in order to solve optimal control problems that involve parametric uncertainties. As explained in Chapter 3, the interesting feature of this approach is that all the variables that are involved in the OCP are described by probability measures. The polynomial optimization method based on measures is particularly suitable for dealing with uncertain systems, by simply imposing the moments of the related probability density functions.

In the particular case under study, we aim at designing a robust optimal control for a dynamical model describing the tumor growth, the parameters of which are supposed to be not perfectly known. This lack of knowledge can be modeled through uncertain parameters characterized by probability distributions, with compact support. Then, in practice, it is sufficient to define an extended state containing both tumor and immune cell populations and the uncertain parameters.

In order to set problem (4.4) in the framework of Chapter 3, we propose to consider

the time invariant uncertainties vector p as a state variable similarly to [85].

$$\begin{cases} \dot{x}(t) &= F\left(x(t), u(t), p\right), \\ \dot{p}(t) &= 0. \end{cases}$$

Therefore, we consider the following state extension $x_e = (x, p)^T$ which results in the following compact form:

$$\dot{x}_e(t) = G\left(x_e(t), u(t)\right). \tag{4.5}$$

The optimal control problem to be solved is the following:

$$\begin{aligned} \min_{u(\cdot)} \quad & \mathbf{E}_{x_e(0)}\left[\int_0^T L(x_e(t), u(t))\, dt + \Phi\left(x_e(T)\right)\right] \\ \text{s.t.} \quad & \dot{x}_e(t) = G\left(x_e(t), u(t)\right), \\ & x_e(t) \in X^e,\ u(t) \in U,\ t \in [0, T], \\ & x_e(T) \in X_T^e, x_e(0) \sim \sigma_0\left(X_0^e\right), \end{aligned}$$

where $x_e(0) \sim \sigma_0\left(X_0^e\right)$ means that $x_e(0)$ follows the probability distribution σ_0 supported on X_0^e.

Similarly to Chapter 3, we assume that L,Φ and G are polynomials and that U,X^e,X_0^e and X_T^e are compact basic semi-algebraic sets.

We denote by σ_0, the probability measure of the initial state $x_e(0) = x_0^e$ which includes the distribution of the time invariant uncertainties vector p. Thus, the initial imposed measure is written $\bar{\mu}_0(dt, dx_e) = \delta_0(dt)\bar{\sigma}_0(dx_e)$, where the notation $\bar{\mu}_0$ highlights the fact that μ_0 is defined by its truncated sequence of moments, and δ_0 allows to impose the initial time to be equal to 0.

Let's denote by $\bar{\mathbf{w}}_0^{(\leq a)}$ the truncated sequence of moments (up to degree a) corresponding to the initial measure $\bar{\mu}_0(dt, dx_e) = \delta_0(dt)\bar{\sigma}_0(dx_e)$ of the extended state. Following the steps explained in Chapter 3, we can derive the finite-dimensional problem on moments as follows:

$$\begin{aligned} \min_{\mathbf{z}, \mathbf{z}_T} \quad & c_L'\, \mathbf{z}^{(\leq b)} + c_\Phi'\, \mathbf{z}_T^{(\leq a)} \\ \text{s.t.} \quad & A_T \mathbf{z}_T^{(\leq a)} = A_0 \mathbf{z}_0^{(\leq a)} + A\mathbf{z}^{(\leq b)}, \\ & \mathbf{z}_0^{(\leq a)} = \bar{\mathbf{w}}_0^{(\leq a)}, \\ & M\left(\mathbf{z}_T^{(\leq a)}\right) \succeq 0, L_{h_{T_i}}\left(\mathbf{z}_T^{(\leq a)}\right) \succeq 0, \forall i = 1, ..., n_{X_T^e}, \\ & M\left(\mathbf{z}^{(\leq b)}\right) \succeq 0,\ L_{h_i}\left(\mathbf{z}^{(\leq b)}\right) \succeq 0\ ,\ \forall i = 1, ..., n_{X^e}, \end{aligned} \tag{4.6}$$

where the minimum is calculated with respect to the moment vectors corresponding to the trajectory and the terminal occupation measures (μ and μ_T). Analogously to (3.7), $n_{X_T^e}$ and n_{X^e} stand for the number of polynomials h_{T_i} and h_i defining X_T^e and X^e respectively. Furthermore a and b are the analogous of d_1 and d_2 in (3.13). The constraint $\mathbf{z}_0^{(\leq a)} = \bar{\mathbf{w}}_0^{(\leq a)}$ enforces the initial occupation measure to describe a given probability distribution on the

initial extended state (including the probability density of p). This means that there is no restriction on the type of the imposed initial probability distribution, as long as one can compute the desired sequence of moments on a compact semi-algebraic set.

Remark 4.1 $\mathbf{z}$ *is the vector of moments corresponding to the average controlled occupation measure.*

After solving the relaxations defined over (4.6), we expect $\mathbf{z}_T$ to contain approximations of the moments corresponding to the terminal occupation measure. Therefore, $\mathbf{z}_T$ characterizes the probability distribution supported on the final state set. Furthermore, $\mathbf{z}$ contains approximations of the moments corresponding to the average controlled occupation measure, that involve time as well as state and control variables. One can use these moments in order to reconstruct the different variables through the different approaches explained in Chapter 3.

4.3.1 Solving moments problems

In the previous section, we showed that the problem of optimal control under uncertainties on initial states as well as model parameters, can be addressed using the moment optimization framework. Thereby, one can derive finite-dimensional moment problems corresponding to problem (4.4), where the cost function is a linear combination of moments corresponding to the defined occupation measures, subject to, linear equality constraints on moments resulting from the system dynamics, semi-definite constraints (on the moment and the localizing matrices) to guarantee that a sequence of moments has a representing nonnegative measure on a compact support, and equality moments constraints which impose the probability distribution on a compact support of the initial extended state.

The SDP relaxations defined on problems (4.6) can be solved with Gloptipoly [45], using SeDuMi [86] or MOSEK [71] as SDP solvers.

4.4 Technical aspects

It is worth recalling that in order to properly link moments to measures, one need to satisfy the additional condition on the definition of the different measures support sets, presented in Assumption 3.1 in Chapter 3. These additional constraints need to be implemented in the constraints of the robust OCP presented in (4.4).

Furthermore, since we are working with polynomials that might have relatively high degrees depending on the relaxation order, we need to scale the different variables involved in the optimal control problems, such as time and state variables, in order to avoid numerical instability.

Since solving moment problems such as (4.6) provides approximations of the moments corresponding to occupation measures, an interesting question that could be asked is: can we have a certificate of convergence to the global optima? Indeed, there exists a certificate of convergence that is based on the rank of the moment matrices up to some degrees, see [53] for more details. This certificate is provided by Gloptipoly [45] after computing the moments approximations. Although for complex problems such as optimal control ones, the rank conditions are often not fulfilled and the only guarantee that one can have is that the obtained cost is a lower bound of the optimal one, we still can have approximations of the moments corresponding to the different occupation measures that can help us to reconstruct the different trajectories. Although these control functions are approximations and not the optimal ones, in the context of control for cancer dynamics, the moment optimization approach allows to have an idea of the control structure, what drugs are preferable to be injected first and at what frequency etc.

Note that this approach is applicable for low dimensional systems having at most six variables (states and controls) [43]. Furthermore, we will see in the sequel that this methodology requires a considerable computational time depending on the relaxation degree, since solving SDP problems in high dimension is numerically expensive.

4.5 Case study and numerical simulations

In this section, we present a case study where we propose to solve nominal and robust optimal control problems for system (4.1). As explained previously, the nominal OCP considers nominal values for the model parameters, whose values are the expectations of the model parameters. Whereas for the robust OCP, some parameters are considered to be uncertain and are defined through probability distributions.

For the nominal OCP, we will present numerical simulations for different cost functions, in order to show how one needs to set the cost function parameters, in order to have the desired state trajectories behavior. Furthermore, we will present numerical simulations for the robust case and highlight the importance of taking into account the parametric uncertainties in optimal control problems. This will lead us to a comparison between the nominal and robust profiles in terms of control robustness to uncertainties.

Moreover, we will provide an idea on the number of moments involved, as well as the required computational time to solve optimal control problems via moment optimization. We will also show how this time evolves with respect to the relaxation order.

4.5.1 Nominal optimal control problem

Similarly to [32] and [82], we assume that the initial state of the system dynamics (4.1) is $(x_1(0), x_2(0)) = (600, 0.1)$, we also consider that the maximum drug dose is 1 for both chemotherapy and immunotherapy. Furthermore, we add constraints on the immune cells

density and the number of tumor cells in order to ensure the compactness of the state set X. Another constraint on the final tumor size is imposed in order to drive the tumor to the benign region. The nominal (*i.e.* considering nominal values of model parameters) optimal control problem that we propose to solve for $t \in [0, 60]$ is the following:

$$\begin{aligned}
\min_{u_1(\cdot),u_2(\cdot)} \quad & J(x_1(\cdot), x_2(\cdot), u_1(\cdot), u_2(\cdot)) \\
\text{s.t.} \quad & \dot{x}_1 = \mu_C x_1 \left(1 - \frac{x_1}{x_\infty}\right) - \gamma x_1 x_2 - \kappa_X x_1 u_1, \\
& \dot{x}_2 = \mu_I \left(x_1 - \beta {x_1}^2\right) x_2 - \delta x_2 + \alpha + \kappa_Y x_2 u_2, \\
& x_1(0) = 600, x_2(0) = 0.1, \\
& x_1(60) \leq 100, \\
& 0 \leq u_1 \leq 1 \ , \ 0 \leq u_2 \leq 1, \\
& 0 \leq x_1 \leq 780 \ , \ 0 \leq x_2 \leq 5, \\
& t \in [0, 60].
\end{aligned} \tag{4.7}$$

The cost J is chosen according to the objectives that one seeks to achieve. It can contain many terms such as final states, integrals of state trajectories and control inputs, with different penalties in order to achieve a trade-off between the different control objectives. Problem (4.7) can be reformulated in the framework of moment optimization via GloptiPoly [45], as explained in Chapter 3, and can be solved using YALMIP [62] and the semidefinite programming solver MOSEK [71].

Note that in this chapter we consider that the minimal allowed density of immune cells is 0, in order to solve a problem that is similar to what we find in the literature. In Chapter 5, we will further investigate this problem by adding a constraint on the minimal density of immune cells, in order to see its effects on the derived control profiles.

The control inputs are approximated, based on the knowledge of their moments, using Christoffel-Darboux kernel briefly described in Chapter 3, see [65] for more details. Although it is not mentioned in problem (4.7), for practical reasons previously explained, time and states trajectories are scaled to $[0, 1]$ in the implementation, therefore, the control inputs presented in this chapter are computed for scaled dynamics.

Let's consider for instance the minimization of the following cost

$$J_1 = x_1(60). \tag{4.8}$$

Figure 4.1 shows the approximations of the control inputs that we obtained after solving the reformulated problem corresponding to (4.7) with $J = J_1$. The evolution of state trajectories with these controls is presented in Figure 4.2, we can see that the tumor burden decreases slowly to reach the final value that lies in the benign region.

Now, if we want the tumor size to decrease faster, we can minimize the following cost:

$$J_2 = \int_0^{60} x_1(t)dt. \tag{4.9}$$

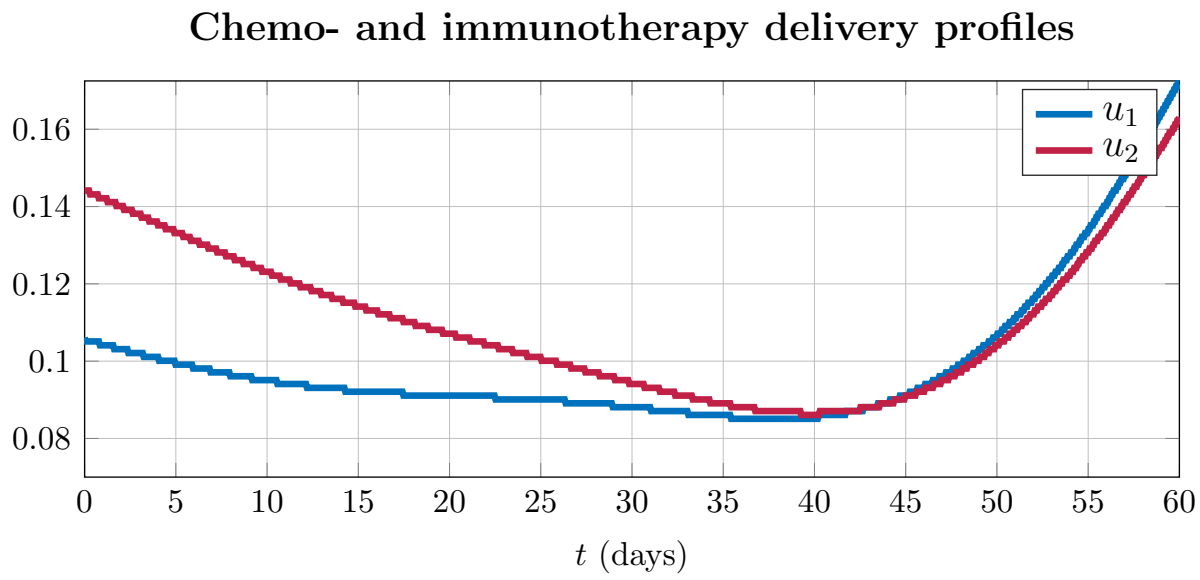

Figure 4.1: Open-loop control input profiles for chemotherapy (u_1) and immunotherapy (u_2), for J_1.

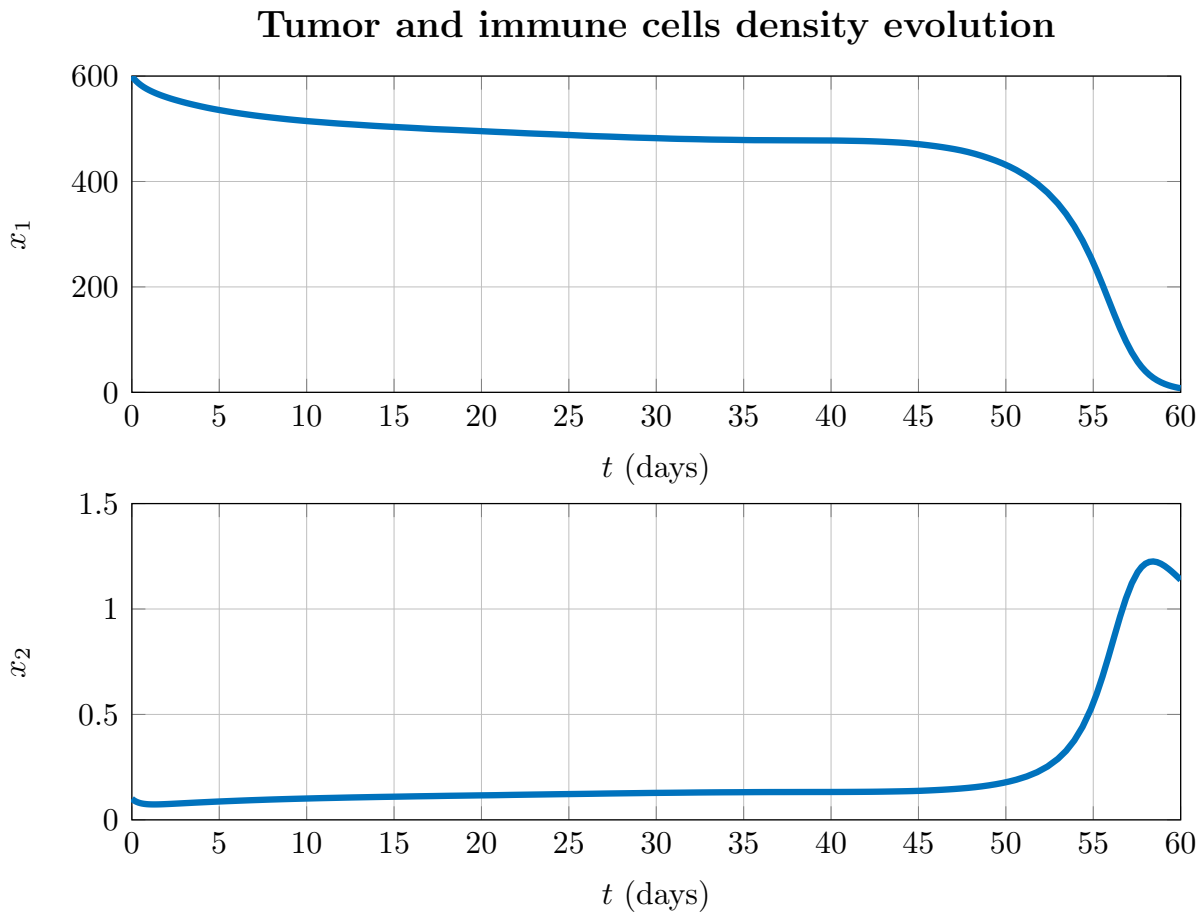

Figure 4.2: States trajectories for J_1.

The approximated control inputs are presented in Figure 4.3, we can notice that the chemotherapy profile is aggressive and persistent, this is due to the choice of the cost

which considers only the minimization of the integral of $x_1(t)$. Such controls might not be allowed practically because of the high toxicity of the cytotoxic agent.

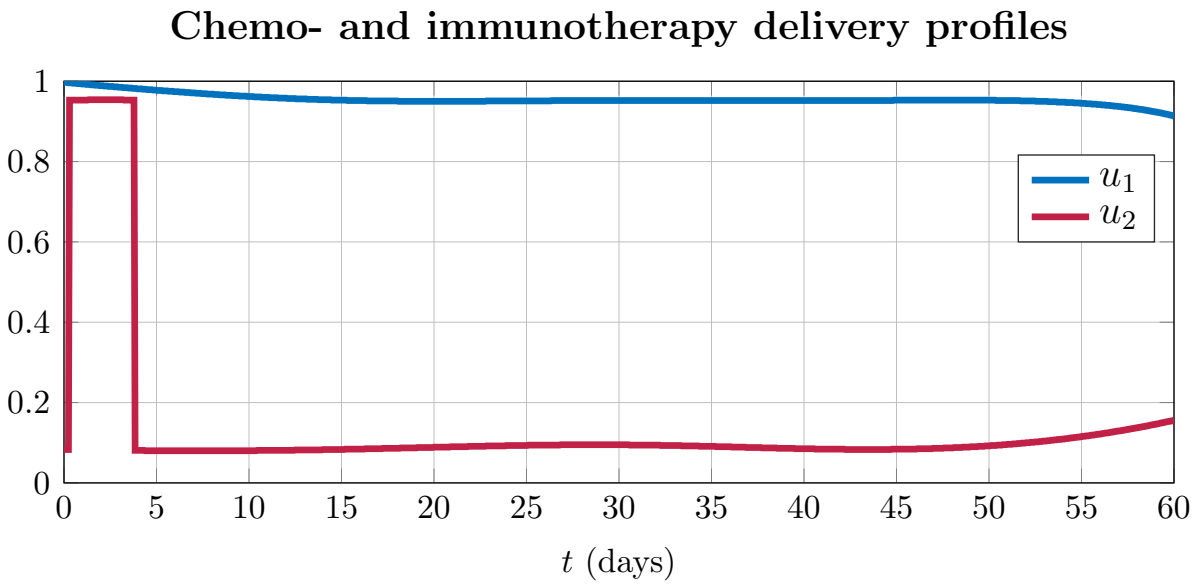

Figure 4.3: Open-loop control input profiles for chemotherapy (u_1) and immunotherapy (u_2), for J_2.

Figure 4.4 shows that the state corresponding to the tumor cells, x_1, goes to 0 faster than in Figure 4.2. Furthermore, we can see that the immune cells density goes up rapidly to reach relatively high values.

Since chemotherapy has damaging side effects on the human body, it is common to frame an optimal control problem so that the total amount of drugs is penalized [25]. It is also important to penalize the use of immunotherapy since the available amount is limited, and for some treatment types, immunotherapy can even be toxic [70]. Furthermore, it is important to look at the evolution of the immune system, because the immune-weakening has damaging effects on the human body. Thereby, one can easily notice that the choice of the cost J, to be minimized, is very important in order to meet the control objectives.

Now, we propose to minimize the following cost:

$$J_3 = x_1(60) + 0.4\int_0^{60} x_1(t)dt + 0.01\int_0^{60} u_1(t)dt + 0.01\int_0^{60} u_2(t)dt. \tag{4.10}$$

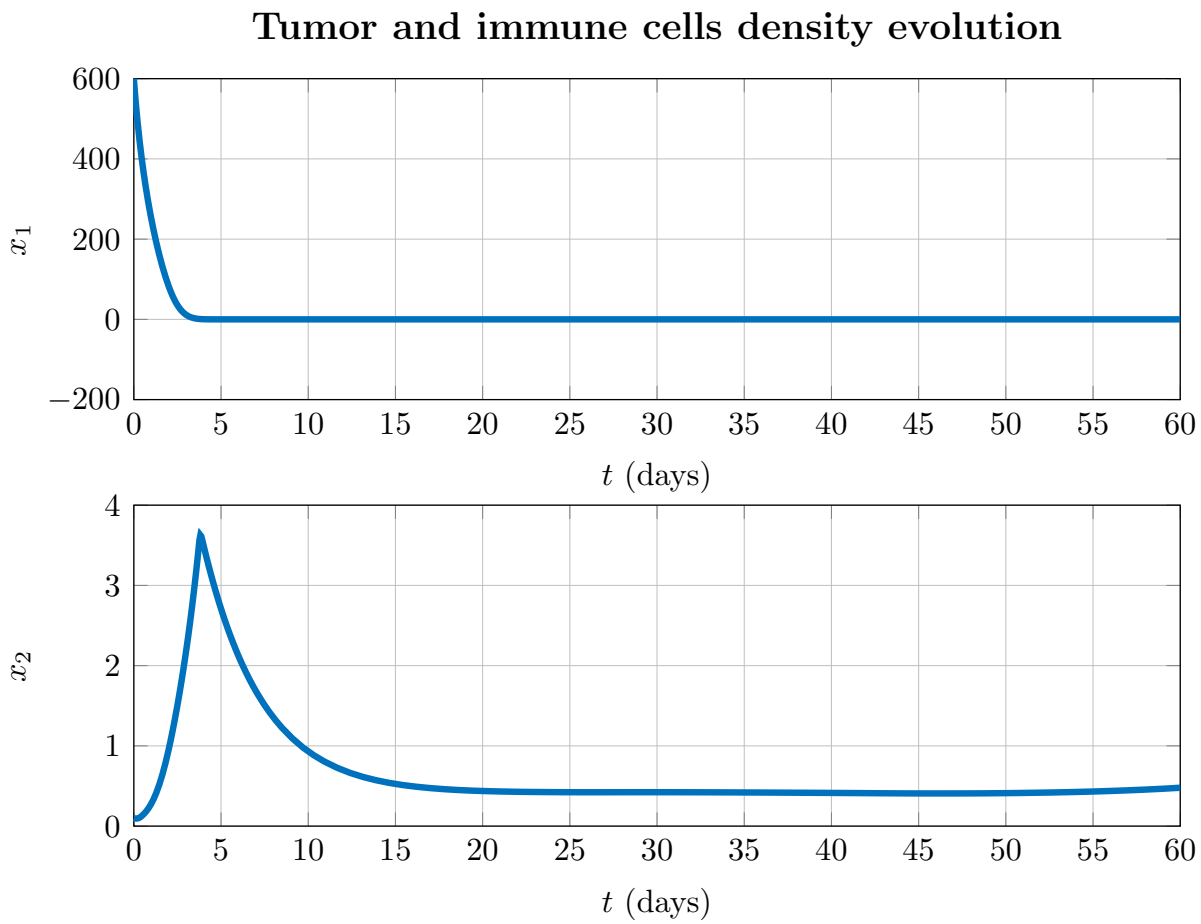

Figure 4.4: States trajectories for J_2.

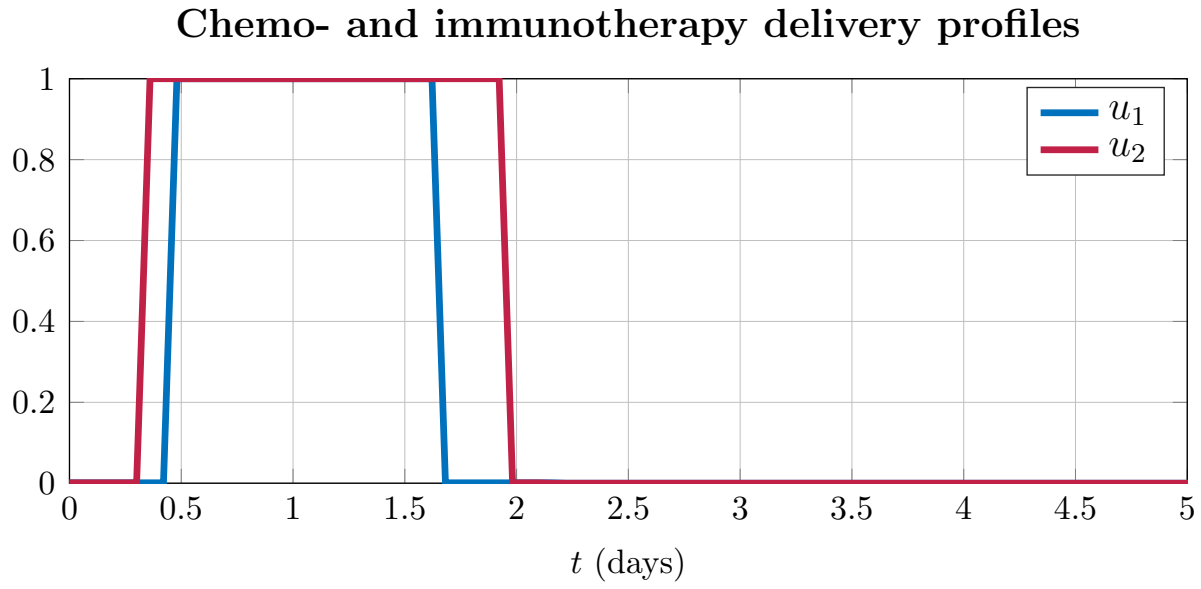

Figure 4.5: Open-loop control input profiles for chemotherapy (u_1) and immunotherapy (u_2), for J_3.

As we can see in Figure 4.5, penalizing the control inputs integrals allows to reduce considerably the injected drugs amounts. In Figure 4.5, we show the graphs in the time interval $[0, 5]$ to emphasize the differences between the two profiles, since for $t \in [5, 60]$, $u_1(t) = 0$ and $u_2(t) = 0$.

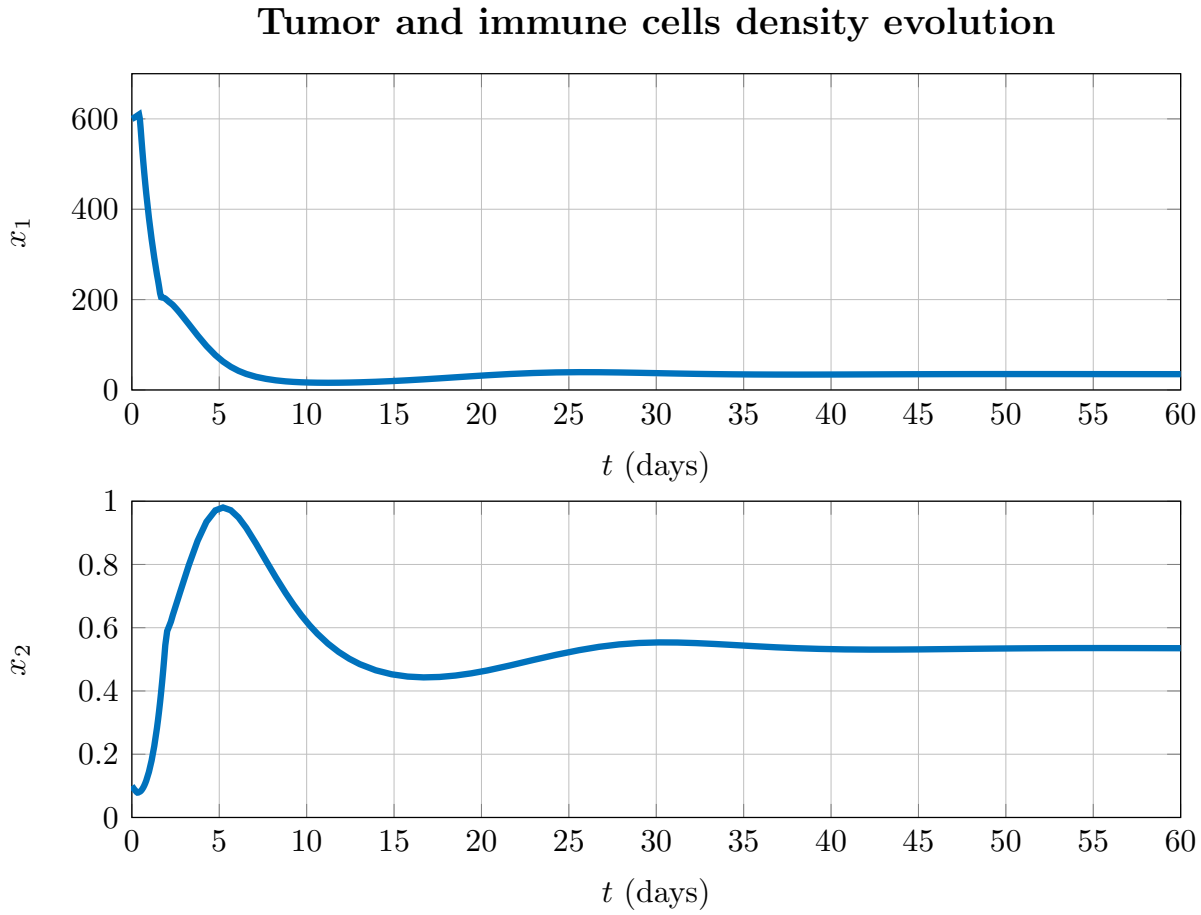

Figure 4.6: States trajectories for J_3.

Figure 4.6 shows that the states converge to the benign equilibrium at around 30 days. Therefore, the control profiles approximated by minimizing J_3 allow to satisfy the standard control objectives, since they drive the states to the benign equilibrium (x_b, y_b). Furthermore, we can notice that these drug injection profiles minimize rapidly the tumor while maintaining a relatively strong immune system.

Table 4.2 presents the evolution of the number of moments involved in the moment problem corresponding to (4.7), as well as the evolution of the required computational time with respect to the relaxation order r. We can notice that both the number of moments and the computational time increase considerably when the relaxation order increases. Furthermore, we can see in Table 4.2 that the cost is the same for the three values of r, therefore we chose to stop the relaxation order at 8 in order to have a low computational time. Figure 4.7 gives an idea about the computational complexity of the nominal optimal control problems using moments, with respect to the relaxation order.

Table 4.2: Number of moments and the required computation time with respect to the relaxation order r for the nominal OCP, the simulations have been performed on a hp EliteBook 2.60GHz Intel Core i7.

Relaxation order r	8	10	12
Number of moments	3333	6760	12538
Average computational time	0.67mn	5.16mn	42.03mn
Cost	$-5.89 \cdot 10^{-3}$	$-5.89 \cdot 10^{-3}$	$-5.89 \cdot 10^{-3}$

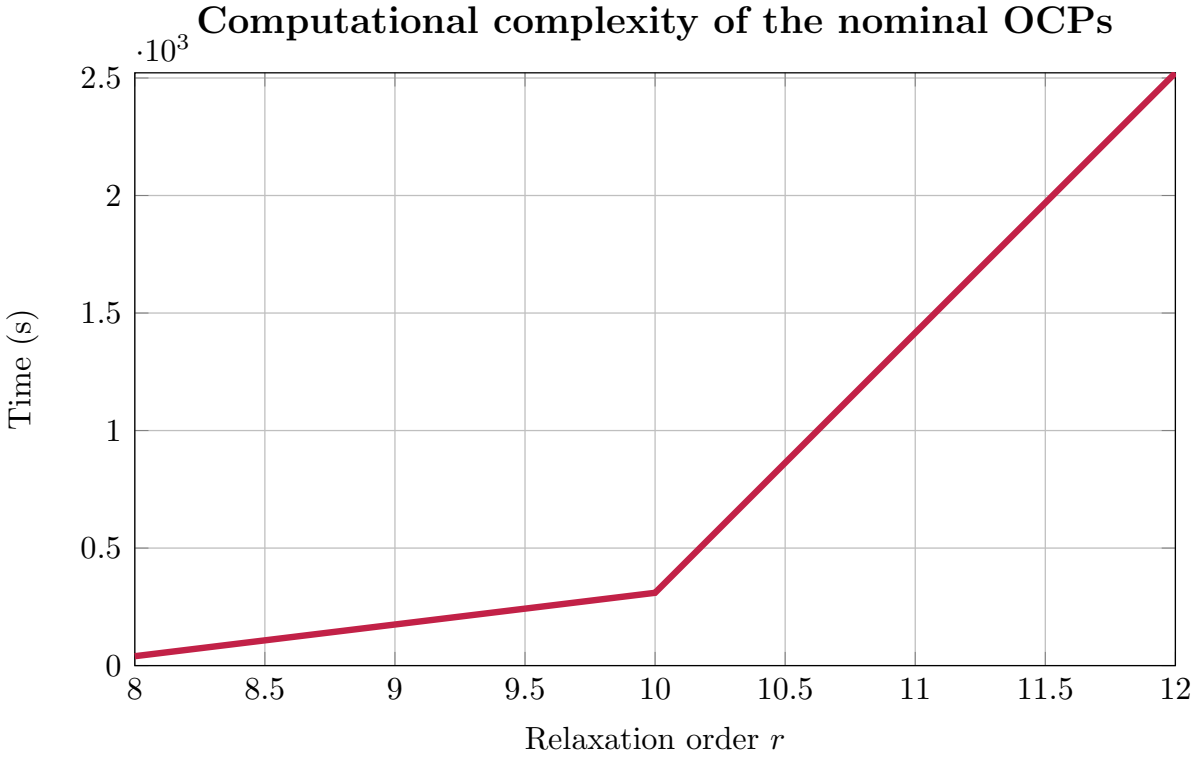

Figure 4.7: Computational complexity of the nominal OCPs for $J = J_3$.

Although the controls in Figure 4.5 satisfy standard objectives in the context of nominal optimal control, we will show that when the dynamics are subject to parameters uncertainties, these controls will not meet the goals set in the optimal control problem.

4.5.1.1 Robustness analysis for the nominal profiles

Let's assume that the tumor growth rate μ_C and the natural influx of immune cells α are uncertain and described by the following distributions: $\mu_C \sim \mathcal{N}(0.5599, 0.1)$ truncated in $[0, 1.1198]$ and $\alpha \sim \mathcal{N}(0.1181, 0.05)$ truncated in $[0, 0.2362]$. The expectations of these distributions are the parameters values presented in Table 4.1. The truncation interval upper bound is the double of the expectation in order to keep the interval symmetric with

respect to the parameters mean value.

Remark 4.2 *The considered distributions are not based on practical knowledge of the system parameters, they are chosen only to illustrate the problem of handling parametric uncertainties. The robust schedules will be designed considering truncated distributions in order to satisfy compactness and positivity conditions.*

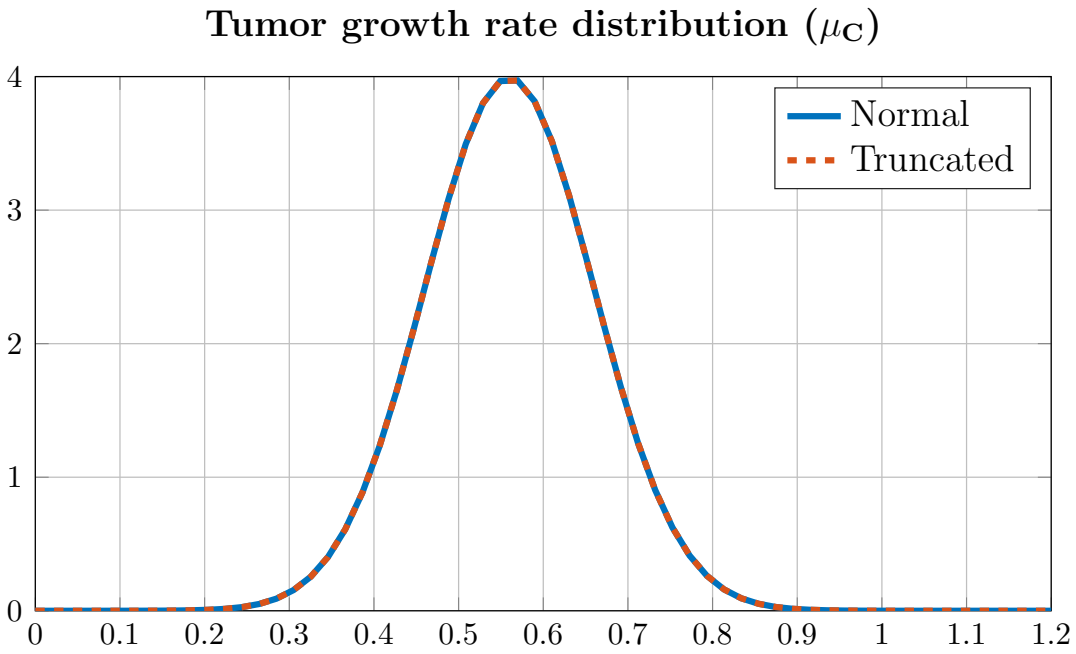

Figure 4.8: Distribution of μ_C.

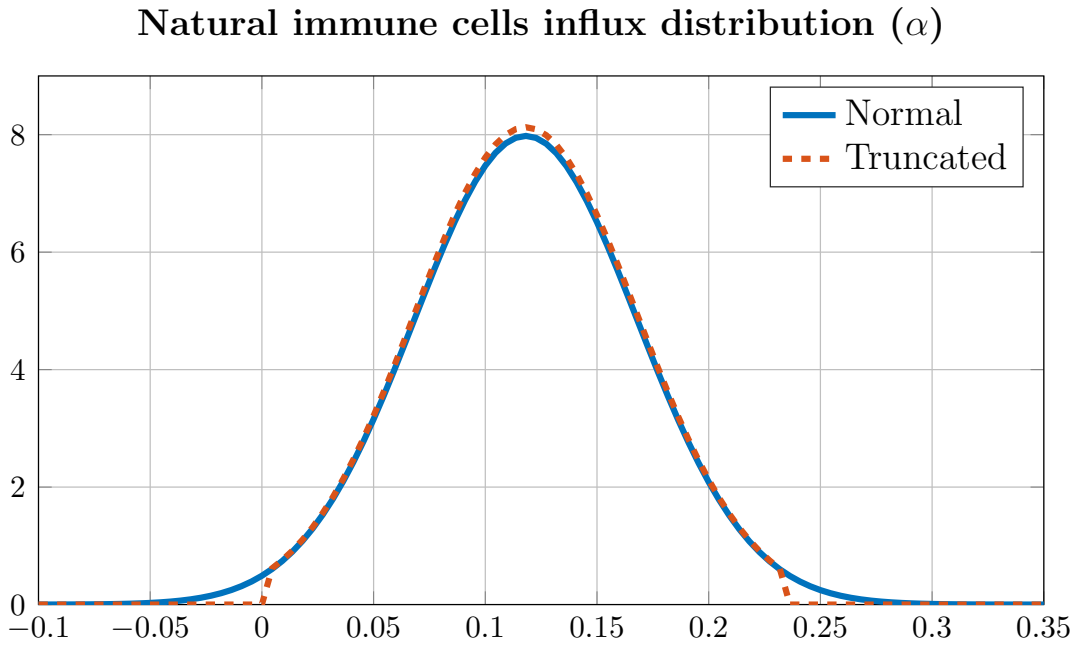

Figure 4.9: Distribution of α.

Remark 4.3 *Note that the lower bounds of the truncation intervals for the distributions of μ_C and α are chosen to be 0 in order to consider small parameters values. Furthermore, for the tumor growth rate μ_C, we can see in Figure 4.8 that due to the choice of the distribution, the probability to have $\mu_C = 0$ is almost 0. Moreover, for the natural influx of immune cells α, we can see in Figure 4.9 that the probability to have $\alpha = 0$ (meaning that there is no natural influx of immune cells) is very low.*

Figure 4.10 presents 100 Monte-Carlo simulations, using the nominal drug profiles, with random values of μ_C and α (the random selection is carried out according to their corresponding probability distributions). It shows that there is a probability of 19% for the states to converge to the malignant equilibrium (x_m, y_m) (*i.e.* leading to patients death). Therefore, it is crucial to consider the potential uncertainties on model parameters.

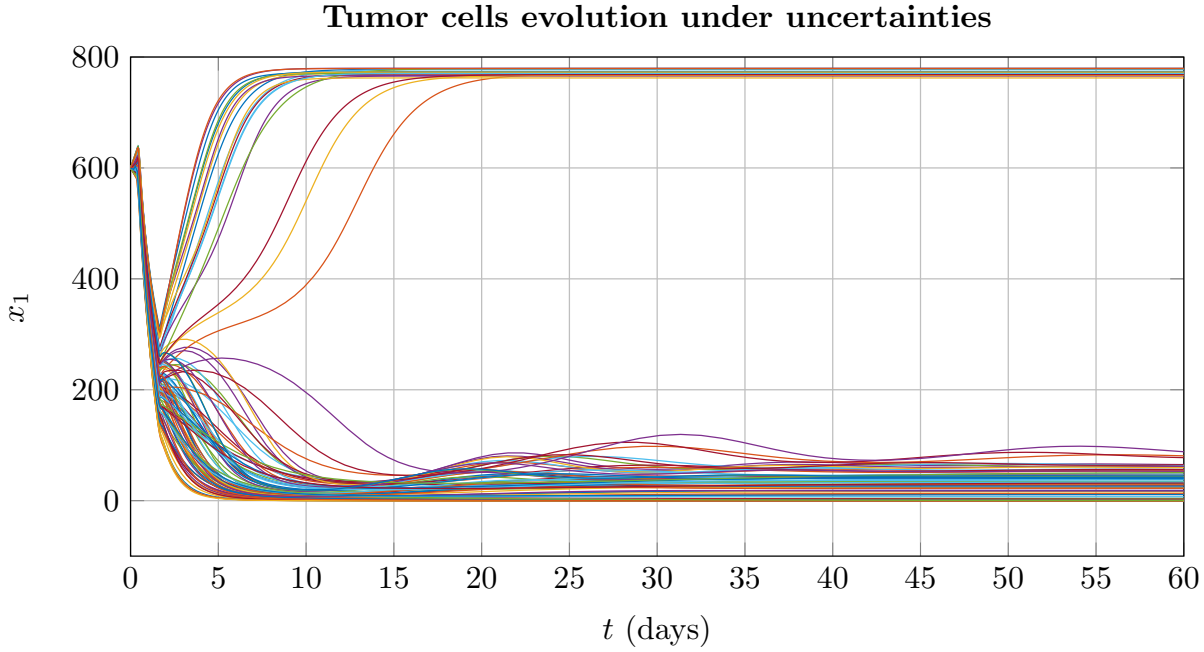

Figure 4.10: Monte-Carlo tests on the nominal schedules.

4.5.2 Robust optimal control problem

Let's consider that the tumor growth rate μ_C and the rate of immune cells influx α are uncertain parameters. As previously, we assume that $\mu_C \sim \mathcal{N}(0.5599, 0.1)$ truncated in $[0, 1.1198]$ and $\alpha \sim \mathcal{N}(0.1181, 0.05)$ truncated in $[0, 0.2362]$.

Let's extend system (4.1) to the following dynamics:

$$\begin{aligned}
\dot{x}_1 &= \mu_C x_1 - \frac{\mu_C}{x_\infty} {x_1}^2 - \gamma_X x_1 x_2 - \kappa_X x_1 u_1, \\
\dot{x}_2 &= \mu_I \left(x_1 - \beta_Y {x_1}^2\right) x_2 - \delta_Y x_2 + \kappa_Y x_2 u_2 + \alpha_Y, \\
\dot{\mu}_C &= 0, \\
\dot{\alpha}_Y &= 0.
\end{aligned} \tag{4.11}$$

The state extension in (4.11) allows to characterize μ_C and α_Y by their probability distributions, and to impose their time invariant characteristic through the dynamics $\dot{\mu_C} = 0$ and $\dot{\alpha_Y} = 0$. Thus, supposing that $\sigma_{\mu_C}(\mu_C)$ and $\sigma_{\alpha_Y}(\alpha_Y)$ denote the probability distributions of parameters μ_C and α_Y, the optimal control problem to be solved should have as initial condition

$$\mu_0\left(t, x_1, x_2, \mu_C, \alpha_Y\right) = \delta_0(t)\, \delta_{x_1(0)}(x_1)\, \delta_{x_2(0)}(x_2)\, \sigma_{\mu_C}(\mu_C)\, \sigma_{\alpha_Y}(\alpha_Y),$$

imposed through moments of the initial measure.

Similarly to problem (4.7), one can reformulate the robust optimal control problem with dynamics (4.11) by including the moments of the parameters distributions.

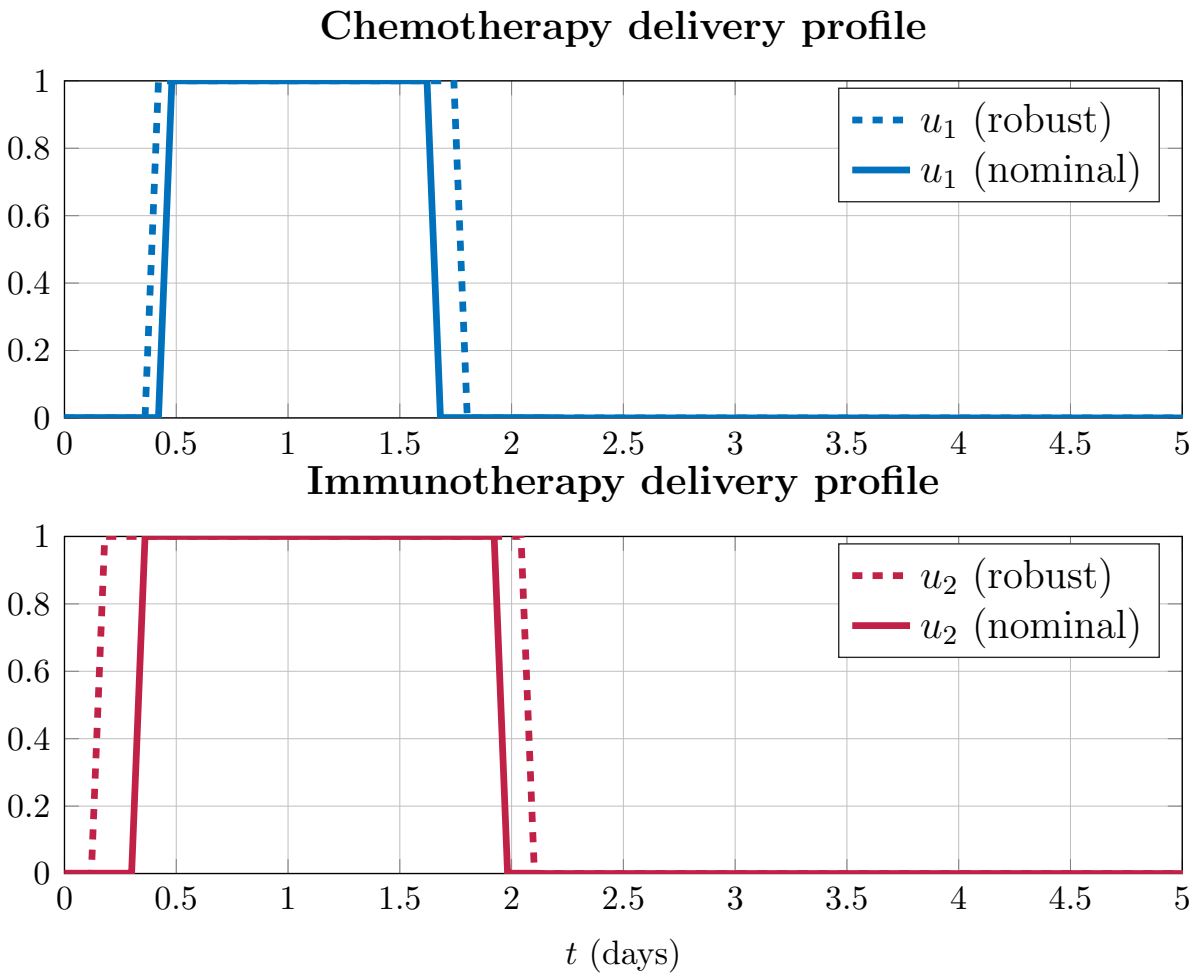

Figure 4.11: Chemo- and immunotherapy schedules (robust and nominal), for J_3.

Figure 4.11 presents a comparison between nominal and robust injection schedules, approximated after minimizing the cost J_3 in the nominal case and $\mathbf{E}_p\left[J_3\right]$ in the robust case (expectation of J_3 with respect to the uncertain parameters), since we have a flow of trajectories generated by the parameters distributions. We can notice that similarly to

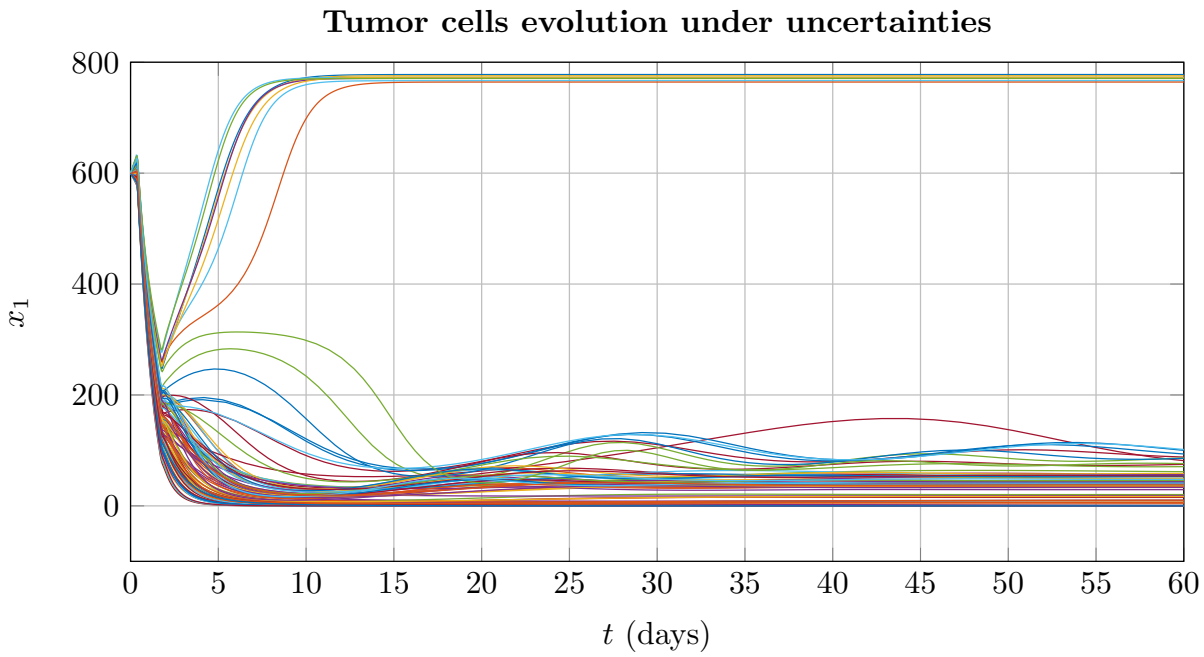

Figure 4.12: Monte-Carlo tests on the robust schedules.

the nominal profiles, the robust ones are also single doses injected at the beginning of the treatment. However, we can see that the robust profiles use more amounts of drugs which highlights the importance of taking into account parametric uncertainties in the optimal control problem.

Figure 4.12 presents 100 Monte-Carlo simulations using the approximated robust injection profiles. We can notice that the probability of convergence to the malignant equilibrium has been reduced from 19%, using the nominal profiles, to 8%, in the case of robust schedules. Note that the moment optimization approach provides solutions allowing to satisfy the imposed constraints. Therefore, if one obtains the optimal control input profiles, no constraint violation should occur and the probability of convergence to the malignant equilibrium should be 0%. However, since the control input profiles are approximated, some constraint violation might occur.

4.5.3 Cost-based performance comparison

Problem (4.7) can be written in a compact form as follows :

$$\begin{aligned} \min_{u_1(\cdot),u_2(\cdot)} \quad & J(x_1(\cdot),x_2(\cdot),u_1(\cdot),u_2(\cdot)) \\ \text{s.t.} \quad & g_C(x_1(\cdot),x_2(\cdot),u_1(\cdot),u_2(\cdot)) \leq 0. \end{aligned} \tag{4.12}$$

In order to effectively compare the performance of nominal and robust schedules, we write the asymptotically equivalent problem of (4.12) as :

$$\min_{u_1(\cdot),u_2(\cdot)} \quad J(x_1,x_2,u_1,u_2) + \rho \max(g_C(x_1,x_2,u_1,u_2),0), \tag{4.13}$$

where $\rho \in \mathbb{R}$ is sufficiently big $\rho = 10^4$.

Using the asymptotic equivalence between (4.12) and (4.13), we computed the costs corresponding to nominal and robust profiles, based on Monte-Carlo simulations that we carried out for both schedules. Table 4.3 and Figure 4.13 show that the mean and variance of the costs corresponding to robust schedules are considerably less than those of the nominal costs. This is mainly due to the excessive number of constraints violations that occur when applying nominal controls.

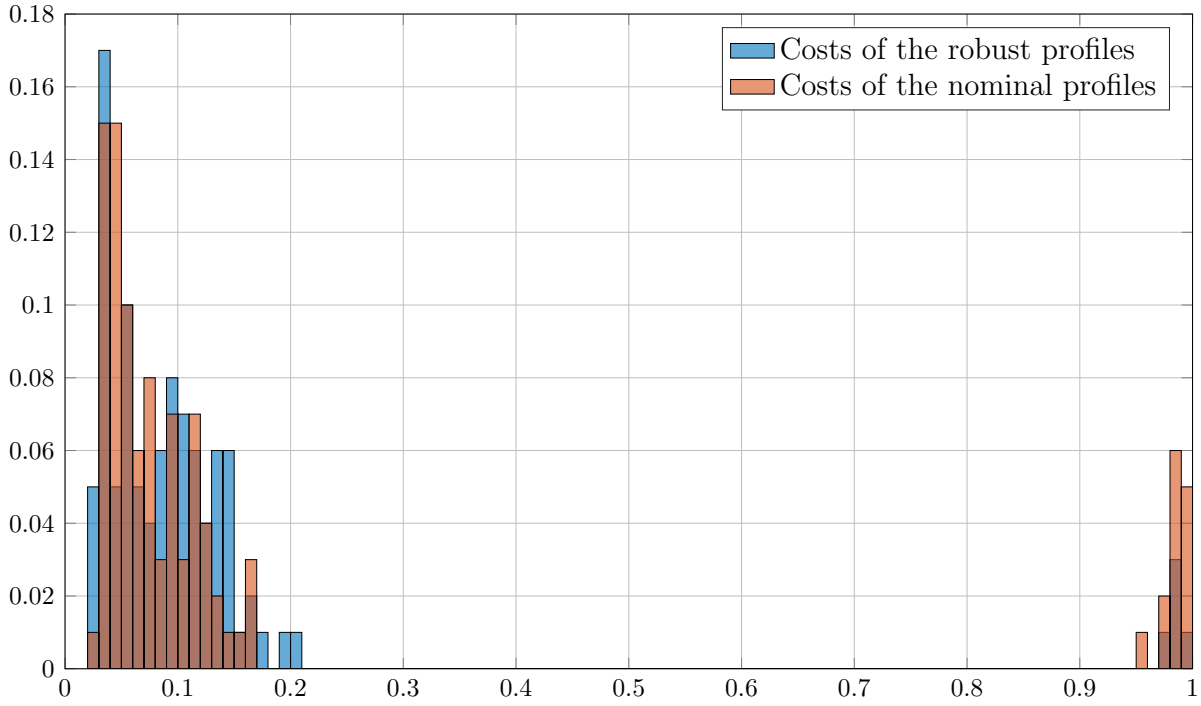

Figure 4.13: Histograms of robust and nominal costs.

Table 4.3: Statistics of the normalized costs (nominal and robust).

	Mean	Variance
Nominal cost	0.20	0.14
Robust cost	0.12	0.07

Table 4.4 presents a comparison between the computational times of the nominal optimal control problem and the robust one. We notice a considerable difference in the computational cost for the same relaxation order, it is mainly due to the increase of the problem dimension, after performing dynamics extension to solve the robust OCP. Increasing the relaxation order r allows to have better approximations of the moments, however, it increases the problem dimension and therefore, the computational time.

Table 4.4: Computation times on hp EliteBook 2.60GHz Intel Core i7.

	Relaxation order r	Average computation time	Number of moments
Nominal OCP	8	0.69mn	3333
Robust OCP	8	62.00mn	22022

4.6 Conclusion and discussion

We presented in this chapter some results on the application of moment optimization theory to schedule cancer treatment. We highlighted the importance of taking into account parametric uncertainties in the optimal control problem. Furthermore, we designed robust and optimal combined chemo- and immunotherapy injection profiles that allow to meet specific objectives.

The moment optimization approach can be very promising for many applications, since it allows to reconstruct optimal injection schedules for a class of nonlinear systems with parametric uncertainties considerations. However, it has some limitations, mainly the restriction on polynomial dynamics and the limited dimension (state and control variables) that can be handled. Although the required computational time is high in the case of solving a robust OCP, in some applications, it remains crucial to guarantee robust performances.

In the next chapter we will explore the consequences of adding a new term in the model that stands for the detrimental effects of chemotherapy on immune cells. Furthermore we will investigate the effects of adding an additional minimal immune cells density constraint on the control profiles and the state trajectories.

Chapter 5

Robust Optimal Scheduling of cancer treatment with considerations on chemotherapy detrimental effects

As pointed out in Chapter 2, the last decades witnessed a real interest in modeling the interaction dynamics between the cancer and the human body in order to better understand and to analyze these phenomena. Since the dynamics of cancer growth are extremely complex, we can find many different models in the literature, depending on the therapies that are used, for example, or the different phenomena that occur in the human body. According to [20], for the specific case of cancer-immune interactions, the mathematical modeling of the entire immune system can be a very complex task, that is one of the reasons for which researchers focus on the elements of the immune system that are known to be significant in controlling the tumor growth.

In this chapter, we further investigate the mathematical model presented in Chapter 4, that describes the interactions between the cancer and the immune system. This model takes into account the detrimental effects of chemotherapy on both cancer and immune cells populations. The problem of cancer treatment scheduling is considered as a robust optimal control problem (ROCP) in the sense that we derive statistically optimal combined strategies of chemo- and immunotherapy treatments, assuming the knowledge of the probability distribution of the chemotherapy killing parameter (effects on the immune population). Furthermore, we add in the ROCP a health constraint on the minimal allowed immune cells density, and we use the moments optimization framework presented in Chapter 3, which allows to explicitly consider uncertainties on model parameters.

In Section 5.1, we present the dynamical model that we use for numerical simulations. In Section 5.2, we present the optimal control problem to be solved with nominal parameters values and we highlight the consequences of adding the new term in the drug profiles. The robust optimal control problem to be solved and its corresponding simulation results are presented in Section 5.3. Finally, in Section 5.4, we summarize the work that we present in this chapter.

5.1 Dynamical model

Similarly to the model illustrated in Chapter 4, we consider in this chapter a modified version of Stepanova's model [84], where we replace the exponential growth term by a logistic one $\left(f(x_1) = \mu_C x_1 \left(1 - \frac{x_1}{x_\infty}\right)\right)$, since the logistic term allows to bound the number of cancer cells by x_∞ which is more realistic.

Unlike the model considered in Chapter 4, we added to model (4.1) the term $-\eta_Y u_1 x_2$ in the dynamics $\dot{x}_2$, which stands for the direct detrimental effects that chemotherapy has on the immune system. This term has been introduced in [32], where the authors proposed a generalized model, based on the Stepanova's model presented in [84]. However, this model has neither been investigated as an optimal control problem nor been considered in numerical simulations.

According to [55], the immune system can be effective in controlling small cancer volumes, but for large volumes, the cancer dynamics overwhelms the immune systems, thus, using a combined therapy is important to achieve patient recovery.

Let's consider the following dynamics :

$$\begin{aligned} \dot{x_1} =& \mu_C x_1 - \frac{\mu_C}{x_\infty} x_1^2 - \gamma_X x_1 x_2 - \kappa_X x_1 u_1, \\ \dot{x_2} =& \mu_I x_1 x_2 - \beta_Y \mu_I x_1^2 x_2 - \delta_Y x_2 + \kappa_Y x_2 u_2 - \eta_Y u_1 x_2 + \alpha_Y, \end{aligned} \tag{5.1}$$

where x_1 and x_2 denote, respectively, the number of tumor cells and the density of effector immune cells (ECs), u_1 and u_2 are, respectively, the delivery profiles of a cytotoxic agent and an immunostimulator. Figure 5.1 presents a scheme describing the different interactions between the tumor and the immune system with the new parameter η_Y.

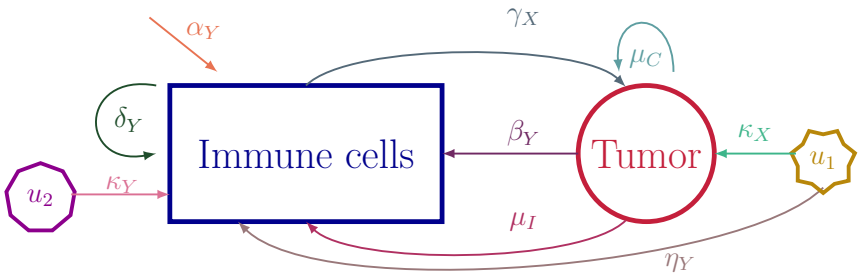

Figure 5.1: A scheme showing the interactions in model (5.1), between the tumor and the immune system, in particular, note the parameter η_Y that is introduced in this chapter yielding a model that differs from the one used before in Chapter 4.

As shown in Figure 5.2, the uncontrolled model (5.1) has two locally asymptotically stable equilibriums. The macroscopic malignant equilibrium is $(x_m, y_m) = (735.9, 0.032)$ and the benign one is $(x_b, y_b) \simeq (34.98, 0.53)$, they are the same as in Chapter 4 since the

new term does not affect the model equilibriums. The trajectory in black represents the evolution of uncontrolled states starting from the initial condition $x_0 = (500, 0.5)$. In this chapter, we are interested in driving the initial condition $x_0 = (500, 0.5)$, which lies in the unsafe region, to the benign equilibrium without violating health constraints, while considering uncertainties on the model parameters.

The initial condition represents the patient health conditions, it can be approximated before the treatment period. Note that the choice of x_0 is made only for illustrative purposes, the methodology that we present in this chapter remains applicable for other initial states values.

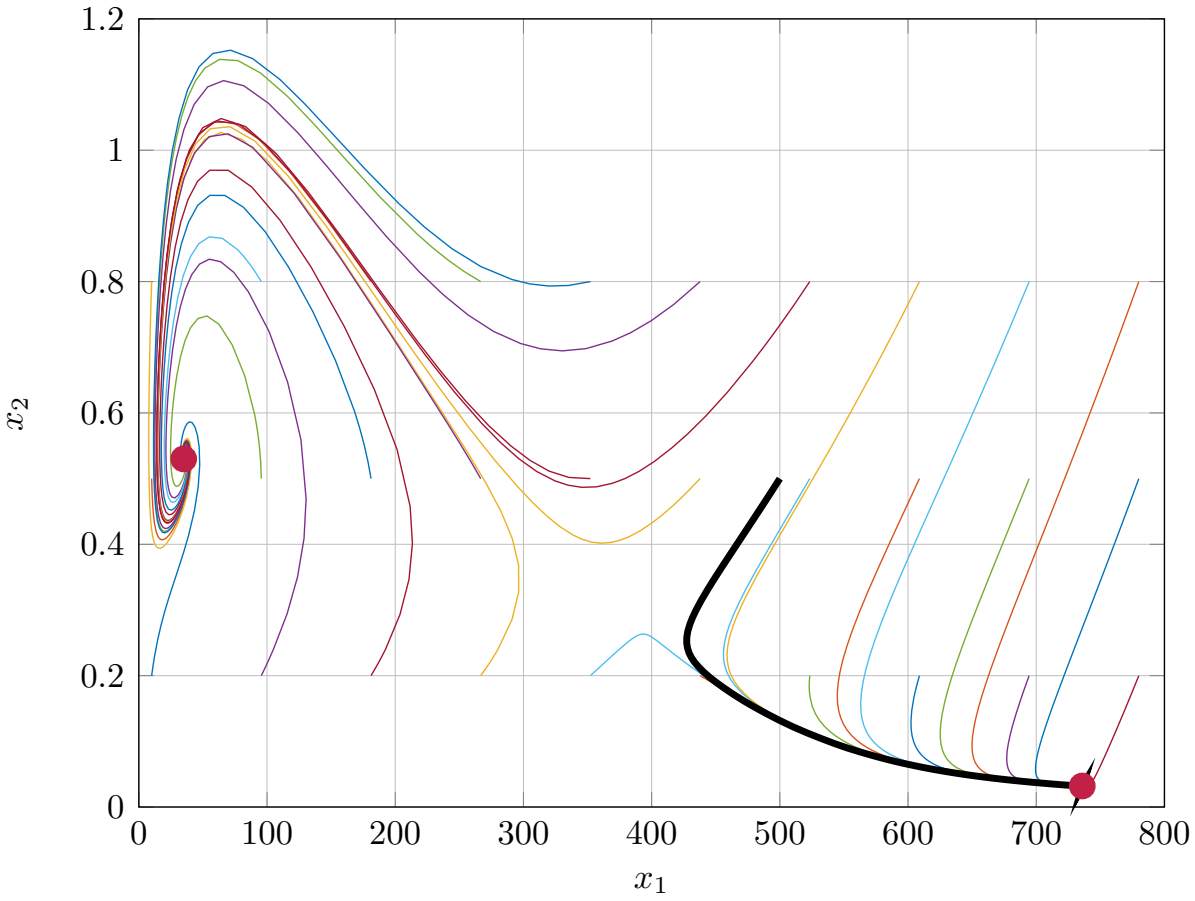

Figure 5.2: Phase portrait of model (5.1), that trajectory in black represents the evolution of the states starting from $x_0 = (500, 0.5)$.

5.2 Optimal design of combined cancer therapies with chemotherapy detrimental effects

We will first consider a nominal value of η_Y in order to solve a nominal optimal control problem, then we will consider η_Y as an uncertain parameter, with a given probability

distribution, and solve the robust optimal control problem. Finally, we compare the effects of both profiles (nominal and robust) for a family of realizations of the parameter vector values, in order to infer on the consequences of adding the chemotherapy-induced damage term and to highlight the importance of considering it in the therapy scheduling design.

Let's suppose that the initial condition is $(x_{10}, x_{20}) = (500, 0.5)$, we can see in Figure 5.2 that without control, the trajectory corresponding to this initial state converges to the malignant equilibrium.

Similarly to Chapter 4, we consider that the maximum drug dose is 1 for both chemotherapy and immunotherapy. Furthermore, we add constraints on the immune cells density and the number of tumor cells in order to ensure the compactness of the state set. We also impose a constraint on the final tumor size in order to drive the tumor to the benign region and a constraint on the minimal immune cells density, recommended to prevent the body from excessive weakening of the immune system. The nominal (*i.e.* considering a nominal value of η_Y) optimal control problem that we propose to solve for $t \in [0, 60]$ is the following:

$$\begin{aligned}
\min_{u_1(\cdot),u_2(\cdot)} \quad & J(x_1(\cdot), x_2(\cdot), u_1(\cdot), u_2(\cdot)) \\
\text{s.t.} \quad & \dot{x}_1 = \mu_C x_1 \left(1 - \frac{x_1}{x_\infty}\right) - \gamma_X x_1 x_2 - \kappa_X x_1 u_1, \\
& \dot{x}_2 = \mu_I \left(x_1 - \beta_Y {x_1}^2\right) x_2 - \delta_Y x_2 + \alpha_Y + \kappa_Y x_2 u_2 - \eta_Y u_1 x_2, \\
& x_1(0) = 500, x_2(0) = 0.5, \\
& x_1(60) \leq 100, \\
& 0 \leq u_1 \leq 1 \ , \ 0 \leq u_2 \leq 1, \\
& 0 \leq x_1 \leq 780 \ , \ 0 \leq x_2 \leq 5, \\
& x_2 \geq 0.1, \\
& t \in [0, 60].
\end{aligned} \tag{5.2}$$

As previously mentioned , in terms of control of cancer dynamics, the expression of the cost J involves many terms that are function of states and control inputs, with different penalties in order to achieve a trade-off between the different control objectives. The cost that has been implemented for this problem is presented bellow. We can reformulate Problem (5.2) in the framework of moments optimization via GloptiPoly 3 [45], as explained in Chapter 3. Similarly to Chapter 4, we solved the moments problem corresponding to (5.2) using YALMIP [62] and the semidefinite programming solver MOSEK [71]. We approximated the control input profiles, with the moments of the different occupation measures, using the Christoffel-Darboux kernel approach [65]. Furthermore, we scale the time and the state trajectories to $[0, 1]$, for the practical reasons previously explained. Therefore, in this chapter, the control inputs are computed for scaled dynamics.

We mentioned in Chapter 4 the importance of considering chemotherapy damaging

side effects on the human body in the optimal control problem. Thereby, it is crucial to minimize the total amount of injected chemotherapy. It is also important to minimize the use of immunotherapy since the available amount is limited, and for some treatment types, immunotherapy can even be toxic [70]. Therefore, one needs to take into account all this information in the definition of the cost function. Here, we focus on the assessment of the methodology by taking the following cost :

$$J = 10x_1(60) + 4\int_0^{60} x_1(t)dt + 0.01\int_0^{60} u_1(t)dt + 0.1\int_0^{60} u_2(t)dt.$$

In Figure 5.3, we show the drug delivery profiles in the time interval $[0, 5]$ to highlight the treatment duration, since for $t \in [5, 60]$, $u_1(t) = 0$ and $u_2(t) = 0$. We can see in this figure that, for $\eta_Y = 1$, the chemotherapy profile is a considerable injection at the beginning of treatment followed by a one day maximal dose injection of immunotherapy.

Figure 5.4 shows the time evolution of state trajectories. We can notice that the tumor burden is considerably reduced during the five first days, due to the considerable amount of chemotherapy drugs injected at the beginning. We can also notice that this important injection of chemotherapy induced a decrease in the density of immune cells (due to the term $-\eta_Y u_1 x_2$) in the dynamics of x_2. However, the minimal constraint is still respected thanks to the immunostimulation (u_2).

Although the control input profiles in Figure 5.3 allow to drive the state trajectories to the benign equilibrium, without any constraint violation, we will show using Monte-Carlo simulations, that when considering uncertainties on the effects of chemotherapy on immune cells, the nominal control profiles will show a lack of robustness.

Let's assume that $\eta_Y \sim \mathcal{U}([0, 2])$, this distribution is not based on practical knowledge of the system parameters, it is chosen only to illustrate the problem of handling parametric uncertainties. The methodology remains applicable for general probability distributions.

Figures 5.5 and 5.6 presents 100 Monte-Carlo simulations using the nominal profiles with random values of η_Y. Figure 5.7 shows the phase portrait corresponding to the Monte-Carlo simulations. We can see in these figures that there are many violations of the immune cells density constraint (*i.e.* leading to critical immune weakening of patients). Another point to notice is that, in some cases, there is a small tumor regrowth due to the weakening of immune system. Therefore, it is crucial to consider the potential uncertainties on chemotherapy detrimental effects.

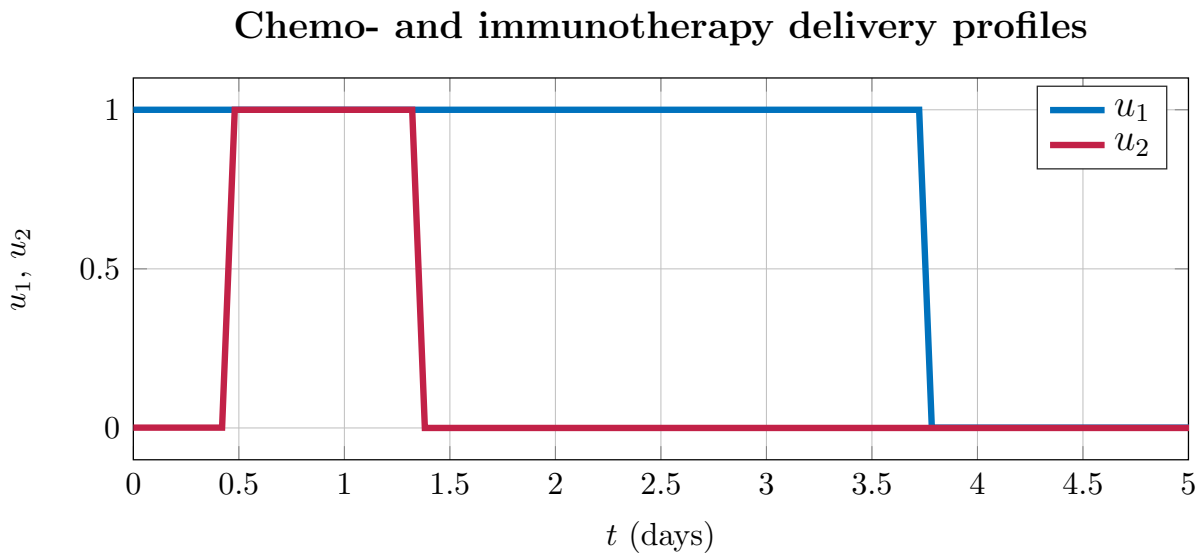

Figure 5.3: Nominal control input profiles (u_1 and u_2), for $\eta_Y = 1$.

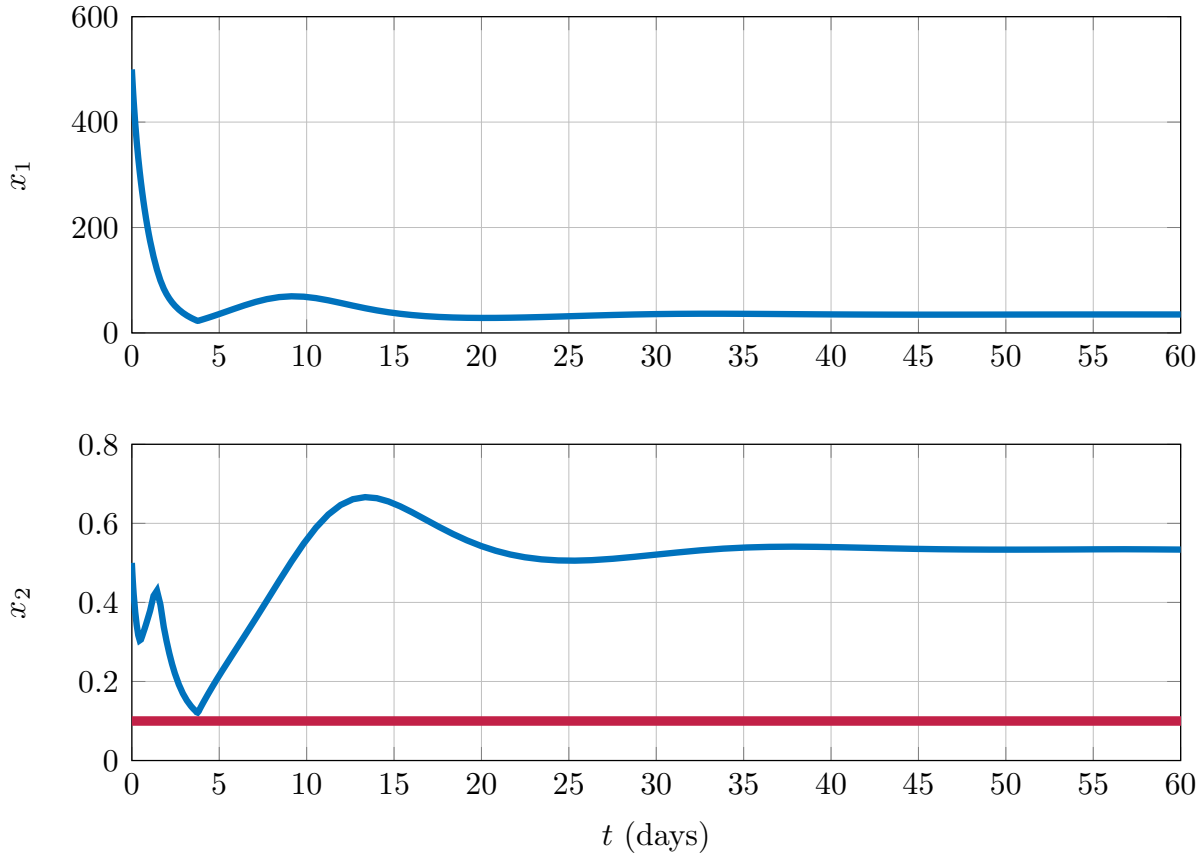

Figure 5.4: States trajectories (x_1 and x_2) using nominal control profiles.

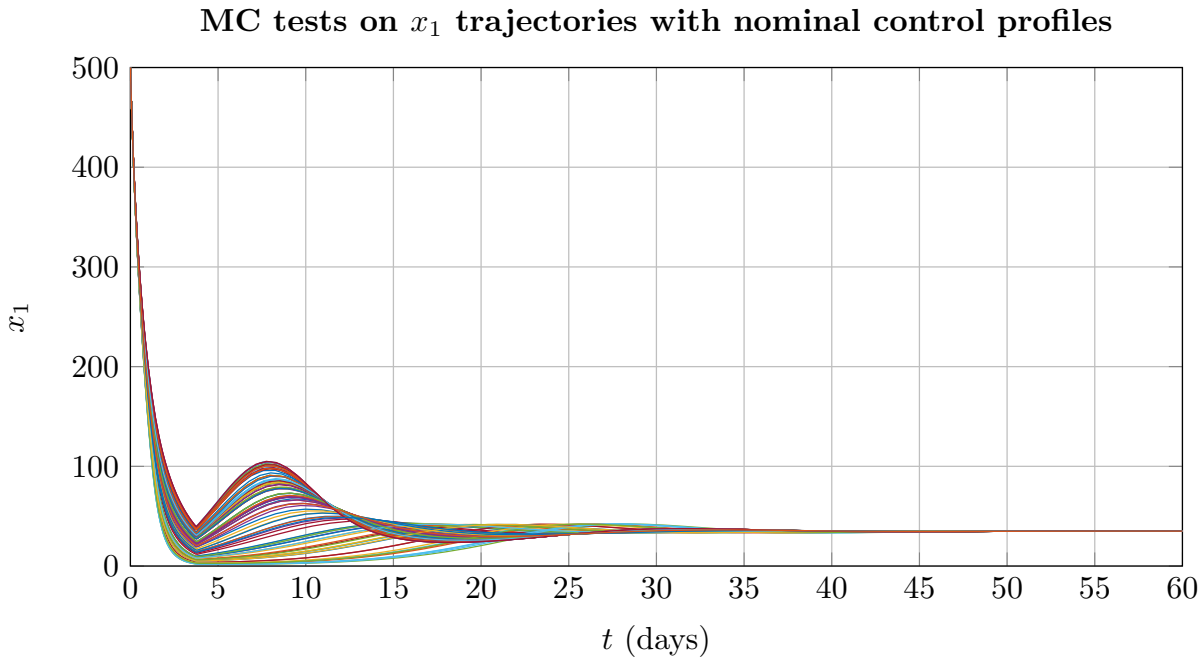

Figure 5.5: Monte-Carlo tests on nominal control profiles, x_1 trajectories.

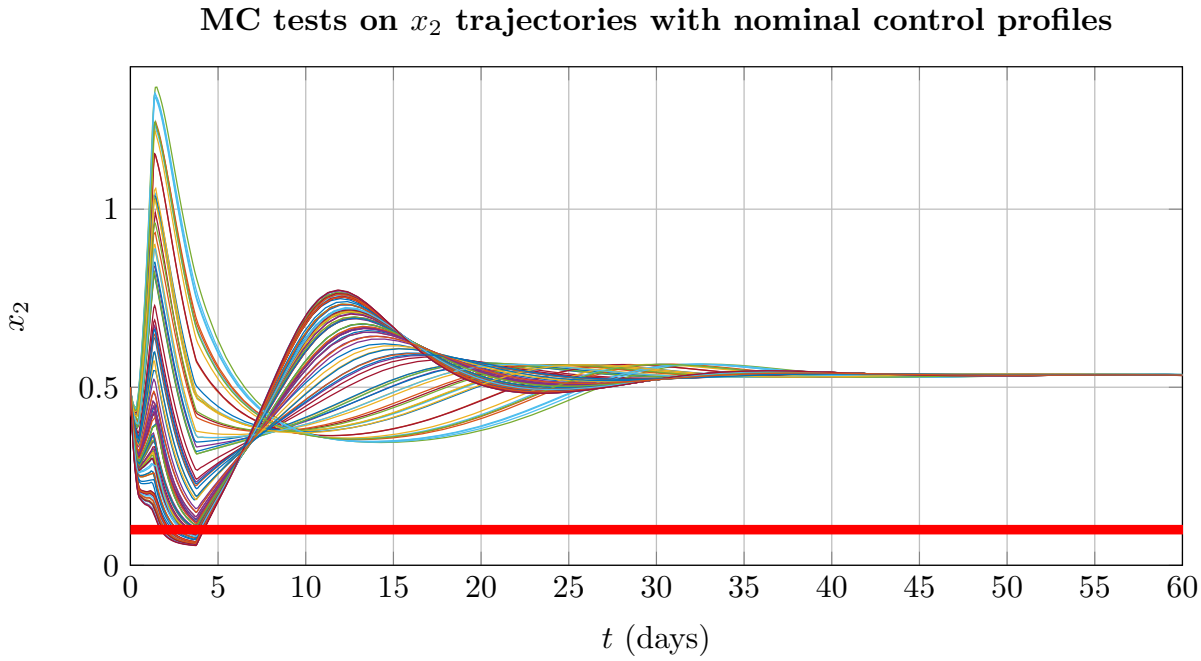

Figure 5.6: Monte-Carlo tests on nominal control profiles, x_2 trajectories.

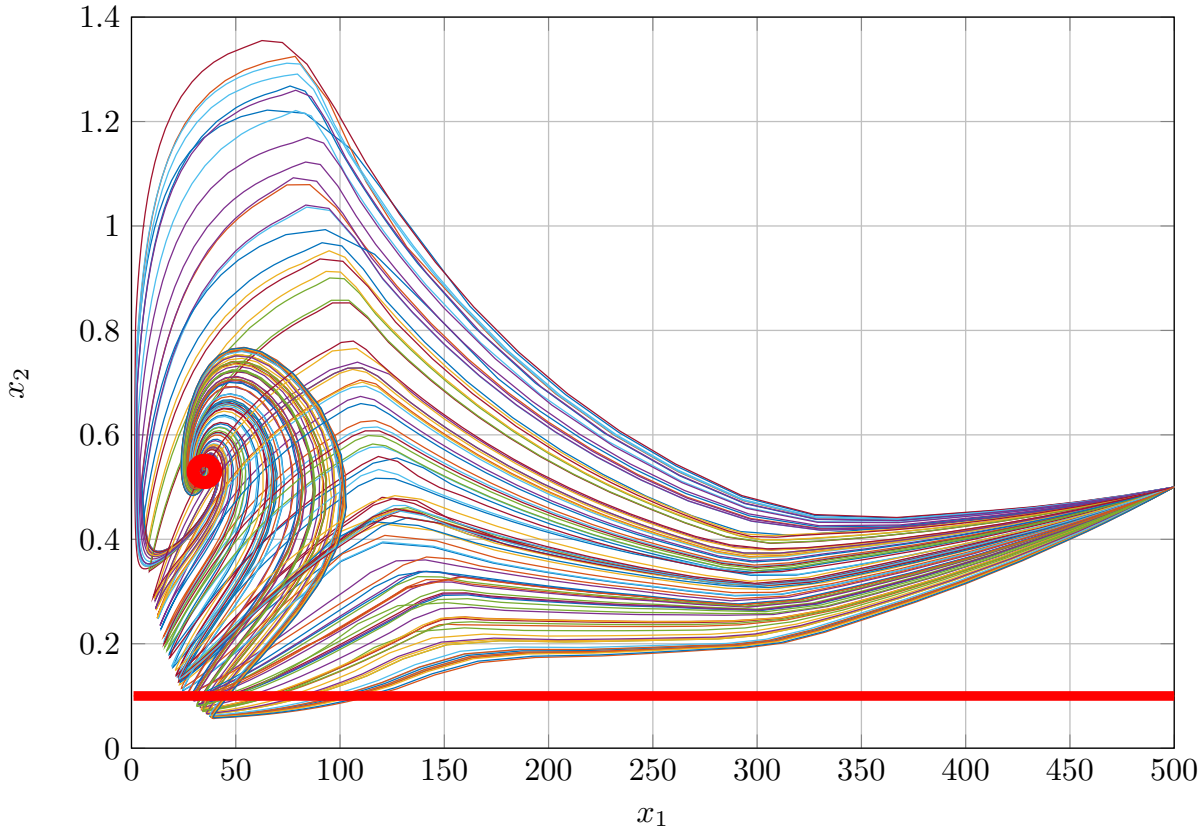

Figure 5.7: Monte-Carlo tests on nominal control profiles, phase portrait.

5.3 Robust optimal scheduling of combined cancer treatment

Let's extend system (5.1) to the following dynamics:

$$\begin{aligned}
\dot{x}_1 &= \mu_C x_1 - \frac{\mu_C}{x_\infty} {x_1}^2 - \gamma_X x_1 x_2 - \kappa_X x_1 u_1, \\
\dot{x}_2 &= \mu_I \left(x_1 - \beta_Y {x_1}^2 \right) x_2 - \delta_Y x_2 + \kappa_Y x_2 u_2 + \alpha_Y - \eta_Y u_1 x_2, \\
\dot{\eta}_Y &= 0.
\end{aligned} \tag{5.3}$$

The state extension in (5.3) allows to characterize η_Y by its probability distribution, as explained in Chapter 4. Similarly to problem (5.2), one can reformulate the robust optimal control problem with dynamics (5.3) by including the moments of the distribution of η_Y. Thus, supposing that $\sigma_{\eta_Y}(\eta_Y)$ denote the probability distribution of η_Y, the optimal control problem to be solved should have as initial condition

$$\mu_0(t, x_1, x_2, \eta_Y) = \delta_0(t)\, \delta_{x_1(0)}(x_1)\, \delta_{x_2(0)}(x_2)\, \sigma_{\eta_Y}(\eta_Y),$$

imposed through the moments of the initial measure.

Figure 5.8 shows the robust chemotherapy injection profile where we minimize the expectation of the nominal cost J that we denote $\mathbf{E}_{\eta_Y}[J]$. We can notice that compared to the nominal case (Figure 5.3), the use of chemotherapy in the robust case has been

considerably reduced in intensity but extended in time. This is due to the presence of constraint on the minimal immune cells density and the new term $-\eta_Y u_1 x_2$ which reduces the amount of immune cells when chemotherapy concentration increases. The robust chemotherapy schedule uses less than 3.5% of the maximal allowed dose, this concentration decreases slowly during the treatment period while in the nominal profile, it is a one maximal dose at the beginning of treatment period.

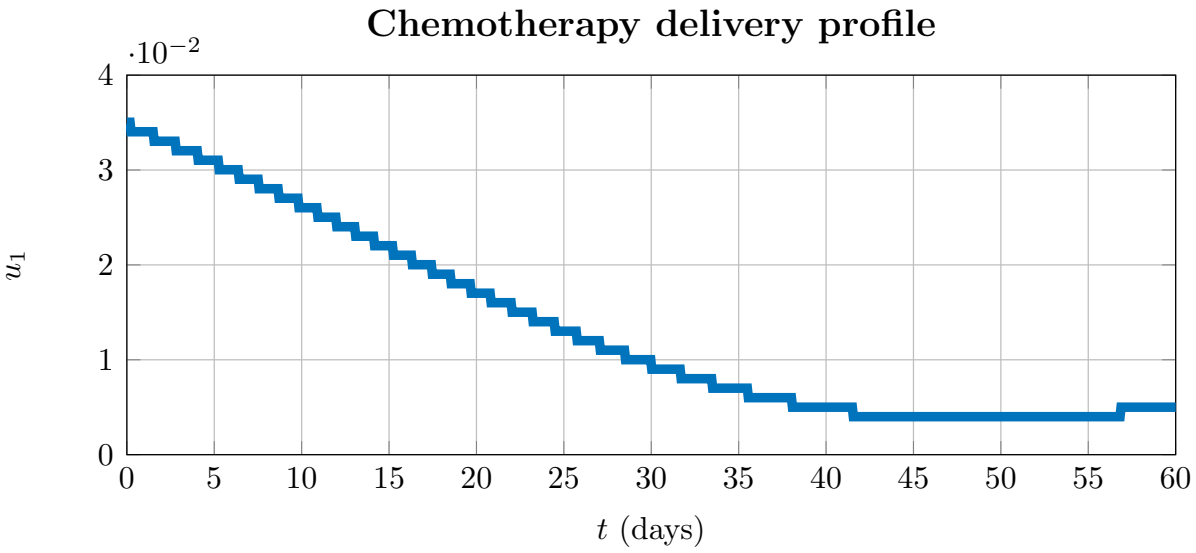

Figure 5.8: Robust control input profile corresponding to chemotherapy (u_1).

Figure 5.9 shows the immunotherapy profile, we can notice that the nominal and robust profiles of immunotherapy are almost the same, it is a one day maximal dose at the beginning of the treatment period.

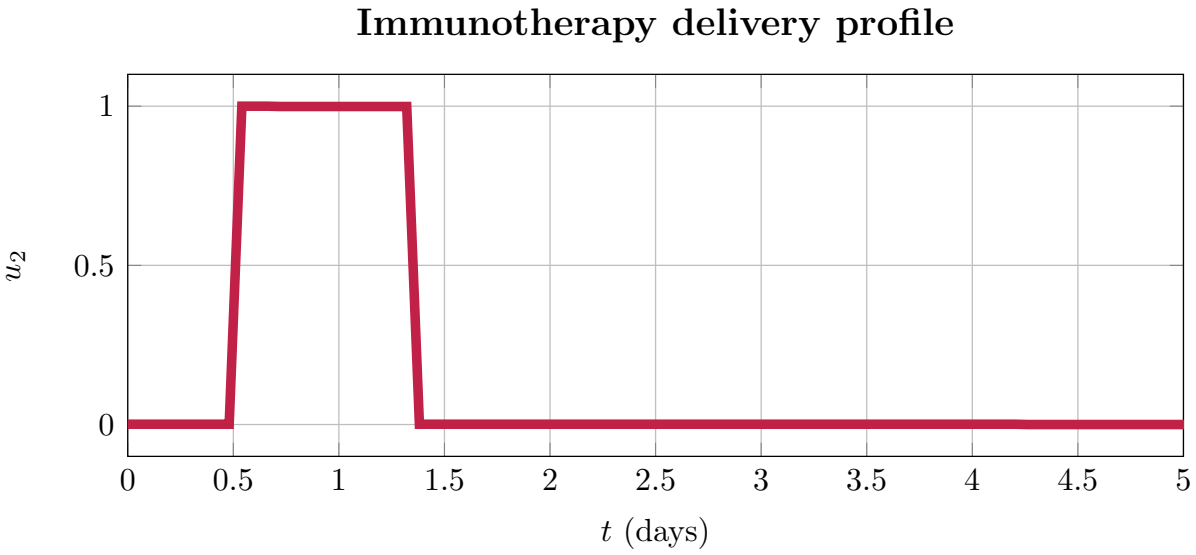

Figure 5.9: Robust control input profile corresponding to immunotherapy (u_2).

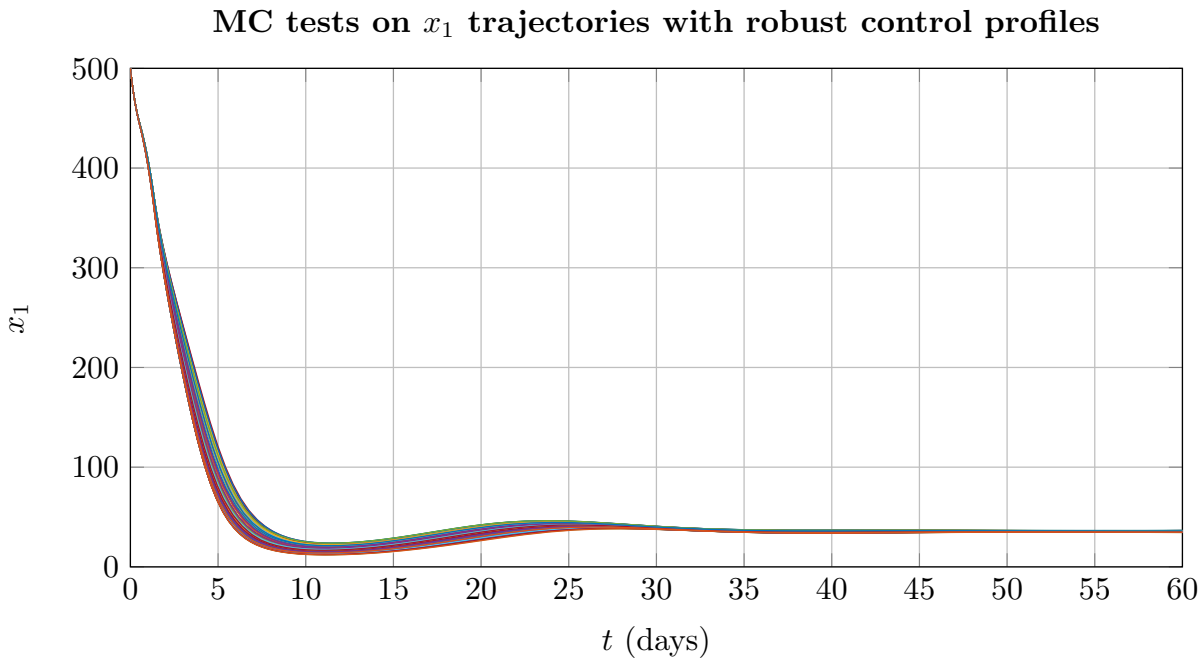

Figure 5.10: Monte-Carlo tests on robust control profiles, x_1 trajectories.

Similarly to the nominal case, we did 100 Monte-Carlo simulations on system (5.1), using robust schedules, the results are presented in Figure 5.10 and 5.11. We can notice in Figure 5.10 that the tumor volume takes more time to be reduced in the robust case. However, as we can see in Figure 5.11, there is no immune constraints violation unlike the nominal case.

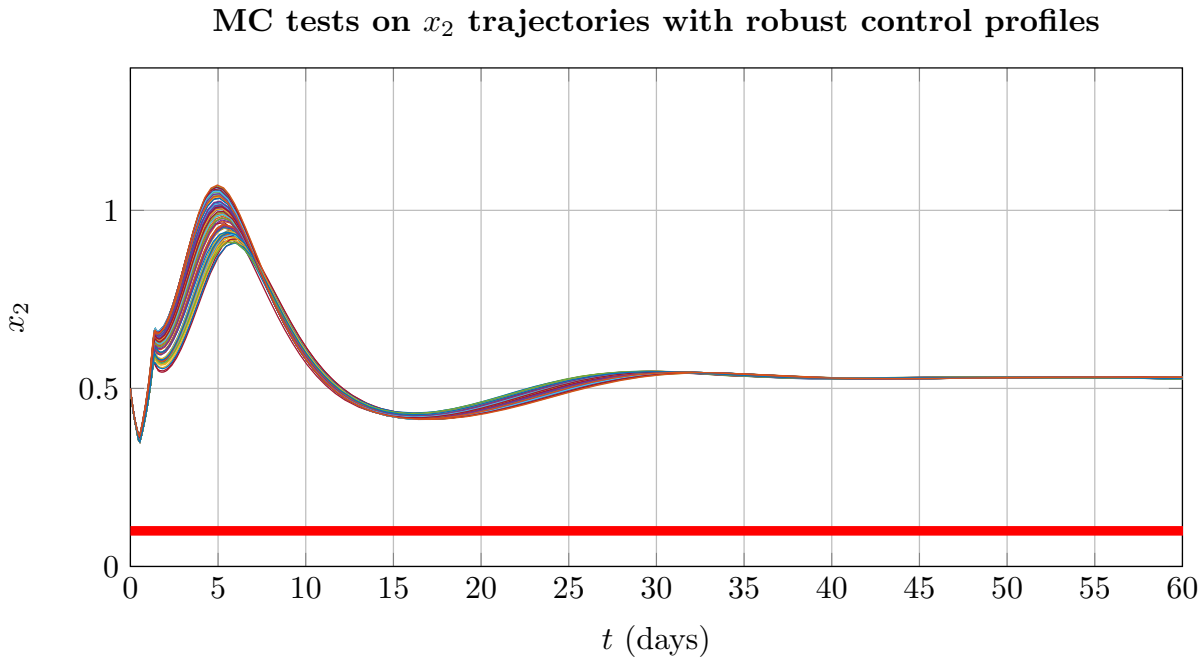

Figure 5.11: Monte-Carlo tests on robust control profiles, x_2 trajectories.

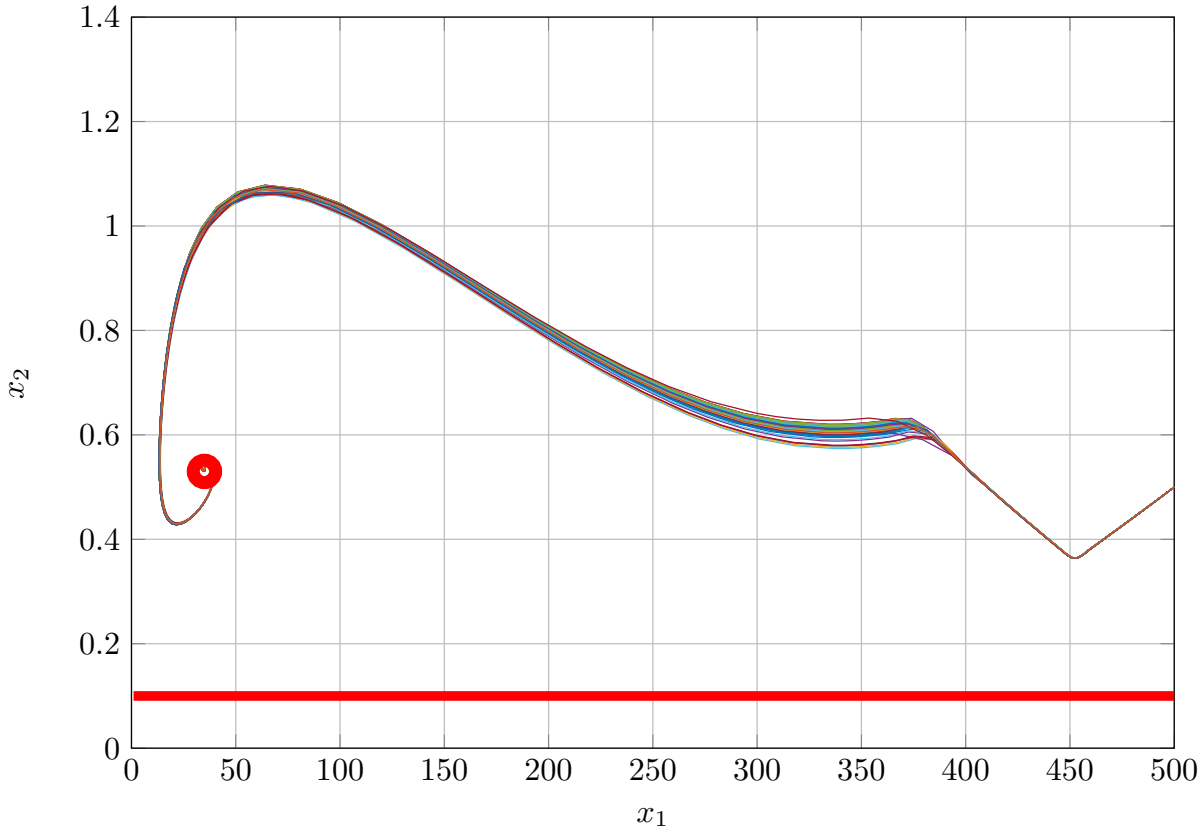

Figure 5.12: Monte-Carlo tests on robust control profiles, phase portrait.

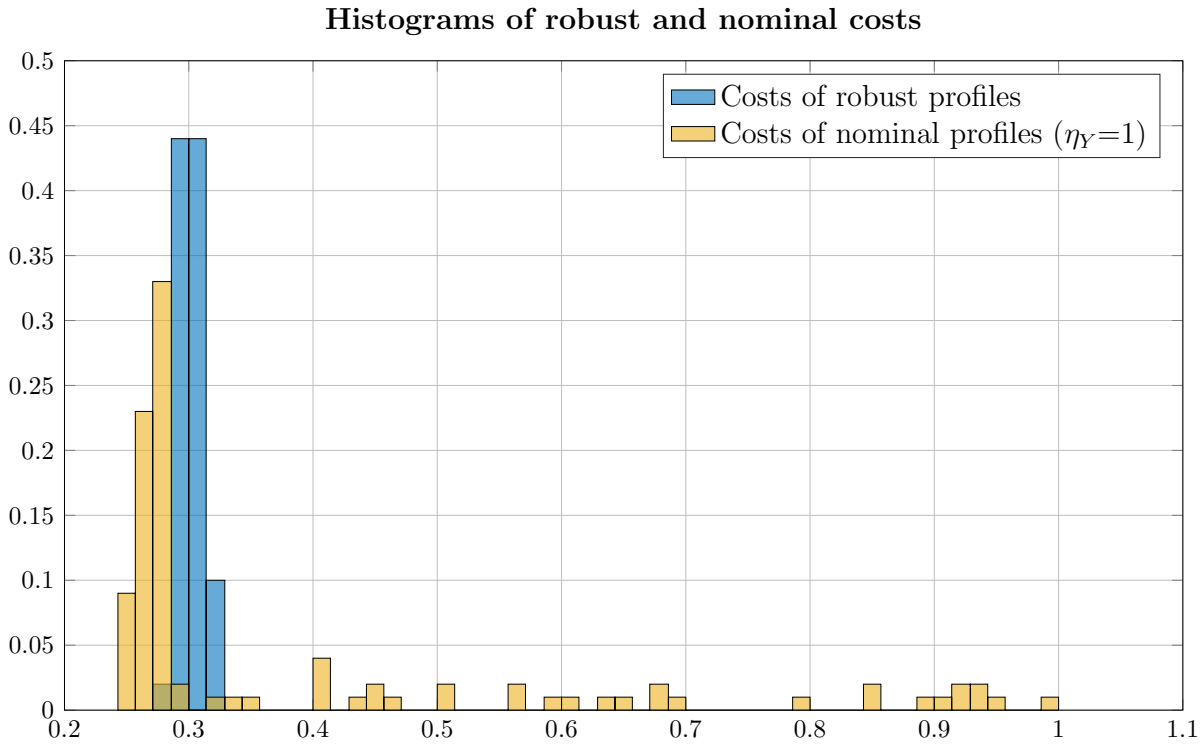

Figure 5.13: Costs comparison.

Figure 5.12 presents the phase portrait of the Monte-Carlo trajectories, showing that

the state trajectories are considerably less dispersed than in the nominal case (Figure 5.7).

Figure 5.13 shows the distributions of nominal and robust costs, obtained using the same cost based comparison methodology presented in Chapter 4. Furthermore, Table 5.1 presents the statistics of the two cost distributions. We can notice that both the mean and the variance are smaller in the robust case than in the nominal one.

Table 5.1: Statistics of the normalized costs (nominal and robust).

	Mean	Variance
Nominal cost	0.39	0.05
Robust cost	0.30	$1{\cdot}10^{-4}$

5.3.1 Computational time comparison

In Table 5.2 we compare the required computational time for a relaxation order $r = 8$, for both the nominal and robust cases. We notice that the computational time required for solving the nominal OCP for $r = 8$ is the same as in Chapter 4, which is explained by the fact that the system dimensions as well as the number of moments are the same for both problems. We also notice that the computation time for the robust OCP with $r = 8$ is considerably less than the one corresponding to the robust problem of Chapter 4, since the number of moments is also smaller. This is due to the difference in the state dimension after extension since in Chapter 4, we considered two uncertain parameters (μ_C and α_Y) adding thereby two extra states to the model. Whereas in this chapter we considered only the parameter standing for chemotherapy detrimental effects on immune cells (η_Y) as uncertain.

Table 5.2: Average computation times on hp EliteBook 2.60GHz Intel Core i7

	Nominal OCP	Robust OCP
Relaxation order r	8	8
Time	0.67mn	6.00mn
Number of moments	3333	8998

5.4 Conclusion

In this chapter, we presented numerical simulation results on optimal control under uncertainties for a cancer interactions model. The model that we considered takes into account the detrimental effects of chemotherapy on the immune system. Furthermore, we added

in the OCP a minimal constraint on the density of immune cells.

Although the nominal profiles allowed to satisfy the constraints for a nominal scenario, it turns out that when considering uncertainties on the chemotherapy effects on immune cells, the tumor burden presents some oscillations and the minimal constraint on immune cells might be violated.

Therefore, we solved a robust OCP which considers the chemotherapy killing parameter (effects of chemotherapy on immune cells) as an uncertain parameter, described by a given probability distribution. We noticed that in this case the intensity of injected chemotherapy is considerably reduced compared to the nominal case. Furthermore, the constraints are satisfied and all state trajectories converge to the benign equilibrium. Thus, we highlighted in this chapter the importance of taking into account the side effects of chemotherapy on immune cells as well as their eventual uncertain behavior.

Although the moment optimization approach does not allow to consider high dimensional systems, it is interesting to use it for such problems in order to investigate the consequences of adding new uncertain terms on the control profiles scheduling.

Part III

Region of attraction estimation under parametric uncertainties for cancer dynamics

Chapter 6

Robust domain of attraction estimation for a cancer model

Estimating the region of attraction (RoA) of equilibrium points is a fundamental problem in systems engineering [18]. This set, called also the domain or the basin of attraction, contains the initial states that can be driven to a stable equilibrium point, without violating the specified constraints. Therefore, the estimation of regions of attraction is a very important and still open field of research [6].

In practical problems, the systems are often affected by different types of uncertainties. Hence, one of the challenging problems in the control of dynamical systems is the estimation of robust regions of attraction for nonlinear and uncertain systems. According to [11], the Lyapunov theory for ODEs initiated the notion of invariant sets for control problems. Deriving the exact RoA for dynamical systems is a challenging task, therefore, researchers focus on determining Lyapunov functions, since the sublevel sets of the latter represent the boundaries of positively invariant sets [88]. In fact, a positively invariant set, for a given dynamical system, is such that if it contains the states at a given time, then, there is a guarantee that it will contain the state trajectories for the future.

One of the commonly used convex sets for the estimation of invariant sets are polyhedrons and ellipsoids. According to [6], invariant ellipsoids have been used in the literature in order to estimate the regions of attraction of nonlinear systems. In [11], a detailed review on invariant sets approaches is provided, with a specific comparison between polyhedrons and ellipsoids, in terms of estimation accuracy and flexibility. According to [12], it is established, in terms of RoA estimation as well as robustness analysis, that the ellipsoidal based approaches are conservative. In contrast to ellipsoids, polyhedral sets provide less conservative solutions, although they might be computationally expensive.

The estimation of regions of attraction for linear systems has received a specific attention in the literature. There exist many works for this class of systems, see for example [10], [11], [12] and [92]. In contrast to linear systems, the characterization of regions of attraction for nonlinear systems is an open research topic. There exist some approaches, that are based on convex difference inclusions (CDIs), allowing to estimate the RoAs for

nonlinear systems, see [5], [38], [37], [40], [39]. Furthermore, in [77], the latter methods were extended to characterize the RoAs for nonlinear systems, subject to different types of uncertainties.

Moreover, there are other methods based on the moment optimization framework, allowing to estimate the RoAs of polynomial dynamical systems and providing a hierarchy of semi-algebraic outer (or inner) approximations of the RoA, by solving a sequence of linear matrix inequalities (LMIs) problems, see [49] and [44]. However, as mentioned in Part II, the moment optimization based methods are limited to low dimensional systems and require a relatively high computational time. Therefore, extending these approaches to uncertain systems might be challenging.

In the context of cancer treatment, the regions of attraction are interpreted as the sets of initial health conditions (tumor volume and immune cells density for example), for which there exists a treatment strategy such that the patient recovers, without any health damage or side effect. Therefore, the characterization of this type of sets is essential for the analysis of cancer related dynamical systems. Furthermore, since this class of systems is known to be highly uncertain, it is crucial to estimate the RoA under uncertainties for such systems.

There exist in the literature few works regarding the estimation of RoAs and robust RoAs for cancer dynamical systems. We cite for example [28] and [91], where the authors proposed different Lyapunov functions based approaches, to estimate the domain of attraction of the tumor free equilibrium point corresponding to autonomous cancer growth models, where no therapies are considered. Furthermore, in [78], an iterative procedure method, based on approximating the uncertain system with CDIs, was presented to estimate the robust region of attraction of a tumor growth model with chemotherapy. However, the model that we consider in this chapter has not been investigated in the literature to estimate its controlled region of attraction.

This part is dedicated to the estimation of regions of attraction under parametric uncertainties, for a model describing cancer dynamics in interaction with the immune system as well as combined therapies. In this chapter, we propose a readily applicable methodology that is in the same line of sliding mode control, in order to characterize the region of attraction of a cancer dynamical model, using bang-bang control strategies. Furthermore, this methodology will be used in order to derive an estimate of the robust region of attraction, where the model parameters are considered to be uncertain. It is worth emphasizing that this approach does not provide the control strategies to be applied, however, it provides the set of initial conditions, such that for every initial condition in this set, there exists a control strategy allowing to drive the states to a benign stable equilibrium. This can also be seen as to provide an estimate of the control invariant set corresponding to the benign stable equilibrium.

This chapter is organized as follows: In Section 6.1, we present the cancer dynamical

model, furthermore, we investigate the parametric space of this model and we analyze the effects of parametric uncertainties on the model equilibrium points. In Section 6.2, we present the methodology allowing to derive the RoA of the cancer benign equilibrium, corresponding to the considered model. We use the latter approach in Section 6.3 in order to derive an estimation of the robust RoA. Finally, Section 6.4 summarizes the work that we present in this chapter and links it to the contribution of Chapter 7.

6.1 Dynamical model

We consider here the same model as in Chapter 5, describing the interaction between a tumor and the immune system under the effects of a combined therapy:

$$\begin{aligned} \dot{x}_1 &= \mu_C x_1 - \frac{\mu_C}{x_\infty} x_1^2 - \gamma_X x_1 x_2 - \kappa_X x_1 u_1, \\ \dot{x}_2 &= \mu_I x_1 x_2 - \beta_Y \mu_I x_1^2 x_2 - \delta_Y x_2 + \kappa_Y x_2 u_2 - \eta_Y u_1 x_2 + \alpha_Y, \\ x(0) &= (x_1(0), x_2(0)) = x_0, \end{aligned} \tag{6.1}$$

where x_1 and x_2 denote, respectively, the number of tumor cells and the density of effector immune cells (ECs), u_1 and u_2 are, respectively, the delivery profiles of a cytotoxic agent (chemotherapy) and an immunostimulator. The initial state of system (6.1) is denoted by x_0.

Table 6.1 summarizes the definitions of the model parameters and their nominal values. We slightly changed the values of some parameters since with the previous set of parameters values (used in Chapter 4 and 5 and taken from [32]), the domain of attraction for the uncontrolled system (6.1) (for $u_1 = 0$ and $u_2 = 0$) was unrealistically big. This allows us to solve a problem which is more reasonable and realistic from a practical point of view. Furthermore, we focus on the assessment of a methodology that remains applicable for different nominal parameters values.

Let's denote by $x = (x_1, x_2)$ and $u = (u_1, u_2)$, respectively, the state and the control input vectors. The uncontrolled nominal model (6.1) (for $u = (0, 0)$) has two locally asymptotically stable equilibrium points. The macroscopic malignant equilibrium is $x_m = (766.44, 0.08)$ and the benign one is $x_b = (41.45, 0.95)$.

In standard control problems for cancer dynamics, the objective of the treatment consists in general in driving the state trajectories from the region of attraction of the malignant equilibrium to the region of attraction of the benign equilibrium. This can be seen as to switch an acute tumor to its chronic state. In this part, we are interested in characterizing the set of initial conditions (tumor volume and immune density) from which the state trajectories can be driven to the safe region.

In the context of cancer treatment, the determination of the region of attraction is an interesting problem, since it provides an information on the possibility of recovery for a patient, given the initial measured health conditions. We mean by recovery reaching a

Table 6.1: Definitions and nominal values of the parameters used in model (6.1).

Parameter	Definition	Numerical value
μ_C	tumor growth rate	$1.0078 \cdot 10^7$ cells/day
μ_I	tumor stimulated proliferation rate	0.0029 day^{-1}
α_Y	rate of immune cells influx	0.0827 day^{-1}
β_Y	inverse threshold	0.0040
γ_X	interaction rate	$1 \cdot 10^7$ cells/day
δ_Y	death rate	0.1873 day^{-1}
κ_X	chemotherapeutic killing parameter	$1 \cdot 10^7$ cells/day
κ_Y	immunotherapy injection parameter	$1 \cdot 10^7$ cells/day
x_∞	fixed carrying capacity	$780 \cdot 10^6$ cells
η_Y	chemo-induced loss on immune cells	1

safe region where the tumor is considered to be harmless, and there is no need to inject drugs. The safe region corresponds to the region of attraction of the locally asymptotically stable benign equilibrium x_b without therapies. This set as well as the region of attraction under treatment will be properly defined in the sequel.

Moreover, we will use the characterization of the domain of attraction of system (6.1) to derive an estimate of the robust region of attraction when the model parameters are considered to be uncertain and belong to a given hyperbox.

In this section, we will provide necessary and sufficient conditions for the equilibriums of system (6.1) to exist, given the vector of model parameters p. We will also investigate the parametric space and show the equilibrium points distributions. Furthermore, we will provide an estimate of the region of attraction of the benign equilibrium x_b when nominal parameters are considered (the parameters values in Table 6.1).

6.1.1 Model equilibriums

We are interested in finding a general equation to obtain the equilibrium points of model (6.1) when no control is applied (*ie*: $u = (0, 0)$). Therefore, we need to solve the following equations:

$$\dot{x}_1 = \mu_C x_1 - \frac{\mu_C}{x_\infty} {x_1}^2 - \gamma_X x_1 x_2 = 0, \tag{6.2}$$

$$\dot{x}_2 = \mu_I \left(x_1 - \beta_Y {x_1}^2 \right) x_2 - \delta_Y x_2 + \alpha_Y = 0. \tag{6.3}$$

The nontrivial solution of (6.2) is:

$$x_1 = \frac{x_\infty}{\mu_C} \left(\mu_C - \gamma_X x_2 \right). \tag{6.4}$$

By replacing (6.4) in (6.3), we obtain that solving $\dot{x}_2 = 0$ implies solving the following polynomial equation:

$$-\frac{\mu_I \beta_Y x_\infty^2 \gamma_X^2}{\mu_C^2} x_2^3 + \left(\frac{2\mu_I \beta_Y x_\infty^2 \gamma_X - \mu_I x_\infty \gamma_X}{\mu_C} \right) x_2^2 + \left(\mu_I x_\infty - \mu_I \beta_Y x_\infty^2 - \delta_Y \right) x_2 + \alpha_Y = 0. \tag{6.5}$$

We denote by $a(x_2)$ the monic polynomial corresponding to the polynomial in (6.5) as follows:

$$a(x_2) = x_2^3 + \mu_C \left(\frac{\mu_I x_\infty \gamma_X - 2\mu_I \beta_Y x_\infty^2 \gamma_X}{\mu_I \beta_X x_\infty^2 \gamma_X^2} \right) x_2^2 + \mu_C^2 \left(\frac{\delta_Y + \mu_I \beta_Y x_\infty^2 - \mu_I x_\infty}{\mu_I \beta_Y x_\infty^2 \gamma_X^2} \right) x_2 - \frac{\mu_C^2 \alpha_Y}{\mu_I \beta_Y x_\infty^2 \gamma_X^2}. \tag{6.6}$$

This notation will be used in the sequel in order to investigate the parametric space corresponding to model (6.1).

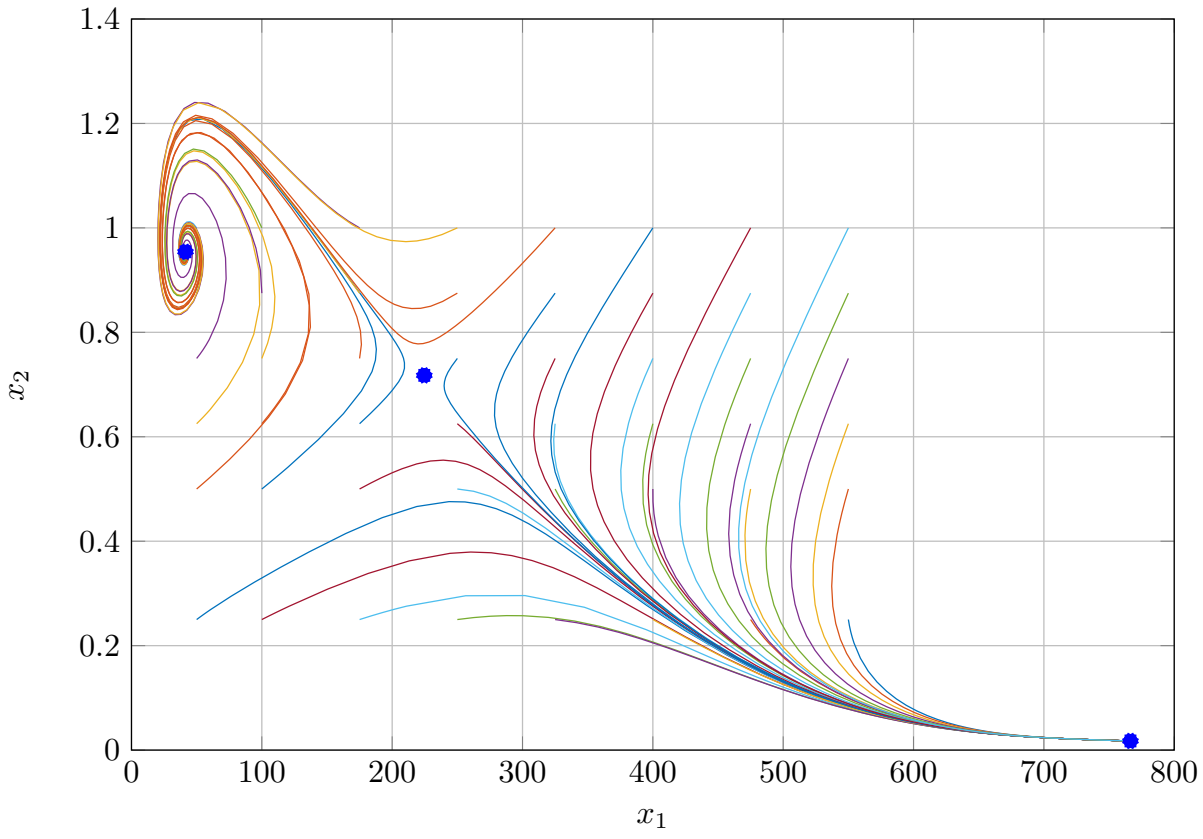

Figure 6.1: Phase portrait of (6.1) with the three equilibrium points.

Considering the nominal parameters in Table 6.1, the polynomial (6.5) has three real solutions. The state x_1 corresponding to the number of tumor cells can be obtained through (6.4) for each root of (6.5). The three equilibriums of system (6.1) are the benign and the malignant ones, which are locally asymptotically stable, and the saddle point which separates the regions of attraction of the benign and malignant equilibriums (see Figure 6.1).

6.1.2 Estimating the domain of attraction of the benign equilibrium

Let's denote by $p \in \mathbb{P} \subset \mathbb{R}_+^{n_p}$ the vector of dimension $n_p = 9$ containing the parameters of model (6.1) such that:

$$p = (\mu_C, \mu_I, \alpha_Y, \beta_Y, \gamma_X, \delta_Y, \kappa_X, \kappa_Y, \eta_Y)^T . \tag{6.7}$$

The uncontrolled system (6.1) can be written in the following form:

$$\dot{x} = F(x, p), \quad x(0) = x_0, \tag{6.8}$$

where x_0 stands for the initial state.

Let $\phi(t, x_0, p)$ be the solution of (6.8) evaluated at time $t \geq 0$ and corresponding to the state initial condition x_0 and the parameters vector p. We denote by x_b^p the benign equilibrium of system (6.1) for a given parameters vector p. Note that the existence of a benign equilibrium depends on the vector of parameters p. We will provide in the sequel necessary and sufficient conditions for the existence of such an equilibrium.

Definition 6.1 *The RoA Ω_0^p of the benign equilibrium of the uncontrolled system (6.8) for a given parameters vector p is defined as follows:*

$$\Omega_0^p = \left\{ x_0 \in \mathbb{R}_+^2 \mid \lim_{t \longrightarrow \infty} \phi(t, x_0, p) = x_b^p \right\}. \tag{6.9}$$

The region of attraction Ω_0^p characterizes the set of initial states that can be driven to the benign equilibrium without any control action. This set can be seen as the safe region previously explained, since there is a guarantee that all trajectories having as initial state $x_0 \in \Omega_0^p$, converge to the benign equilibrium x_b^p after some time, and without control. Therefore, Ω_0^p can be used as a target set for any control strategy.

Let's denote by $p_{nom} \in \mathbb{R}_+^{n_p}$ the vector containing the nominal parameters of model (6.1) (presented in Table 6.1), such that:

$$p_{nom} = (1.0078, 0.0029, 0.0827, 0.004, 1, 0.1873, 1, 1, 1)^T . \tag{6.10}$$

As mentioned in [32], finding an analytic description for the domain of attraction of the benign equilibrium denoted $\Omega_0^{p_{nom}}$ might be challenging. However, there exist some methods for approximating these sets, see for example [41] and [35].

Definition 6.2 *We denote by* $\hat{\Omega}_0^{p_{nom}}$ *an estimate of the nominal uncontrolled RoA of the benign equilibrium denoted* $\Omega_0^{p_{nom}}$.

Note that $x_b^{p_{nom}}$ is the same previously defined benign equilibrium point $x_b = (41.45, 0.95)$, when nominal parameters are considered.

Figure 6.2 shows the phase portrait of system (6.1) with an estimation of the nominal uncontrolled region of attraction of the benign equilibrium. We can notice that this set is considerably smaller than the region of attraction of the benign equilibrium with the previous set of parameters used in Chapter 4 and 5, see Figure 5.2.

In the context of standard control, where deterministic parameters are considered, the set shown in Figure 6.2 can be used as a target set for the defined control strategy, since all the trajectories starting in this set converge to the corresponding benign equilibrium without any control action.

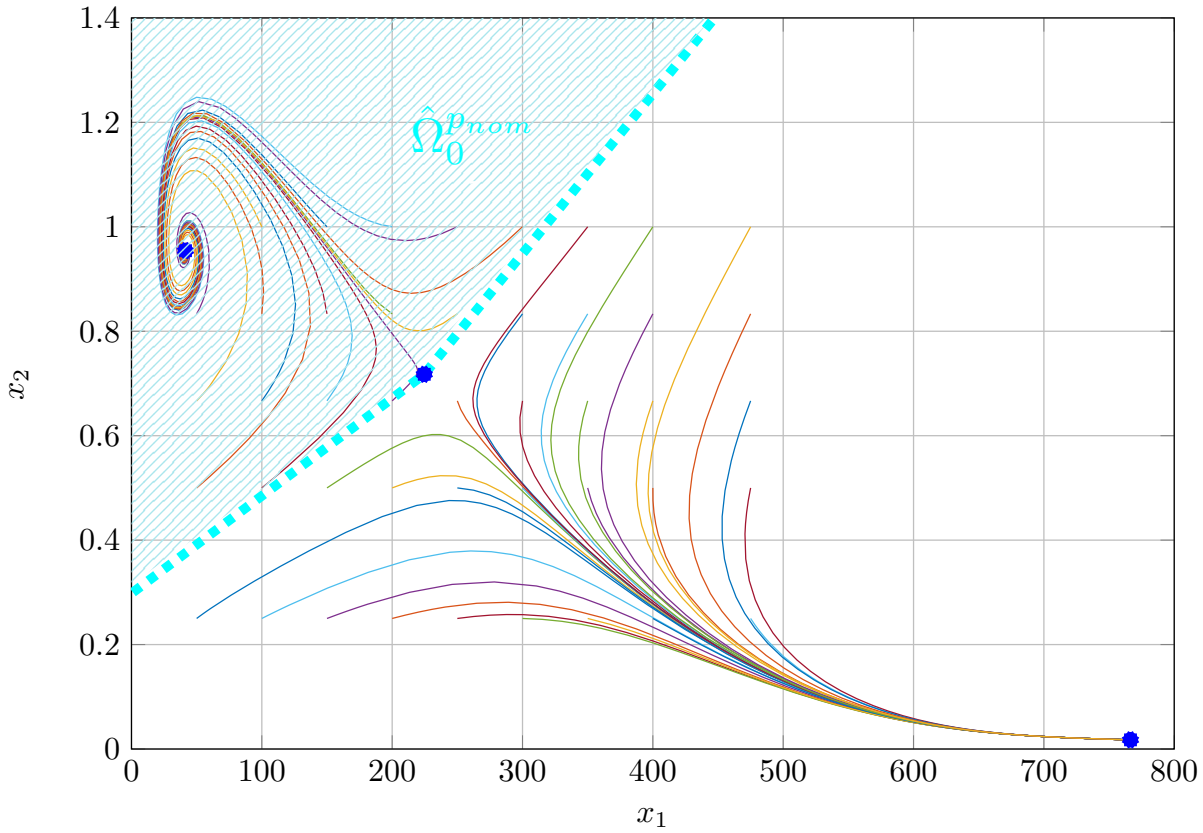

Figure 6.2: Phase portrait of (6.1) with nominal parameters p_{nom}, estimate of the nominal uncontrolled RoA of the benign equilibrium $\hat{\Omega}_0^{p_{nom}}$ in dashed cyan.

6.1.3 Parametric space investigation

In the previous section, we presented the general equations providing the equilibriums of system (6.1). The roots of the polynomial (6.6) can be either real or complex depending on the parameters vector p. In this chapter, we are interested in providing an estimation

of the robust region of attraction of system (6.1) subject to parametric uncertainties. Therefore, it is interesting to investigate the parametric space, since there might be some inadmissible parameter vectors, for which the polynomial (6.6) has complex roots, this case being unrealistic in the context of cancer dynamics modeling.

In the sequel, we provide necessary and sufficient conditions for system (6.1) to have real distinct equilibrium points. Furthermore, we illustrate these conditions with examples in both cases, when the polynomial equation allowing to derive the equilibrium points of system (6.1) has only real roots, as well as in the case when it has complex roots.

Theorem 6.1 *The system (6.1) for a given parameters vector p has three real distinct equilibrium points if and only if the following condition is satisfied:*

$$\mathcal{H}(a_p) := \begin{pmatrix} s_0 & s_1 & s_2 \\ s_1 & s_2 & s_3 \\ s_2 & s_3 & s_4 \end{pmatrix} \succ 0 \tag{6.11}$$

where a_p stands for the coefficients vector corresponding to the polynomial $a(x_2)$ (6.6), and $\mathcal{H}(a_p)$ denotes the Hermit matrix of the polynomial $a(x_2)$. The coefficients of the Hermit matrix s_0, s_1, s_2, s_3 and s_4 have the following expressions:

$$\begin{cases} s_0 = 3 \\ \\ s_1 = \mu_C \left(\dfrac{2\beta x_\infty - 1}{\beta_Y x_\infty \gamma_X} \right) \\ \\ s_2 = \dfrac{\mu_C^2}{\mu_I \beta_Y^2 x_\infty^2 \gamma_X^2} \left(\mu_I - 2\delta_Y \beta_Y - 2\mu_I \beta_Y x_\infty + 2\mu_I \beta_Y^2 x_\infty^2 \right) \\ \\ s_3 = \dfrac{\mu_C^2}{\mu_I \beta_Y^3 x_\infty^3 \gamma_X^3} \left(-\mu_C \mu_I + 3\mu_C \mu_I \beta_Y x_\infty - 3\mu_C \mu_I \beta_Y^2 x_\infty^2 + 8\mu_C \mu_I \beta_Y^3 x_\infty^3 + 3\mu_C \beta_Y \delta_Y \right. \\ \quad \left. -6\mu_C \mu_I \beta_Y^2 x_\infty \delta_Y - 6\mu_C \mu_I^2 \beta_Y^3 x_\infty^3 + 3\alpha_Y \beta_Y^2 x_\infty \gamma_X \right) \\ \\ s_4 = (1 - 4\beta_Y x_\infty + 4\beta_Y^2 x_\infty) \left(\dfrac{\mu_C^4 \left(1 - 4\beta_Y x_\infty + 4\beta_Y^2 x_\infty^2\right)}{\beta_Y^4 x_\infty^4 \gamma_Y^4} - \dfrac{4\mu_C^4 \left(\delta_Y + \mu_I \beta_Y x_\infty^2 - \mu_I x_\infty\right)}{\mu_I \beta_Y^3 x_\infty x_\infty^4 \gamma_X^4} \right) \end{cases}$$

The proof of Theorem 6.1 is given in Appendix A. The condition (6.11) provided by Theorem 6.1 is satisfied if and only if the eigenvalues of the Hermit matrix $\mathcal{H}(a_p)$ are strictly positive. Let's denote by Λ the vector containing the eigenvalues of the Hermit matrix $\mathcal{H}(a_p)$.

Example 6.1 *Considering the vector of nominal parameters p_{nom} defined in Table (6.1), we check the condition in Theorem 6.1 by computing the eigenvalues of the corresponding Hermit matrix:*

$$\Lambda = \begin{pmatrix} 0.9543 \\ 0.7176 \\ 0.0175 \end{pmatrix}$$

we can notice that the condition of Theorem 6.1 is satisfied, which is directly related to the fact that system (6.1) has the three real distinct equilibrium points $(41.45, 0.95)$, $(224.64, 0.72)$ *and* $(766.44, 0.02)$ *(see Figure 6.1).*

Example 6.2 *Let's consider the following parameters:*

$$\begin{cases} \mu_C = & 1.1497 \\ \mu_I = & 0.0024 \\ \delta_Y = & 0.2210 \\ \alpha_Y = & 0.0739 \\ \beta_Y = & 0.0046 \\ \gamma_X = & 1.0391 \\ x_\infty = & 780 \end{cases}$$

In this case, we obtain that the Hermit matrix has the following eigenvalues:

$$\Lambda = \begin{pmatrix} -0.003 \\ 0.5902 \\ 6.1589 \end{pmatrix}$$

which does not satisfy the condition in Theorem 6.1 since we have one negative eigenvalue. The roots of polynomial (6.6) obtained for this set of parameters are the following:

$$x_2 = \begin{pmatrix} 0.98 \pm 0.06i \\ 0.02 \end{pmatrix}$$

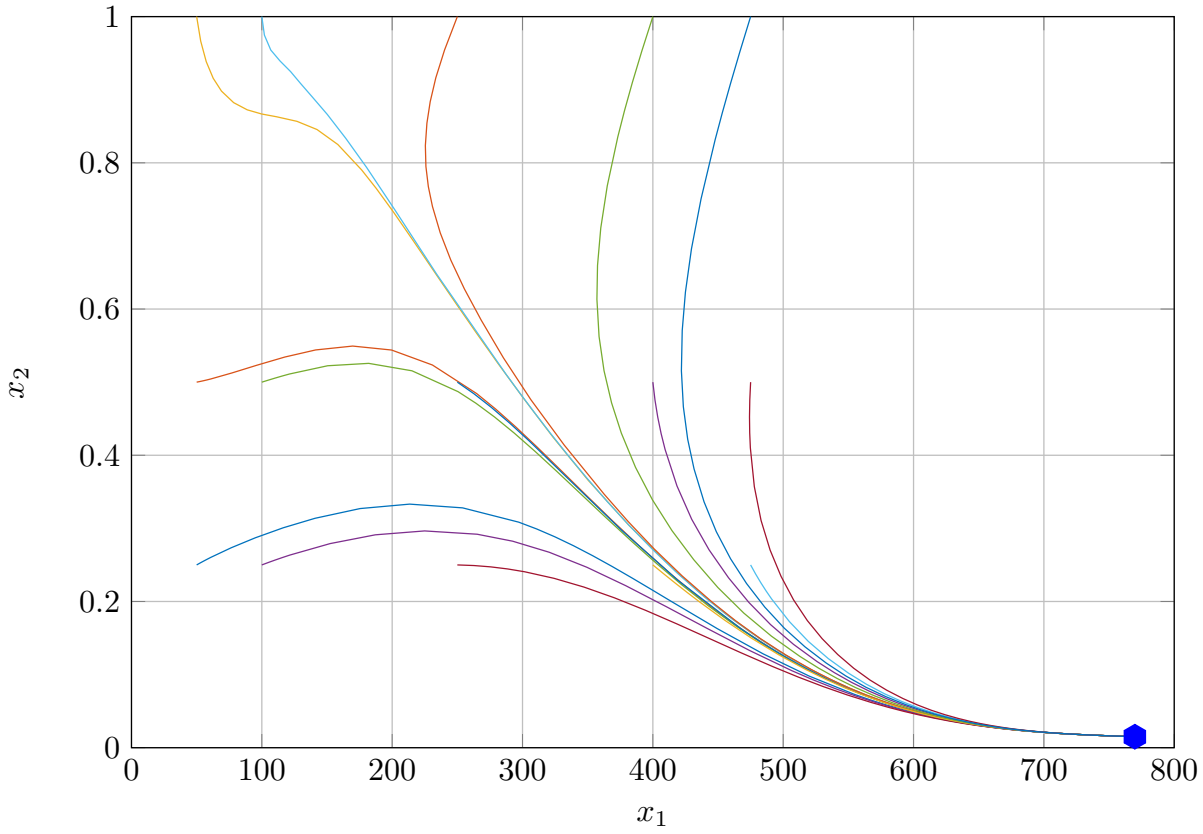

Figure 6.3: Example of the phase portrait of system (6.1), when its corresponding polynomial (6.6) has two complex roots.

In this case, we have only one real equilibrium point $(769.80, 0.02)$ *corresponding to the malignant equilibrium. Figure 6.3 shows the phase portrait corresponding to the set of parameters considered in this example. We can see that this phase portrait does not have the same characteristics as in Figure 6.1, where we have two locally asymptotically stable equilibria, the benign one corresponding to an acute tumor and the malignant one corresponding to its chronic state as well as the real saddle point.*

The condition of Theorem 6.1 allows us to check the admissibility of a given parameters vector. In addition to the satisfaction of this condition, one can check the positivity of the real equilibrium points after solving (6.5).

Definition 6.3 (Admissibility of p) *We say that a vector of parameters p is admissible if the condition of Theorem 6.1 is satisfied and the real distinct roots of (6.6) are positive.*

Definition 6.3 will be used in the sequel in the algorithm that we suggest to estimate the robust region of attraction of system (6.1).

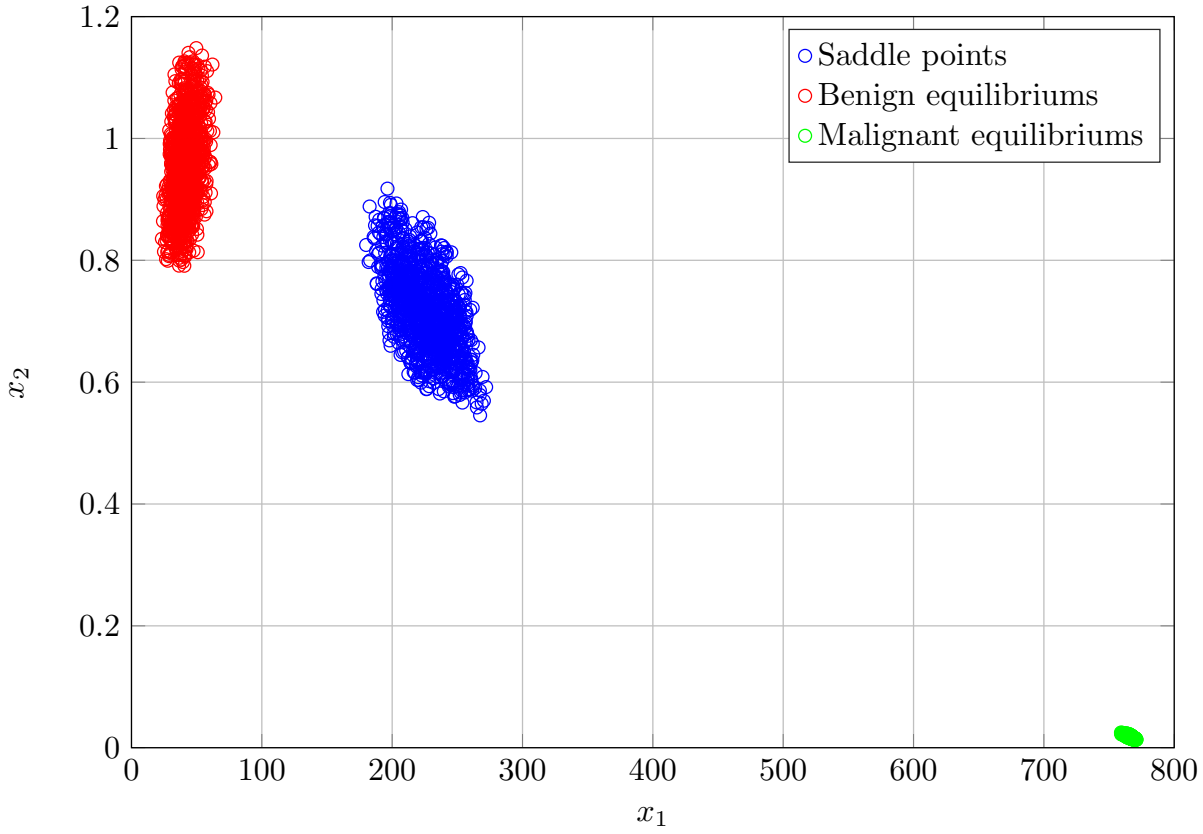

Figure 6.4: Distribution of equilibrium points under uncertainties, in red the benign equilibriums, in blue the saddle points and in green the malignant equilibriums.

6.1.4 Equilibrium points distribution

Let's consider that the vector of model parameters p is unknown and belong to the following interval:

$$[0.9p_{nom}, 1.1p_{nom}], \tag{6.12}$$

where p_{nom} stand for the vector containing nominal parameters in Table 6.1. We can draw the distribution of the equilibrium points of model (6.1), using Monte-Carlo tests corresponding to random selections of the model parameters in the given interval.

Figure 6.4 shows the distribution of the equilibriums of system (6.1) for 1600 uniformally distributed samples of model parameters in the given interval. This figure shows that the malignant equilibrium points are considerably less dispersed than the benign ones and the saddle points. For this choice of uncertainties interval, all the selected parameters vectors were admissible.

The distribution of the benign equilibrium points presented in Figure 6.4 will be used in Chapter 7, in order to characterize a certified set where the state trajectories converge to their respective benign equilibriums in spite of all possible parametric uncertainties meeting (6.12).

6.2 RoA estimation with bang-bang control

The cancer dynamical system (6.1) can be written as:

$$\dot{x} = F(x, u, p), \quad x(0) = x_0. \tag{6.13}$$

We denote by $\Phi_u(T, x_0, p)$ the solution of this system evaluated at time $T \geq 0$ for a given initial state x_0 using a control strategy $u(\cdot)$. Let's denote by Ω_u^p the controlled domain of attraction of system (6.1) with a bang-bang control strategy, for a given vector of parameters p. We consider the following state and input constraints sets:

$$\mathbb{X} = \left\{x \in \mathbb{R}_+^2 \mid \ x_2 \geq c\right\} \tag{6.14}$$

$$\mathbb{U} = \left\{u \in \mathbb{R}_+^2 \mid \ u_1, u_2 \in \{0, 1\}\right\} \tag{6.15}$$

The control input constraint set $\mathbb{U}$ in (6.15) allows to consider bang-bang control strategies.

Definition 6.4 *The RoA Ω_u^p of the controlled system (6.1) is defined as follows:*

$$\Omega_u^p = \left\{x_0 \in \mathbb{R}_+^2 | \ \exists u(\cdot) \ s.t. \ \Phi_u(T, x_0, p) \in \Omega_0^p, \ x \in \mathbb{X}, \ u \in \mathbb{U}\right\}. \tag{6.16}$$

where Ω_0^p is the previously defined region of attraction of the benign equilibrium x_b^p of system (6.1), without drugs, corresponding to the admissible parameters vector p. We

denote by $\mathbb{X} \subset \mathbb{R}^n$ and $\mathbb{U} \subset \mathbb{R}^m$ the sets of admissible values corresponding the state x and the control u, respectively.

Practically, (6.16) means that we set a therapy time T, then we characterize the set of initial conditions Ω_u^p such that for each initial state x_0 (information about the patient health) belonging to Ω_u^p, there exists at least one control law $u(\cdot)$, which allows to drive the states trajectories to the safe region Ω_0^p without violating the constraints on states and control inputs.

Problem 6.1 (Estimation of the nominal controlled RoA) *Given the nominal parameters vector p_{nom} and considering bang-bang control strategies, characterize the region of attraction of the controlled system (6.1).*

This region is denoted $\Omega_u^{p_{nom}}$ and provides the set of state initial conditions for which there exists a bang-bang control strategy denoted $u(\cdot)$, such that the states at the end of the treatment period (at time T) belong to the region of attraction of the benign equilibrium $\Omega_0^{p_{nom}}$ (the safe region for the nominal parameters vector p_{nom} without control inputs). Additionally, the state trajectories as well as the control inputs have to satisfy the constraints defined by the sets $\mathbb{X}$ and $\mathbb{U}$.

In this section, we present a methodology to estimate the region of attraction of system (6.1). Firstly, we characterize the domain of attraction for a given admissible parameters vector p. Then, in the next section, we provide a heuristic estimate of the robust region of attraction for model (6.1).

6.2.1 Characterizing the RoA for the nominal controlled system

Let's consider the vector of nominal parameters p_{nom} and bang-bang control strategies. Since we have only two control inputs u_1 and u_2 corresponding to chemotherapy and immunotherapy injections respectively, there are only four possible instantaneous injection strategies. We inject only chemotherapy, only immunotherapy, both of them or neither chemotherapy nor immunotherapy.

Let's denote these injection strategies as follows:

$\mathcal{S}_{0,0}$ No drug injection $u = (0, 0)$.

$\mathcal{S}_{1,0}$ Injection of chemotherapy $u = (1, 0)$.

$\mathcal{S}_{0,1}$ Injection of immunotherapy $u = (0, 1)$.

$\mathcal{S}_{1,1}$ Injection of both chemotherapy and immunotherapy $u = (1, 1)$.

By drawing the phase portrait of the injection strategies previously listed, we can have an information on all possible bang-bang strategies allowing to drive the states to the safe region, without constraints violation. This can help us to derive an estimate the set $\Omega_u^{p_{nom}}$ previously defined. This choice of strategies makes the constraints in (6.15) directly satisfied. The satisfaction of state constraints specified by (6.14) can be checked by drawing it in the phase portrait as well.

Figure 6.5 shows the phase portrait of system (6.1) using the drug injection schedules listed above. In this figure, we can notice that all the black trajectories corresponding to a continuous injection of chemotherapy violate the minimal constraint on immune cells density. We can notice also that the continuous injection of immunotherapy (represented by blue trajectories) allows to enlarge the domain of attraction of the benign equilibrium. Moreover, all the magenta trajectories, corresponding to a continuous injection of both chemo- and immunotherapy, converge to the safe region, which further enlarges the domain of attraction of the benign equilibrium. However, we can notice that for bigger initial cancer volumes, the magenta trajectories violate the minimal constraint on immune cells density.

Figure 6.5 shows all the possibilities of switching between the different strategies in order to drive the states to the safe region. An interesting option is to choose the strategy allowing to reduce the quantity of injected drugs or to minimize the hospitalization time. We do not further investigate this idea here, since we are interested in estimating the domain of attraction of system (6.1). Therefore, the only relevant information is the existence of at least one control strategy allowing to drive the states to the region of attraction of the benign equilibrium.

Since the strategy of injecting both therapies provides the biggest domain of attraction, we focus on the magenta trajectory that is tangential to the minimal constraint $x_2 \geq c$. This trajectory is depicted by **(1)** in Figure 6.6, we can notice also that in this region of the state space, the blue trajectories (with immunotherapy only) evolve above the constraint line, before converging to the malignant equilibrium. We are interested in characterizing the blue trajectory that is tangential to the magenta one (depicted by **(2)** in Figure 6.6) in order to further enlarge the domain of attraction of the controlled system (6.1). Note that for this specific initial state (represented in green in Figure (6.6)), the strategy to consider is to use immunotherapy till the state reaches the yellow point and then to use both chemotherapy and immunotherapy in order to satisfy the specified constraint.

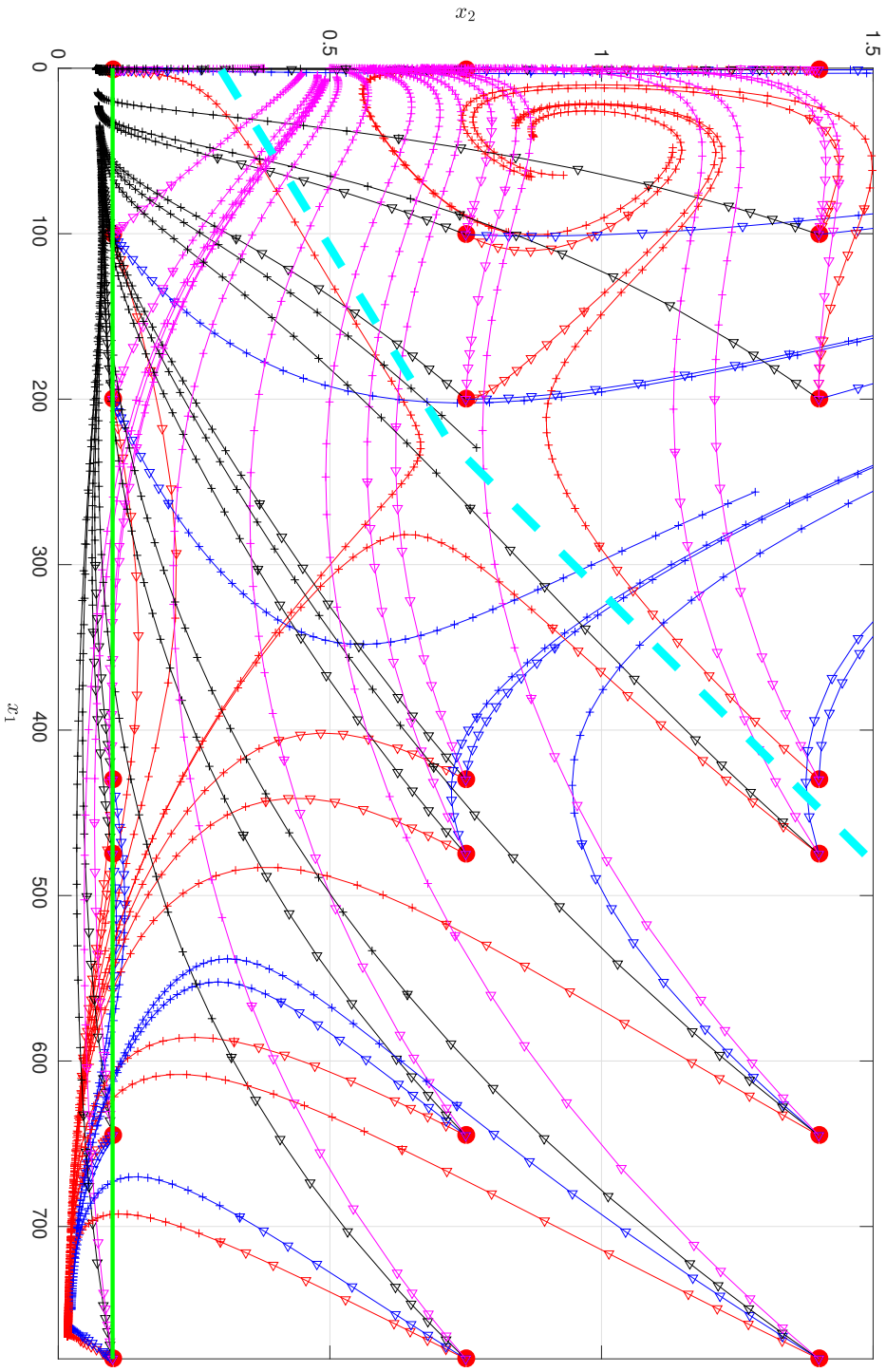

Figure 6.5: Phase portrait of system (6.1) with different drug injection strategies, the red trajectories correspond to $\mathcal{S}_{0,0}$, the black ones to $\mathcal{S}_{1,0}$, the blue ones to $\mathcal{S}_{0,1}$ and the magenta ones to $\mathcal{S}_{1,1}$, in green the minimal constraint on immune cells density, in dashed cyan the estimated nominal uncontrolled region of attraction of the benign equilibrium. The triangle sign denotes the beginning of a trajectory, whereas the sign + denotes its ending.

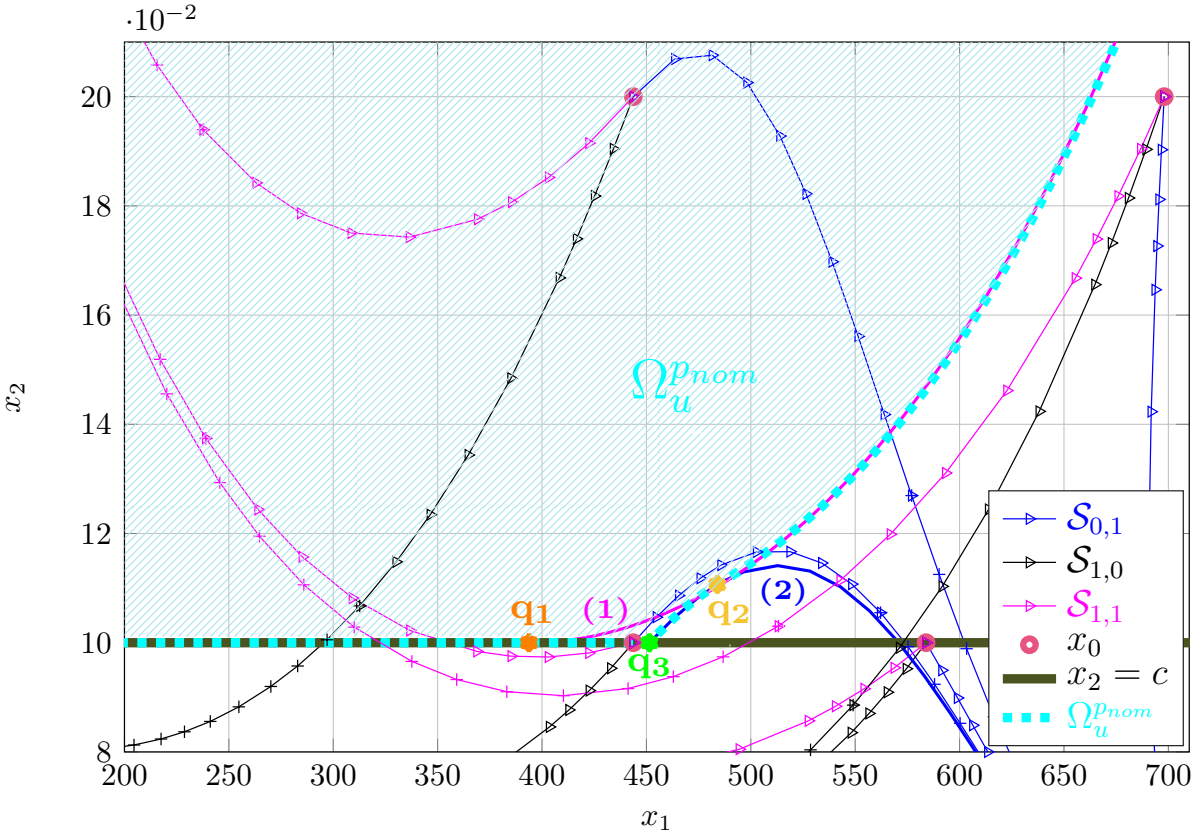

Figure 6.6: The three points q_1, q_2 and q_3 characterizing the RoA of model (6.1), and the resulting RoA that is an estimate of $\Omega_u^{p_{nom}}$ using nominal parameters is shown in cyan dashed line. The triangle sign denotes the beginning of a trajectory, whereas the sign + denotes its ending.

Let's denote the points characterizing the domain of attraction as follows:

$\mathbf{q_1} = (\mathbf{q_{11}}, \mathbf{q_{12}})$ The point where the magenta trajectory is tangential to the minimal constraint on immune cells density $x_2 \geq c$.

$\mathbf{q_2} = (\mathbf{q_{21}}, \mathbf{q_{22}})$ The point where the blue trajectory is tangential to the magenta one.

$\mathbf{q_3} = (\mathbf{q_{31}}, \mathbf{q_{32}})$ The point where the blue trajectory intersects with the constraint line.

In the sequel, we provide a generic methodology to derive the three points characterizing the domain of attraction of the controlled system (6.1).

Computing q_1

System (6.1) can be written as :

$$\begin{aligned} \dot{x}_1 &= F_1(x, u, p), \\ \dot{x}_2 &= F_2(x, u, p). \end{aligned} \tag{6.17}$$

In order to find q_1 we have to solve $F_2 = 0$ for $x_2 = c$ and $u = (1, 1)$, it implies solving the following equation:

$$-c\mu_I\beta_Y x_1^2 + c\mu_I x_1 + \alpha_Y - c\delta_Y + c\kappa_Y - c\eta_Y = 0. \tag{6.18}$$

Let q_{11} be the positive solution of (6.18), q_1 is defined as follows:

$$q_1 = (q_{11}, c). \tag{6.19}$$

Computing q_2

Let's denote the time inverse trajectory of (6.13) for $u = (1, 1)$, having as final point q_1, as $x_2 = g(x_1)$ and g_p as the polynomial approximation of g up to some degree. In order to find q_2, we have to solve the following equations:

$$\begin{aligned} &F(x, (0, 1), p) \times F(x, (1, 1), p) = 0, \\ &x_2 = g_p(x_1). \end{aligned} \tag{6.20}$$

Solving (6.20) implies solving the following equations system:

$$\begin{cases} -\mu_I\beta_Y\kappa_X x_1^3 x_2 + \left(\dfrac{\mu_c}{x_\infty} + \mu_I\kappa_X\right) x_1^2 x_2 + \gamma_X\eta_Y x_1 x_2^2 + \left(\kappa_X\kappa_Y - \delta_Y\kappa_X - \mu_c\eta_Y\right) x_1 x_2 \\ \quad +\kappa_X\alpha_Y x_1 = 0 \\ x_2 = g_p(x_1) \end{cases} \tag{6.21}$$

Finally, solving (6.21) provides an approximation of q_2.

Computing q_3

Let $x_2 = h(x_1)$ be the time inverse trajectory of (6.13) for $u = (0, 1)$, having as final point q_2. We denote by $x_2 = h_p(x_1)$ the polynomial approximation of this trajectory. Therefore, in order to find q_3, we need to solve the following equation:

$$h_p(x_1) - c = 0. \tag{6.22}$$

Solving (6.22) provides an approximation of q_{31} and q_3 is defined as follows:

$$q_3 = (q_{31}, c). \tag{6.23}$$

Note that the solutions of the equations allowing to derive the points q_1, q_2 and q_3 depend on the parameters vector p. However, one can validate the RoA structure afterwards, by checking the following conditions:

$$\begin{cases} q_{11} > 0, & q_{31} > q_{11} \\ q_{21} > q_{31}, & q_{22} > c \end{cases} \tag{6.24}$$

Remark 6.1 *The methodology allowing to derive the points q_1, q_2 and q_3 has been tested over 2000 scenarios, corresponding to uncertain parameters vectors, as defined in (6.12). We also checked, using the conditions in (6.24), that all these scenarios have the same characterization shown in Figure 6.6.*

6.2.2 Algorithm for the estimation of domains of attraction

After deriving the characteristic points as explained in the previous section, the region of attraction of the controlled system (6.1) is characterized by the following trajectory (see Figure 6.6):

$$x_2 = \mathcal{D}^p(x_1) = \begin{cases} c & \text{if } x_1 < q_{31} \\ h_p(x_1) & \text{if } q_{31} \leq x_1 \leq q_{21} \\ g_p(x_1) & \text{if } x_1 > q_{21} \end{cases} \tag{6.25}$$

The region of attraction Ω_u^p is defined as follows:

$$\Omega_u^p = \left\{ x \in \mathbb{R}^2 \mid x_2 \geq \mathcal{D}^p(x_1) \right\} \tag{6.26}$$

Algorithm 6.1 summarizes the methodology previously explained, allowing to derive the domain of attraction of the controlled system (6.1) for a given vector of parameters p and considering bang-bang control strategies.

Algorithm 6.1 Estimation of the RoA of the controlled system (6.1)

Input: p

Check if p is admissible (Definition 6.3)
Solve (6.18) to obtain q_1
Solve (6.20) to obtain q_2
Solve (6.22) to obtain q_3
Check the conditions in (6.24)
Derive Ω_u^p using (6.25)–(6.26)

Output: Ω_u^p

Figure 6.6 shows the estimated domain of attraction of system (6.1) denoted $\Omega_u^{p_{nom}}$, for nominal parameters p_{nom}, that we obtained using Algorithm 6.1. It also shows the trajectories corresponding to $\mathcal{S}_{1,0}$, $\mathcal{S}_{0,1}$ and $\mathcal{S}_{1,1}$ for different initial states, highlighting the fact that the state trajectories starting out of the estimated region of attraction, either converge to the malignant equilibrium or violate the specified constraint.

6.2.3 RoA sensitivity analysis

We showed in the previous section that the nominal domain of attraction of system (6.1) can be characterized by the points q_1,q_2 and q_3 (see Figure 6.6). In this section, we are

interested in investigating the sensitivity of the RoA estimation with uncertainties on the model parameters. Therefore, we change the parameters values with some percentages, in order to see the effect of this change on the estimation of the ROA.

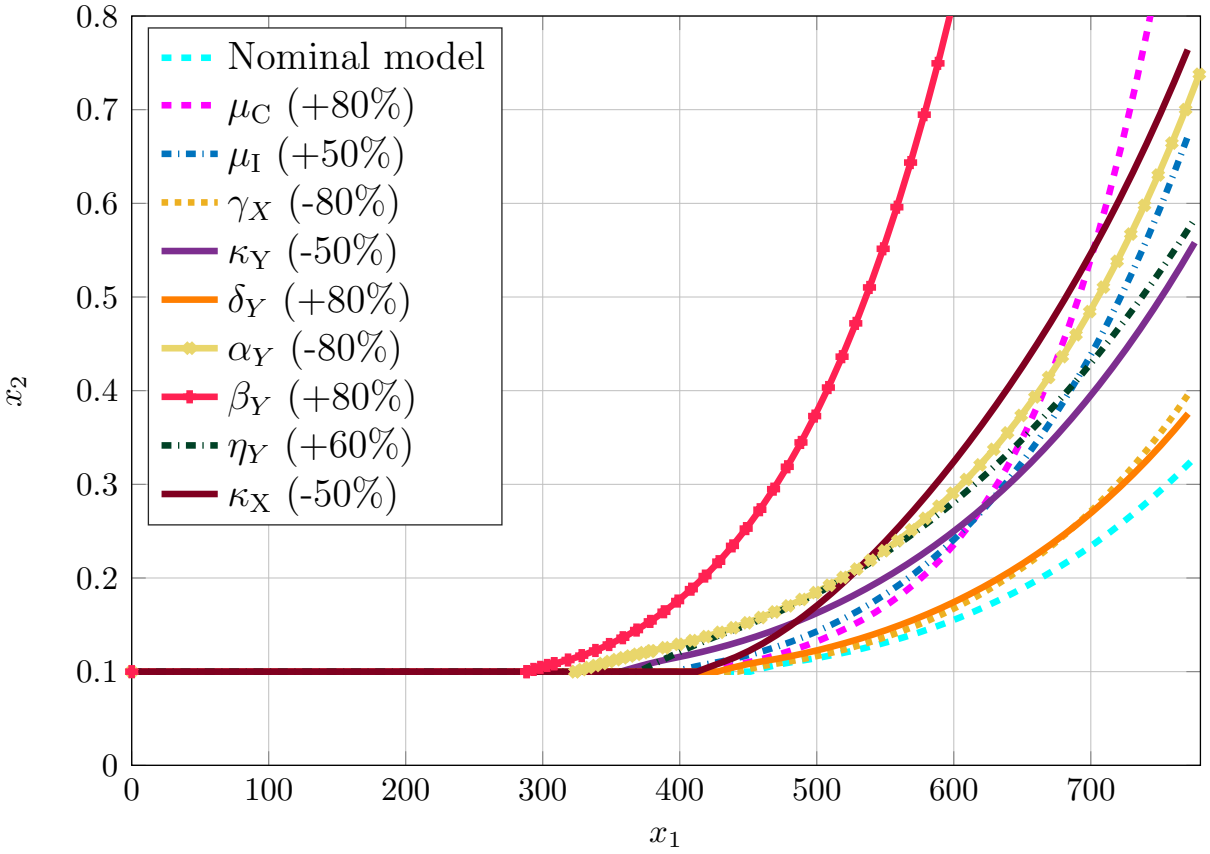

Figure 6.7: The sensitivity of RoA estimation with respect to the model parameters.

Figure 6.7 shows the nominal controlled RoA denoted $\Omega_u^{p_{nom}}$ in cyan dashed line. This figure shows also the RoA of system (6.1) for different changes in the model parameters. We notice that changing the parameters δ_Y and γ_X changes slightly the RoA estimation, whereas by changing the parameter β_Y the RoA volume decreases drastically. The other parameters show more or less the same sensitivity.

Remark 6.2 *The RoAs shown in Figure 6.7 are derived for deterministic parameters vectors, in the sense that we change one parameter value and derive the RoA for a fixed parameters vector.*

Note that the parameters changing signs (either + or −) have been chosen such that the RoA volume is reduced. Furthermore, the percentage of change has been chosen such that the parameters vector p remains admissible.

6.3 Heuristic estimate of the robust RoA

The characterization of the domain of attraction of a given system as explained in Problem 6.1 is interesting since it provides the set of initial conditions that can be driven to the safe region. However the common assumption made for such deterministic approaches is that the system parameters are perfectly known [18], which is not realistic for practical problems. As previously mentioned, system parameters are generally affected by uncertainties that can be described by probability distributions or belong to given intervals.

After characterizing the region of attraction of system (6.1) for a given parameters vector, it is interesting to find the domain of attraction when the model parameters are uncertain. This set is called the robust region of attraction and represents the set of initial conditions that can be driven to the safe region in spite of all possible uncertainties. The robust region of attraction is defined as the intersection of all the regions of attraction governed by (6.1) for all possible realizations of p [88].

Definition 6.5 *The robust region of attraction of system (6.13), for a given set of parameters $\mathbb{P}$, denoted $\Omega_u^{\mathbb{P}}$ is defined as follows:*

$$\Omega_u^{\mathbb{P}} = \bigcap_{p \in \mathbb{P}} \Omega_u^p. \tag{6.27}$$

Remark 6.3 *Note that this definition of the robust RoA means that there exists a control u for each initial state x_0 and parameters vector p. This can be seen as an outer approximation of the real robust RoA, which is indeed bigger.*

Problem 6.2 (Estimation of the robust controlled RoA) *Given an uncertain parameters vector p belonging to a set $\mathbb{P}$, we are interested in estimating the robust region of attraction of system (6.1), such that the state trajectories corresponding to the initial states in this set, belong to the safe region after some time and do not violate the specified constraints, in spite of all possible parametric uncertainties.*

It is commonly known that finding the exact robust region of attraction for a nonlinear system is a challenging task. Therefore, we aim here at providing a tighter estimate of the robust region of attraction $\Omega_u^{\mathbb{P}}$ that we denote Ω_R.

Let's denote by $\left\{p^{(j)}\right\}_{j=1}^{N}$ a collection of samples of the parameters vector p corresponding to model (6.1), uniformly drawn in the following interval:

$$[0.9p_{nom}, 1.1p_{nom}]\,. \tag{6.28}$$

In the previous section, a characterization of the RoA of system (6.1) for nominal parameters p_{nom} denoted by the set $\Omega_u^{p_{nom}}$ had been provided. This procedure can be

applied in order to derive the RoA of system (6.1) for each parameters sample $p^{(j)}$, by checking the validity of the characterization through the conditions (6.24).

We denote by $\Omega_u^{p^{(j)}}$ the RoA of the controlled system (6.1) considering the parameters vector $p^{(j)}$ and bang-bang control strategies.

In order to characterize the robust region of attraction, we perform N Monte-Carlo tests assuming that the samples $\left\{p^{(j)}\right\}_{j=1}^{N}$ are uniformly distributed in the interval (6.28). The intersection of all the sets $\Omega_u^{p^{(j)}}$, estimated for each sample $p^{(j)}$, is defined by the maximum of all the corresponding functions $\mathcal{D}^{p^{(j)}}$ (defined in (6.25)). Thus, the estimated robust region of attraction is the following:

$$\Omega_R = \{x \in \mathbb{R}^2 \mid x_2 \geq \mathcal{D}_R(x_1)\}, \tag{6.29}$$

where $\mathcal{D}_R(x_1)$ is defined as follows:

$$\mathcal{D}_R(x_1) = \max\left(\mathcal{D}^{p^{(1)}}(x_1), \cdots, \mathcal{D}^{p^{(N)}}(x_1)\right). \tag{6.30}$$

Algorithm 6.2 Robust RoA estimation

Input: $\left\{p^{(j)}\right\}_{j=1}^{N}, N$
  $\Omega_R \leftarrow \mathbb{X}$
  while $j \leq N$ **do**
    $\Omega_u^{p^{(j)}} \leftarrow$ Algorithm 6.1$\left(p^{(j)}\right)$
    $\Omega_R \leftarrow \Omega_R \cap \Omega_u^{p^{(j)}}$
    $j \leftarrow j + 1$
  end while
Output: Ω_R

Algorithm 6.2 allows to derive a heuristic estimate of the robust region of attraction of system (6.1), for N samples of parameters vectors, by intersecting their corresponding controlled regions of attraction.

Figure 6.8 shows the regions of attraction derived for N samples $p^{(j)}$, the estimated robust region of attraction for different number of samples N, using Algorithm 6.2. We can notice that the estimation of Ω_R is enhanced and the robust RoA volume is reduced as the number of samples N grows. We stopped running Algorithm 6.2 at $N = 2000$ since for bigger values of N the estimations of the robust RoA was almost the same as for $N = 2000$. Note also that the estimated robust RoA is considerably smaller than the nominal one, even with the uncertainties rate that is only $\pm 10\%$.

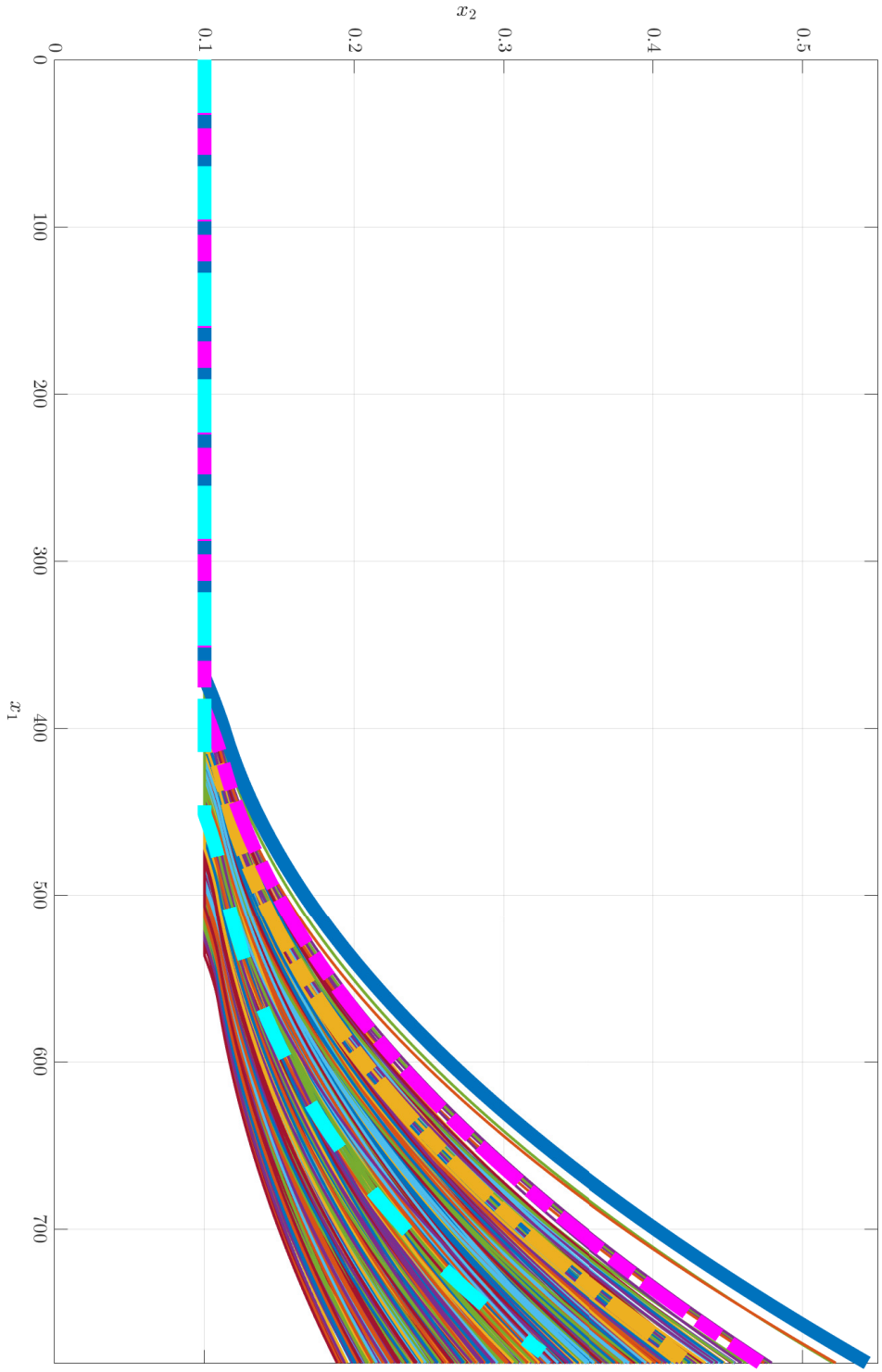

Figure 6.8: Monte-Carlo tests for the RoA estimation under ±10% of parametric uncertainties, the blue bold trajectory defines the estimated robust region of attraction of system (6.1) denoted Ω_R, for $N = 2000$, the pink trajectory defines the estimated robust RoA for $N = 1000$ and the orange one for $N = 200$, the dashed cyan trajectory is the estimated nominal domain of attraction $\Omega_u^{p_{nom}}$.

6.4 Conclusion

We presented in this chapter an extensive parametric analysis for a cancer dynamical system. This allowed us to provide necessary and sufficient conditions for the admissibility of the model parameters vectors. Furthermore, we investigated the effects of parametric uncertainties on the system equilibrium points, as well as on the estimation of regions of attraction.

Therefore, we used a readily applicable methodology, allowing to characterize the domain of attraction of a nonlinear system describing cancer dynamics, with bang-bang control strategies. Then, we used this approach to derive an estimation of the robust region of attraction.

It is important to point out the fact that regions of attraction might be highly sensitive to parametric uncertainties, and can be considerably reduced when considering even small uncertainties on the model parameters. This is critical in the context of cancer treatment, since such sets provide an information on the patients that can be healed, using appropriate treatments.

As previously mentioned, the methodology that we presented in this chapter characterizes the set of initial states for which there exists a control input, such that the state are driven to a stable equilibrium, however, it does not provide the control strategies to be used. In the next chapter, we propose a methodology to estimate a probabilistically certified region of attraction for a cancer model. Furthermore, we provide the corresponding control strategies allowing to drive the states to the benign stable equilibrium, in spite of all uncertainties realizations. The probabilistically certified RoA is intended to be less conservative than the robust one, since in the latter we consider the worst-case scenario for the RoA design. We will use the results of this chapter for comparison purposes.

Chapter 7

Probabilistically certified region of attraction of a tumor growth model

In this chapter, we are interested in estimating regions of attraction (RoAs) under parametric uncertainties for a cancer growth model with combined therapies. We propose to investigate a cancer growth dynamical model that is widely used in the literature. However, this model has never been investigated to estimate its region of attraction. Therefore, we aim at pointing out the importance of uncertainties considerations in RoA estimation for such models.

As mentioned in Chapter 6, the estimation of the region of attraction for cancer models is an interesting problem since it provides a set of possible initial conditions (tumor volume and immune density for example) that can be driven to a desired target set (benign region). This problem becomes complex when dealing with nonlinear systems and even more challenging for uncertain systems. There are some works which dealt with the problem of estimating the RoA for cancer models, see [69] and references therein, but only few of them considered model uncertainties. In particular, in [78], an iterative method to estimate the robust RoA was presented. However, robust RoA estimation is based on the worst-case scenario analysis leading to potentially pessimistic design. This because the worst-case is considered no matter how small its probability of occurrence is.

As shown in the previous chapters, even for low dimensional systems, the presence of parametric uncertainties can affect drastically the efficiency of a nominal controller as well as the size of the estimated RoAs. Therefore, we propose a framework of probabilistic certification, based on the randomized methods, in order to derive probabilistically certified RoAs of a cancer growth model. The model that we consider in this chapter describes the interaction between a tumor and the immune system in presence of a combined chemo- and immunotherapy. Furthermore, we model the concentration of the chemotherapy agent in the body via a pharmacokinetic equation.

The approach that we propose consists in probabilistically certifying the existence of a control structure, that drives the states corresponding to tumor cells and immune cells density, from an initial state set to a certified target set. This probabilistic certification

framework is based on the randomized methods proposed in [7] and [8], which, unlike the robust classical design, avoids focusing on few unlikely very bad scenarios allowing to overcome the conservatism of the robust RoA design.

The methodology that we suggest consists mainly of two steps. Firstly, we derive an ordered sequence of sets and a control strategy over each of them such that the states can be driven from a set to the previous with a certain probabilistic guarantee. The appropriate choice of the first set allows to insure that the union of the sets is a probabilistically certified approximation of the RoA. The second step consists in providing a global certification on the probability of convergence to the initial certified target set.

This chapter is organized as follows: In Section 7.1, the dynamical cancer model and the problem of RoA probabilistic certification are introduced. Section 7.2 recalls the randomized algorithms approach for probabilistic certification. In Section 7.3, a framework for RoA probabilistic certification is proposed, based on the randomized methods presented in [7] and [8]. In Section 7.4, the proposed RoA probabilistic certification framework is applied to the considered cancer model. Finally, Section 7.5 summarizes the contribution that we present in this chapter and compare it to the results of Chapter 6.

7.1 Dynamical model

The following nonlinear dynamical system describes the interaction between a tumor and the immune system in presence of chemotherapy and immunotherapy drugs:

$$\begin{aligned} \dot{x}_1 &= \mu_C x_1 - \frac{\mu_C}{x_\infty} x_1^2 - \gamma_X x_1 x_2 - \kappa_X x_1 x_3, \\ \dot{x}_2 &= \mu_I x_1 x_2 - \beta_Y \mu_I x_1^2 x_2 - \delta_Y x_2 + \kappa_Y x_2 u_2 - \eta_Y x_3 x_2 + \alpha_Y, \\ \dot{x}_3 &= -a_c x_3 + b_c u_1, \\ x(0) &= (x_1(0), x_2(0), x_3(0)) = x_0, \end{aligned} \tag{7.1}$$

where x_1, x_2 and x_3 denote, respectively, the number of tumor cells, the density of effector immune cells (ECs) and the concentration of chemotherapy in the body, u_1 and u_2 are, respectively, the dosages of a cytotoxic agent and an immuno-stimulator. This model has the advantage of being a low dimensional system that nevertheless includes the main aspects of cancer-immune interactions.

In many models it is assumed that the drug concentration is equal to its dosage which is an oversimplification. Therefore, we revisited the model proposed in [32] by adding a pharmacokinetic (PK) equation that allows to model the concentration of chemotherapy in the body. As previously mentioned, this model has been widely used in the literature for cancer drug scheduling.

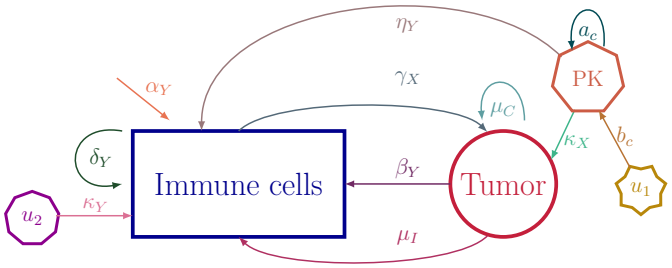

Figure 7.1: Schematic representation of the different interactions in model (7.1), between the tumor, the immune system and the drug dosages.

Table 7.1: Definitions and nominal values of the parameters used in model (7.1).

Parameter	Definition	Numerical value
μ_C	tumor growth rate	$1.0078 \cdot 10^7$ cells/day
μ_I	tumor stimulated proliferation rate	0.0029 day^{-1}
α_Y	rate of immune cells influx	0.0827 day^{-1}
β_Y	inverse threshold	0.0040
γ_X	interaction rate	$1 \cdot 10^7$ cells/day
δ_Y	death rate	0.1873 day^{-1}
κ_X	chemotherapeutic killing parameter	$1 \cdot 10^7$ cells/day
κ_Y	immunotherapy injection parameter	$1 \cdot 10^7$ cells/day
x_∞	fixed carrying capacity	$780 \cdot 10^6$ cells
η_Y	chemo-induced loss on immune cells	1
a_c	chemotherapy concentration decay	0.5
b_c	drug rate effect on the concentration of chemotherapy	1

Figure 7.1 presents a scheme describing the different interactions between the tumor and the immune system as well as the different injected drugs. Table 7.1 summarizes the definitions of the model parameters and their nominal values. We slightly tuned the values of some parameters since with the previous set of parameters values (used in Chapter 4 and 5 and taken from [32]), the domain of attraction of the benign equilibrium for the uncontrolled system (7.1) (for $u_1 = 0$ and $u_2 = 0$) was unrealistically big. This allowed us to solve a more challenging and seemingly realistic problem. Moreover, we properly chose the parameters a_c and b_c of the PK dynamics, such that the drug concentration reaches

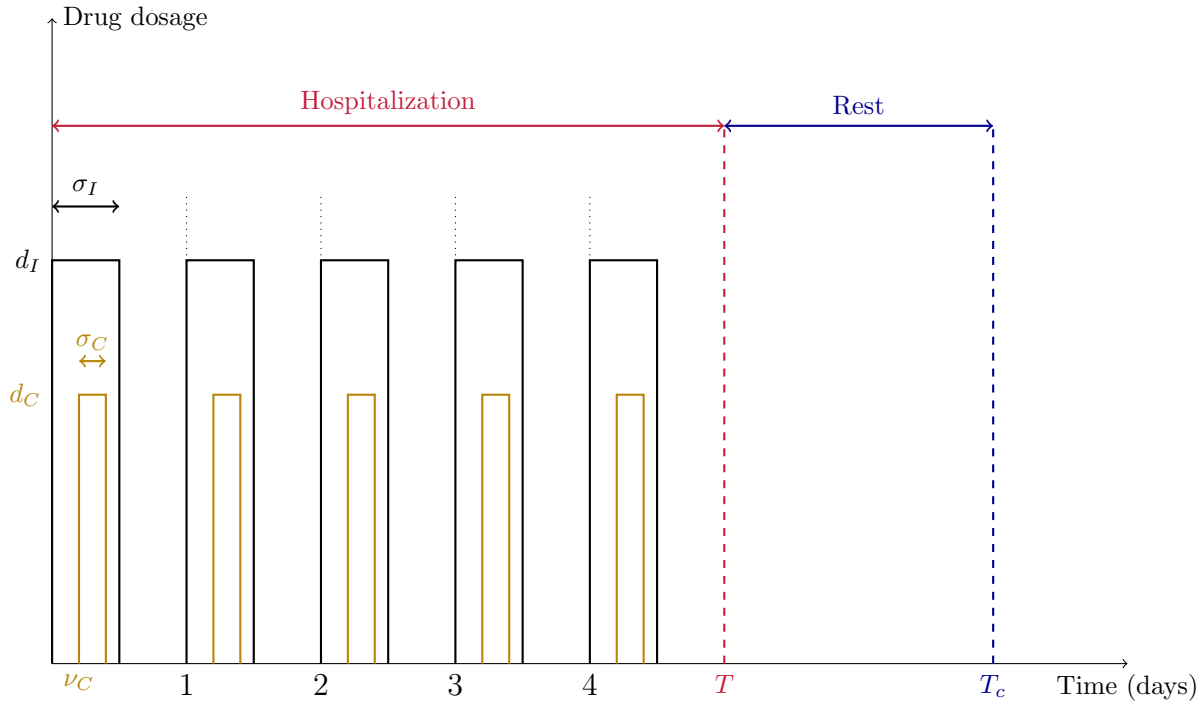

Figure 7.2: Temporal open-loop control structure for each cycle, in black and yellow, respectively, the immunotherapy and the chemotherapy profiles.

its maximum in $4.8h$ and starts decreasing towards a negligible value after a period of 15 days. Note that this is an example of a treatment protocol, nevertheless, it is worth emphasizing that in this chapter, we focus on the assessment of a methodology that remains applicable for different nominal and PK parameters values.

Let's denote by $x = (x_1, x_2, x_3)$ and $u = (u_1, u_2)$ respectively, the state and the control input vectors. In this chapter, we consider a cycle-based treatment, where the drugs are injected following N_C therapeutic cycles. Each cycle having two phases, a hospitalization period lasting 5 days, where the patient receives one injection per day, and a rest period where the patient recovers. Figure 7.2 shows a typical temporal combined control structure, the different notations in this figure are defined as follows:

$$\begin{cases} \sigma_I, \sigma_C : & \text{duration of immunotherapy and chemotherapy injections, respectively.} \\ d_I, d_C : & \text{concentration of immunotherapy and chemotherapy injections, respectively.} \\ \nu_C : & \text{the delay between chemotherapy and immunotherapy injections.} \\ T = 5 : & \text{hospitalization duration.} \\ T_c = 15 : & \text{cycle duration.} \end{cases}$$

Let's denotes by $\bar{d}_C$ the maximal desired concentration of x_3. Since x_3 and u_1 are linked through first order dynamics, $\bar{d}_C$ allows to monitor d_C. Therefore, for a given treatment cycle, the therapeutic profile considered in this chapter is completely defined by the following control parametrization θ:

$$\theta = [\nu_C, \sigma_C, \bar{d}_C, \sigma_I, d_I]. \tag{7.2}$$

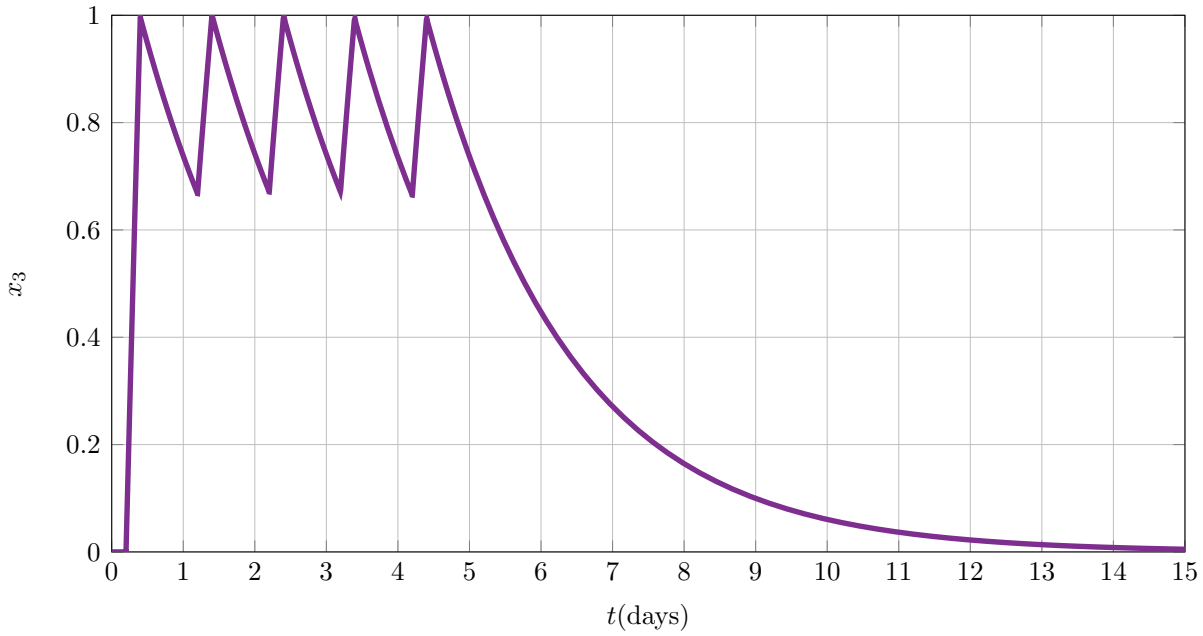

Figure 7.3: A typical PK evolution profile for chemotherapy, with 5 consecutive doses lasting $4.8h$, during the 5 first days of the therapy period, at a rate of one dose per day.

In cancer treatment design, we usually have some constraints to satisfy, they can be defined either on the states or on the control inputs. These constraints allow to prevent from drug toxicity and immune weakening. In this chapter, we consider the following constraints for all $t \in [0, T]$, with $T \in \mathbb{R}_+$:

$$x_2(t) \geq c, \text{ with } c \in \mathbb{R}_+, \tag{7.3}$$
$$0 \leq x_3(t) \leq 1, \tag{7.4}$$
$$0 \leq u_2(t) \leq 1, \tag{7.5}$$

where (7.3) is a health constraint on the minimal density of immune cells. The constraints on $x_3(t)$ and $u_2(t)$ for all t, are drug toxicity constraints. The constraint (7.4) on x_3 can be satisfied by properly choosing a constraint on u_1, given the PK parameters (a_c and b_c) since these two variables are linked through simple first order dynamics.

Figure 7.3 shows a typical PK evolution profile, where 5 consecutive doses of chemotherapy are injected, at a rate of 1 dose per day, each dose lasting $4.8h$. We can notice that thanks to a proper choice of the constraint on u_1, the constraint on x_3 is satisfied even for successive drug doses injections. Furthermore, the constraints on the control inputs, u_1 and u_2, can be satisfied by properly choosing the parametrization θ (namely, $\bar{d}_C$ and d_I) of the control input u. Therefore, we will consider only the constraint (7.3), since the satisfaction of the other constraints can be monitored by a proper choice of θ.

The uncontrolled model (7.1) (for $u = (0, 0)$) has two locally asymptotically stable equilibriums points. The macroscopic malignant equilibrium is $x_m = (766.4, 0.018, 0)$ and

the benign one is $x_b = (41.45, 0.954, 0)$. In general, the objective of the treatment is to drive the state initial conditions to the region of attraction of the benign equilibrium (safe region), without constraints violation. We are interested specifically in characterizing the set of initial conditions (tumor volume and immune density) from which the trajectories of (7.1) can be driven to the safe region under parametric uncertainties.

In Chapter 6, we proposed a methodology to characterize the controlled region of attraction of model (7.1) with bang-bang controls (without pharmacokinetics). Then, we used this approach to derive and estimate of the robust region of attraction. In this chapter, we propose to derive a probabilistically certified RoA for model (7.1), that is based on chance-constrained problems, tolerating some constraints violations provided that their corresponding probability is small enough. In the sequel, we will properly define what we mean by the probability of constraints violations being small enough, and we will introduce the problem of deriving probabilistically certified RoAs.

Definition 7.1 *We denote by Ω_0 a probabilistically certified region of attraction of many benign equilibrium points, corresponding to many parameters vector samples, when no control is applied to model (7.1), i.e. $u = (0, 0)$.*

The set Ω_0 can be interpreted here as a safe region, where we have a guarantee that if the state trajectories belong to Ω_0, they will converge to their respective benign equilibriums, in spite of all uncertainties realizations, with a confidence probability.

Problem 7.1 (Estimation of a probabilistically certified RoA) *We aim at computing a sequence of sets $\{\Omega_k\}_{k=1}^{N_C}$, for N_C therapeutic cycles. Those sets are determined in the space of the cancer burden (defined by the number of cancer cells) and the ECs density, such that, in the family of control parametrizations that we consider, there exists a therapeutic protocol that drives, with a desired probability, the states from Ω_{k+1} to $\bigcup_{j=0}^{k} \Omega_j$ without safety constraints violations.*

Similarly to Chapter 6, we denote by $\hat{\Omega}_0^{p_{nom}}$ an estimation of the region of attraction of the benign equilibrium for $u = (0, 0)$, when nominal model parameters (in Table 7.1) are considered.

7.2 Recall of the randomized algorithms for probabilistic certification

The randomized algorithms were presented in [87], [7] and [8] in order to solve optimization problems with probabilistic constraints satisfaction. In contrast to the standard robust control design, which is based on the worst-case scenario analysis leading hence to potentially pessimistic design, the randomized methods provide the possibility to avoid focusing on the worst scenarios if their probability of occurrence is small. Therefore, this framework is very interesting from the cancer treatment point of view, since the latter involves many uncertainties that have to be considered as mentioned in Chapter 2.

This section aims at briefly recalling the main key-points of the randomized methods that are important for the assessment of the approach that we propose in this chapter, in which we present a framework of estimation of probabilistically certified regions of attraction for a cancer therapies dynamical model.

Let's consider the following optimization problem :

$$\begin{array}{ll} \min\limits_{\theta\in\Theta} & J(\theta) \\ \text{s.t.} & \forall p \quad g_c(\theta,p)=0, \end{array} \tag{7.6}$$

where $\theta \in \Theta \subset \mathbb{R}^{n_\theta}$ is the decision variable (which can be a parametrization of a control law) and p is the uncertainties vector following the probability measure $\mathcal{P}$ defined in the set $\mathbb{P}$ (the vector p can contain for example model parameters that are considered to be uncertain), J is the cost to be minimized. In terms of control design for dynamical systems, the cost J can involve the states, the input variables, their respective integrals with respect to time or any combination of these indicators. Finally, g_c is an indicator function on the violation of some given constraints and is defined as follows:

$$g_c(\theta,p) := \begin{cases} 0 & \text{if all the constraints are satisfied} \\ 1 & \text{otherwise} \end{cases}$$

The randomized method consists in replacing the original hard problem in (7.6) by the following problem:

$$\begin{array}{ll} \min\limits_{\theta\in\Theta} & J(\theta) \\ \text{s.t.} & \Pr_{\mathcal{P}}\{g_c(\theta,p)=1\} \leq \eta, \end{array} \tag{7.7}$$

where the constraint is on the probability of constraints violation, giving therefore a soft constraint in the sense that we can accept a value of θ which minimizes the cost J, even if the constraints are violated for some realizations of p, provided that the probability of these violations is less than or equal to η (small enough). Even though the constraint in (7.7) simplifies the previous constraint in (7.6), the computation of the violation probability remains expensive. Authors in [7] and [8] proposed a simplification which consists

in replacing the probability by the mean value over N_p drawn independent identically distributed (i.i.d.) samples of p in $\mathbb{P}$ according to the probability distribution $\mathcal{P}$. Therefore, the simplified optimization problem is the following:

$$\begin{aligned} \min_{\theta\in\Theta} \quad & J(\theta) \\ \text{s.t.} \quad & \frac{\sum_{i=1}^{N_p} g_c\left(\theta, p^{(i)}\right)}{N_p} \leq \frac{m}{N_p}, \end{aligned} \tag{7.8}$$

where m is the number of constraints violations. In [7] and [8], several bounds on N_p are given such that the fulfillment of the constraint in (7.8) implies that the probability condition in (7.7) is satisfied with a confidence probability greater than or equal to $1-\delta$. Therefore, the N_p bounds that are derived involve the precision η and the confidence of fulfillment δ.

In this chapter, we are interested in specific control structures, since cancer treatment schedules are often defined by cycles with a hospitalization period where the patient receives several drug injections and a rest period for recovery. Therefore, it is more adequate in this case to consider that the controls are parametrized by a discrete variable θ with cardinality $n_\Theta \in \mathbb{N}$. This choice of θ simplifies the optimization problem (7.7), since it can be solved by a simple enumeration. In this case, the following proposition from [8] holds:

Proposition 7.1 *Let $m \in \mathbb{N}$ be any integer representing the number of accepted failures. Let $\delta \in (0,1)$ be a targeted confidence parameter. Take N_p satisfying*

$$N_p \geq \frac{1}{\eta}\left(m + ln\left(\frac{n_\Theta}{\delta}\right) + \left(2mln\left(\frac{n_\Theta}{\delta}\right)\right)^{\frac{1}{2}}\right) \tag{7.9}$$

then any solution of (7.8) in which $\{p^{(j)}\}_{j=1}^{N_p}$ are i.i.d. following the probability distribution $\mathcal{P}$ satisfies the constraint in (7.7) with a probability greater than or equal to $1-\delta$

The inequality (7.9) is mathematically based on the binomial distribution. In this section, we presented a concise overview of the basic theoretical aspects of this methodology, the readers interested in further mathematical proofs should refer to [8].

It is interesting to notice that the bound on N_p provided by Proposition 7.1 does not depend on the dimension of p which is useful when having many uncertain parameters in the certification problem. Furthermore, as we can see in Table 7.2, since the confidence parameter δ affects the bound logarithmically, we can have a highly confident certification with a tractable number of random samples.

Table 7.2: The evolution of the number of samples N_p required to achieve the certification, with respect to the confidence design parameter δ and the number of control parametrizations n_Θ, for $\eta = 10^{-2}$ and $m = 1$.

n_Θ	$\delta = 0.1$	$\delta = 0.01$	$\delta = 0.001$
10	864	1162	1451
100	1162	1451	1732
1000	1451	1732	2008
10000	1732	2008	2280

Furthermore, for a specific desired confidence parameter $\delta = 10^{-3}$, Table 7.3 provides an idea on the evolution of the number of trials N_p that should be performed for each possible control law θ, with respect to the precision parameter η and the number of control parametrizations n_Θ. Therefore, the total number of simulations is $N_{sim} = N_p \cdot n_\Theta$.

Table 7.3: The evolution of the number of samples N_p required to achieve the certification, with respect to the precision design parameter η and the number of control parametrizations n_Θ, for $\delta = 10^{-3}$ and $m = 1$.

n_Θ	$\eta = 0.1$	$\eta = 0.01$	$\eta = 0.001$
10	146	1451	14503
100	174	1732	17312
1000	201	2008	20073
10000	228	2280	22796

This approach provides a powerful pragmatic tool allowing to certify control strategies. In [4], a randomized method based framework for probabilistic certification of feedback control strategies has been proposed for a combined cancer therapy model.

7.3 Probabilistic certification of ROA

In this section, we will establish a framework of RoA probabilistic certification, based on the randomized methods presented in the previous section. We propose to use this general framework in order to probabilistically certify the existence of a control structure which allows to drive initial states from a given set to a target set under parametric uncertainties.

Let's rewrite system (7.1) into the following form:

$$\dot{x} = F(x, u, p), \tag{7.10}$$

where p is the vector of parameters that model (7.1) involves. Furthermore, we consider that the variables of system (7.10) are subject to the following constraints:

$$x \in \mathbb{X}, \quad x(T) \in \Omega, \quad u \in \mathbb{U}. \tag{7.11}$$

As previously mentioned, we consider that the control inputs are parametrized by a vector θ which lies in a discrete set Θ with cardinality $n_\Theta \in \mathbb{N}$. This choice of θ fits particularly to the case of cancer therapy design, since some of the parameters involved in the treatment scheduling are naturally quantified.

Suppose that the parameters vector p is a random variable following the probability distribution $\mathcal{P}$ that we denote $p \sim \mathcal{P}$. Given a set $\Gamma \subseteq \mathbb{R}^n$ (to be more precise, Γ must belong to the σ-algebra defined on $\mathbb{R}^n$) and a parameterization of the input $\theta \in \Theta$, let's consider the following optimization problem:

$$\begin{aligned} \min_{\theta \in \Theta} \quad & J(\theta) \\ \text{s.t.} \quad & \forall\, (x_0, p) \in (\Gamma \times \mathbb{P}) \qquad g_c(\theta, x_0, p) = 0, \end{aligned} \tag{7.12}$$

where $J(\theta)$ is a cost function to be minimized. In terms of cancer treatment design, this function can be a combination of many objectives that one seeks to achieve, for example reducing the quantity of injected drugs, to prevent from toxicity, or reducing the duty cycle in order to reduce the hospitalization duration. g_c is the failure indicator function, defined on the state trajectories of (7.10). The function g_c is deterministic such that, for a given initial state, an input parametrization θ and a model parameters vector $p \in \mathbb{P}$, it is equal to one if the constraints (7.11) are violated, during at least some instant on the trajectory, zero otherwise. Problem (7.12), then, aims at selecting the optimal control strategy such that no constraints violation occurs.

As previously explained, the randomized method consists in replacing the original problem in (7.12) by the following chance-constrained problem tolerating some violations:

$$\begin{aligned} \min_{\theta \in \Theta} \quad & J(\theta) \\ \text{s.t.} \quad & \Pr_{\mathcal{X}_0(\Gamma) \times \mathcal{P}} \{ g_c(\theta, x_0, p) = 1 \} \leq \eta, \end{aligned} \tag{7.13}$$

where the constraint is on the probability of violation, with respect to the distribution of x_0 on Γ, that we denote $\mathcal{X}_0(\Gamma)$, and $p \sim \mathcal{P}$. This problem gives therefore a chance-constrained formulation in the sense that we can accept a vector θ which minimizes the cost J, even if the constraints are violated for some realizations of (x_0, p), provided that the probability of these violations is lower than η, hence small enough.

Since problem (7.13) is hard to solve, it can be simplified into the following problem, employing the empirical mean instead of the probability of the constraints violation:

$$\begin{aligned} \min_{\theta\in\Theta} \quad & J(\theta) \\ \text{s.t.} \quad & \sum_{i=1}^{N} g_c\left(\theta, x_0^{(i)}, p^{(i)}\right) \leq m, \\ & (x_0, p)^{(i)} \sim \left(\mathcal{X}_0(\Gamma) \times \mathcal{P}\right), \ \forall i = 1, \ldots, N, \end{aligned} \tag{7.14}$$

where m is the maximum number of allowed constraints violation.

Theorem 7.1 *Given $\Gamma \subseteq \mathbb{R}^n$, let $m \in \mathbb{N}$ be any integer, and $\delta \in (0,1)$ a targeted confidence parameter, and suppose that problem (7.14) has a solution, that we denote $\hat{\theta}$, for N i.i.d. samples of (x_0, p), with N satisfying the following condition from [8]:*

$$N \geq \frac{1}{\eta}\left(m + \ln\left(\frac{n_\Theta}{\delta}\right) + \left(2m\ln\left(\frac{n_\Theta}{\delta}\right)\right)^{\frac{1}{2}}\right)$$

Then the solution $\hat{\theta}$ satisfies the constraint in problem (7.13) with a probability higher than $1-\delta$.

In the next section, we will explain how the iterative resolution of problems of the type (7.14) allows one to generate a sequence of sets $\{\Omega_k\}_{k=1}^{N_C}$ such that the constraints violation on passing from Ω_{k+1} to $\bigcup_{j=0}^{k}\Omega_j$ is smaller then η with a certain desired confidence probability $1-\delta$.

7.3.1 Algorithm for RoA estimation

Given a target set Ω, our objective is to certify that the set Γ is such that there exists a control parametrization θ, for which at least $100\cdot(1-\eta)\%$ of the trajectories of (7.10), generated by the distributions of the initial states $x_0 \in \Gamma$ and the uncertain parameters p, converge to Ω at time T, while satisfying constraints (7.11), with a confidence higher than $1-\delta$. Any solution of (7.14) defines a local control strategy that satisfies the constraints while minimizing the cost $J(\theta)$.

Γ generator

We suppose that we have a generator of sets Γ with a parametrized geometry providing a family of nested potential sets Γ, then we can compute the biggest one that is probabilistically certified through (7.14). In the case under study, we consider that the sets Γ have a polytopic form.

Therefore, starting from Ω_0 which is in the certified region of attraction of many benign equilibriums without therapies, an iterative procedure can be designed to generate

the sequence $\{\Omega_k\}_{k=0}^{N_C}$ such that the trajectories starting in Ω_{k+1} end in $\bigcup_{j=0}^{k}\Omega_j$ with the desired probability and without violating the constraints. In particular, we will consider sequences of sets such that $\Omega_k \cap \Omega_{k+1} = \emptyset$. Then, we keep doing this certification process until given Ω_{k-1}, the set Ω_k is empty. Once the RoA probabilistic certification algorithm terminates, the candidate to be a probabilisitically certified RoA is the set $\Omega_C = \bigcup_{i=1}^{N_C}\Omega_i$.

Note that, if $x_0 \in \Omega_k$, for $k = 1, \cdots, N_C$, this means that the trajectory of length T will end in $\bigcup_{j=0}^{k-1}\Omega_j$ without violating the constraint with a certain probability, but no direct probabilistic guarantee is given regarding the convergence to the set Ω_0.

It is not straightforward to derive a probabilistic bound on driving the states directly from the last set of the sequence Ω_{N_C} to Ω_0. This is because the latter probability involves the accuracy and confidence parameters, η and δ. Another reason is that, there is no guarantee that, given the initial state distribution $\mathcal{X}_0(\Omega_k)$, the distribution of the state at the end of the k-th therapeutic cycle is $\mathcal{X}_0(\Omega_{k-1})$, for which the probabilistic validation is performed. However, after deriving the sequence of certified sets, we can approximate the probability of driving the states from Ω_{N_C} to Ω_0, with the corresponding certified control strategy, using Monte-Carlo simulations.

Algorithm 7.1 Sequence of probabilistically certified sets

Input: Ω_0

$k \leftarrow 0$

while $\Omega_k \neq \emptyset$ **do**

$\Omega \leftarrow \bigcup_{j=0}^{k}\Omega_j$

repeat

Generate Γ

until (7.14) is unfeasible for Γ

$k \leftarrow k + 1$

$\Omega_k \leftarrow \Gamma$

end while

$N_C \leftarrow k - 1$

Output: $\Omega_C \leftarrow \bigcup_{i=0}^{N_C}\Omega_i$

Finally, by using Algorithm 7.1, we can obtain a sequence of certified sets, such that the output is the candidate to be a probabilistically certified RoA Ω_C.

7.4 Probabilistically certified RoA for a cancer model

As previously explained, considering N_C treatment cycles, our objective consists in estimating the probabilistically certified RoA of model (7.1) that we denote Ω_C. To this end, we certify a sequence of successive disjoint sets such that their union is the candidate to be a probabilistically certified RoA.

Moreover, the temporal control profiles that we consider correspond only to the hospitalization period (see Figure 7.2), meaning that the rest period is not included in the decision variable θ defined in Section 7.1, since we assume that this parameter can be estimated afterwards depending on the health conditions of the patient.

Therefore, we propose a feedback control strategy that can be seen in an implicit way, such that at the end of each therapy period, we measure the states (patient health and tumor volume) and depending on the certified set Ω_k where this measure lies, we can estimate the maximal possible recovery time $(T_c - T)$ that the patient can take. At the end of the rest period, the certified therapy corresponding to this set is then applied, we keep doing this process until we reach the safe region Ω_0.

The initial condition x_0 is assumed to be uniformly distributed in the set Γ while the parameters of model (7.1) are assumed to be normally distributed in the following interval:

$$[0.9p_{nom}, 1.1p_{nom}], \tag{7.15}$$

where p_{nom} is the nominal value of each parameter and the variance of these distributions is 0.01. The parameter x_∞ is supposed to be known.

The failure indicator function, which determines whether the constraints (7.3)–(7.5) are satisfied or not, is defined on $x(t|x_0, p, \theta)$ which is the state trajectory of (7.1) for a given control parametrization θ and a random sample of x_0 and p. We denote by $x(T|x_0, p, \theta)$ the state trajectory evaluated at the end of the hospitalization period. Therefore, the failure indicator is defined as:

$$g_c(\theta, x_0, p, \Omega) := \begin{cases} 0 & \text{if } x_2(t|x_0, p, \theta) \geq c \ \ \forall t \ \text{ and } \ x(T|x_0, p, \theta) \in \Omega \\ 1 & \text{otherwise} \end{cases}$$

where Ω is a probabilistically certified target set which can be seen as the safe region to attain at the end of the cycle.

Using Algorithm 7.1, we can derive a sequence of probabilistically certified sets providing the probabilistically certified RoA. Firstly, we need to derive an initial target set Ω_0, in order to initialize the certification algorithm.

7.4.1 Probabilistically certified initial target set Ω_0

Definition 7.2 *Given $p \in \mathbb{P}$ (drawn according to the probability distribution $\mathcal{P}$) and x_0 following a uniform distribution on Ω_{eq}, we denote by Ω_{eq} a certified set in a neighbor-*

hood of benign equilibriums of (7.1), generated by the realizations of p according to the probability distribution $\mathcal{P}$. Therefore Ω_{eq} is derived such that:

$$\Pr_{\mathcal{U}(\Omega_{eq})\times\mathcal{P}}\{x_2(t|x_0,p)\geq c,\ \forall t>0 \text{ and } x(T|x_0,p)\in\Omega_{eq}\}>1-\eta. \tag{7.16}$$

Note that Ω_{eq} is slightly different than a probabilistically certified invariant set, since we don't require that the trajectories starting in Ω_{eq} stay in it, we rather require that these trajectories satisfy the constraints (7.3)–(7.5) and converge to Ω_{eq} after some time T.

Given p belonging to $\mathbb{P}$ and x_0 following a uniform distribution on Ω_0, that we denote $\mathcal{U}(\Omega_0)$, Ω_0 is determined such that:

$$\Pr_{\mathcal{U}(\Omega_0)\times\mathcal{P}}\{x_2(t|x_0,p)\geq c,\ \forall t>0 \text{ and } x(T|x_0,p)\in\Omega_{eq}\}>1-\eta, \tag{7.17}$$

for a given time T. Note that the set Ω_{eq} is derived to be used as a target set for the determination of Ω_0.

In order to provide an estimation of Ω_{eq}, we draw the distribution of the benign equilibriums of model (7.1) for many parameters vector samples (selected according to the probability distribution $\mathcal{P}$). Then, we choose a geometry for Ω_{eq} surrounding the benign equilibriums of the sample shown in Figure 7.4. Finally, we expand this set until (7.16) is not satisfied.

After finding a proper geometry for the set Ω_{eq} such that it satisfies (7.16), we use Algorithm 7.1 in order to provide an estimation of the certified set Ω_0. Note that in this case $\mathcal{X}_0(\Gamma)$ corresponds to $\mathcal{U}(\Omega_0)$ since we assume that x_0 is uniformly distributed on Ω_0, and the target set for the states at time T denoted Ω in the definition of g_c corresponds to Ω_{eq}. Furthermore, since we deal with an uncontrolled problem, we have $\theta=0$. Therefore, (7.7) turns out to be a feasibility problem, where we need only to guarantee the probability condition in (7.17) by using the empirical mean over g_c for N i.i.d. samples of (x_0,p) mentioned in (7.14), with $\theta=0$ and $n_\Theta=1$, with the bound N given by Theorem 7.1.

We assume that the set Ω_0 to be certified has the same geometry as the estimated nominal uncontrolled region of attraction $\hat{\Omega}_0^{p_{nom}}$ (derived in Chapter 6) that we shrink until (7.17) is not satisfied given the confidence probability $1-\delta$. There is clearly no guarantee that the set Ω_0 that we obtain is the biggest possible certified set, however, in this case, proving the existence of a set Ω_0 satisfying (7.17) is enough, since Ω_0 is only used as a target set for the Algorithm 7.1 allowing therefore to compute the sequence of certified sets.

Figure 7.4 shows the probabilistically certified RoA of the benign equilibriums Ω_{eq}, the estimated uncontrolled nominal region of attraction $\hat{\Omega}_0^{p_{nom}}$ and the initial probabilistically certified target set Ω_0 for different T. Figure 7.5 shows the phase portrait of (7.1) with both the estimated nominal RoA $\hat{\Omega}_0^{p_{nom}}$ without control, and the certified initial target set Ω_0 for $T=60$. We can see that the Ω_0 is smaller than $\hat{\Omega}_0^{p_{nom}}$ which shows the effects of parametric uncertainties consideration.

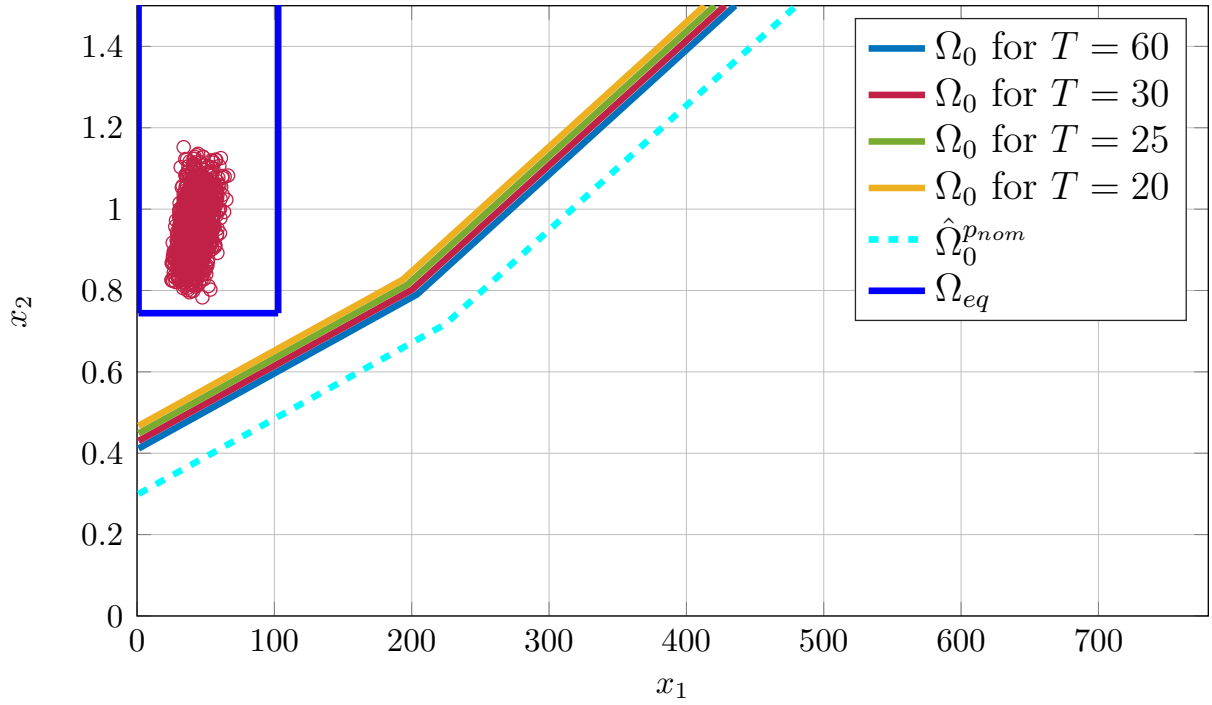

Figure 7.4: Probabilistically certified sets Ω_0 for different horizons T.

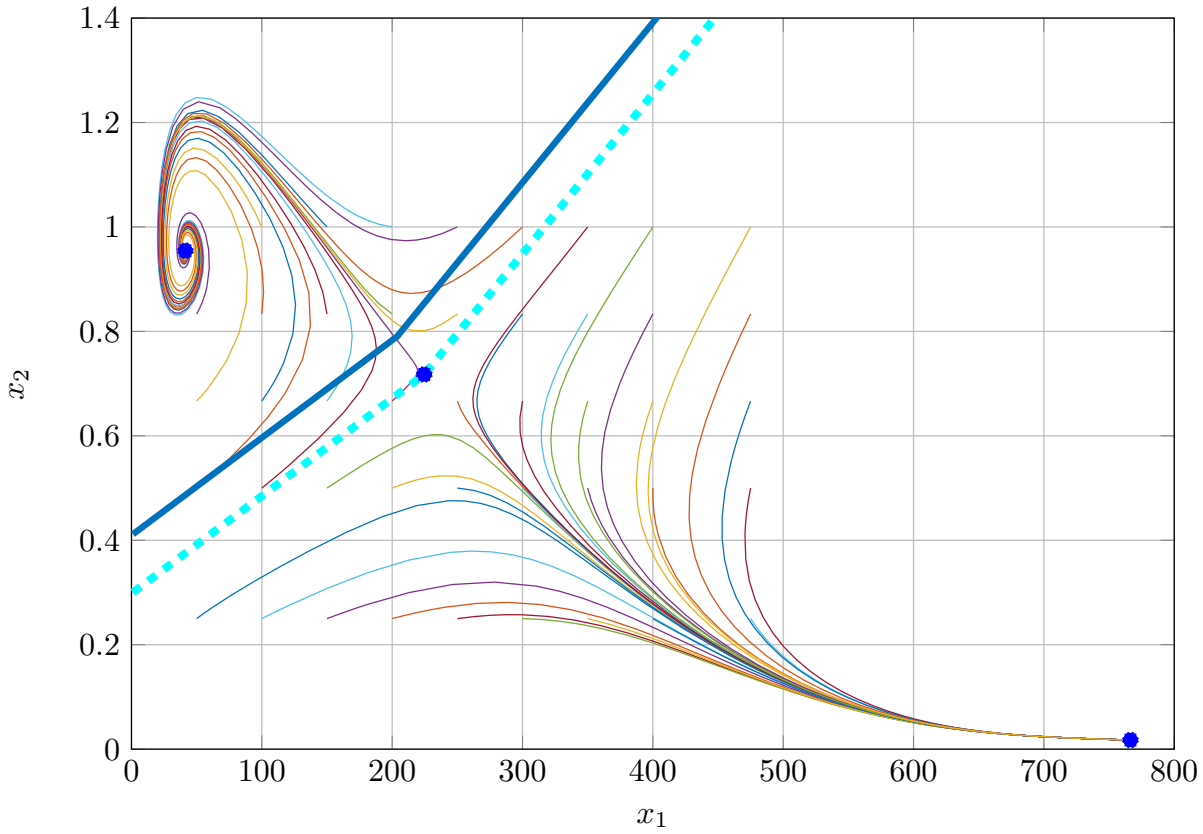

Figure 7.5: Phase portrait of (7.1), estimated nominal uncontrolled RoA $\hat{\Omega}_0^{p_{nom}}$ in dashed cyan and the estimated certified initial target set Ω_0 for $T = 60$ in blue.

7.4.2 Validation of the estimation of Ω_0

In order to validate the estimation of the target set Ω_0, we carry out 5000 Monte-Carlo simulations by randomly selecting the initial states as well as the model parameters according to their respective probability distributions. We can notice that in Figure 7.6 there are only 11 trajectories that converge to the malignant equilibrium, violating thereby the specified constraints. This corresponds to 99.78% of successful trajectories, validating therefore the imposed probabilistic bound.

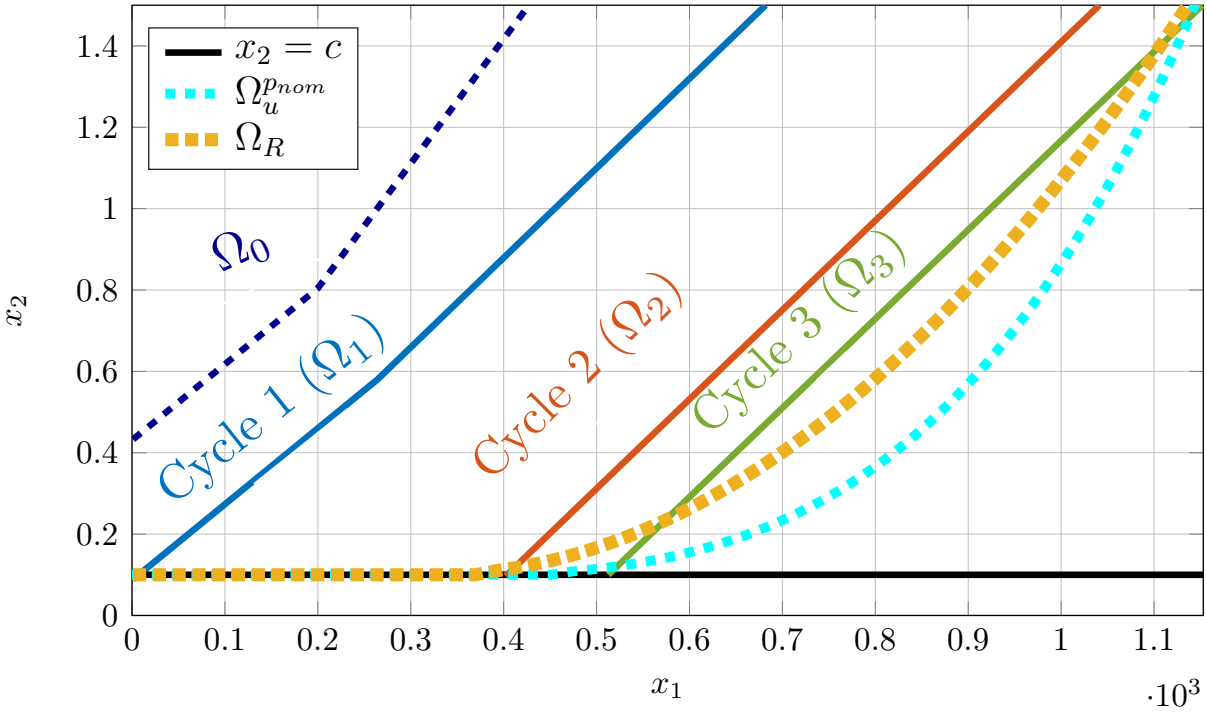

Figure 7.7: Probabilistically certified RoAs for 3 injection cycles.

7.4.3 Probabilistically certified region of attraction Ω_C

We denote by Ω_C the probabilistically certified region of attraction of system (7.1). We initialize Algorithm 7.1 with Ω_0 in order to derive the sequence of probabilistically certified sets providing the certified RoA for model (7.1).

We consider that the decision variable θ is defined by the following variables:

$$\begin{cases} \sigma_I \in \{0, 0.16, 0.32, 0.48, 0.64, 0.8\}, \\ \sigma_C = 0.2, \quad \nu_C = 0.2, \\ d_I \in \{0, 0.25, 0.5, 0.75, 1\}, \\ \bar{d}_C \in \{0, 0.11, 0.22, 0.33, 0.44, 0.56, 0.67, 0.78, 0.89, 1\}. \end{cases}$$

Therefore, the cardinality of Θ is $n_\Theta = 300$ giving the bound $N \geq 1863$ according to Theorem 7.1, for $m = 1$, $\eta = 10^{-2}$ and $\delta = 10^{-3}$. The number of simulations to be performed for each set certification is $N_{sim} = N \cdot n_\Theta = 558900$. The required computational time to perform N_{sim} simulations is less than 6 mn using Matlab coder toolbox.

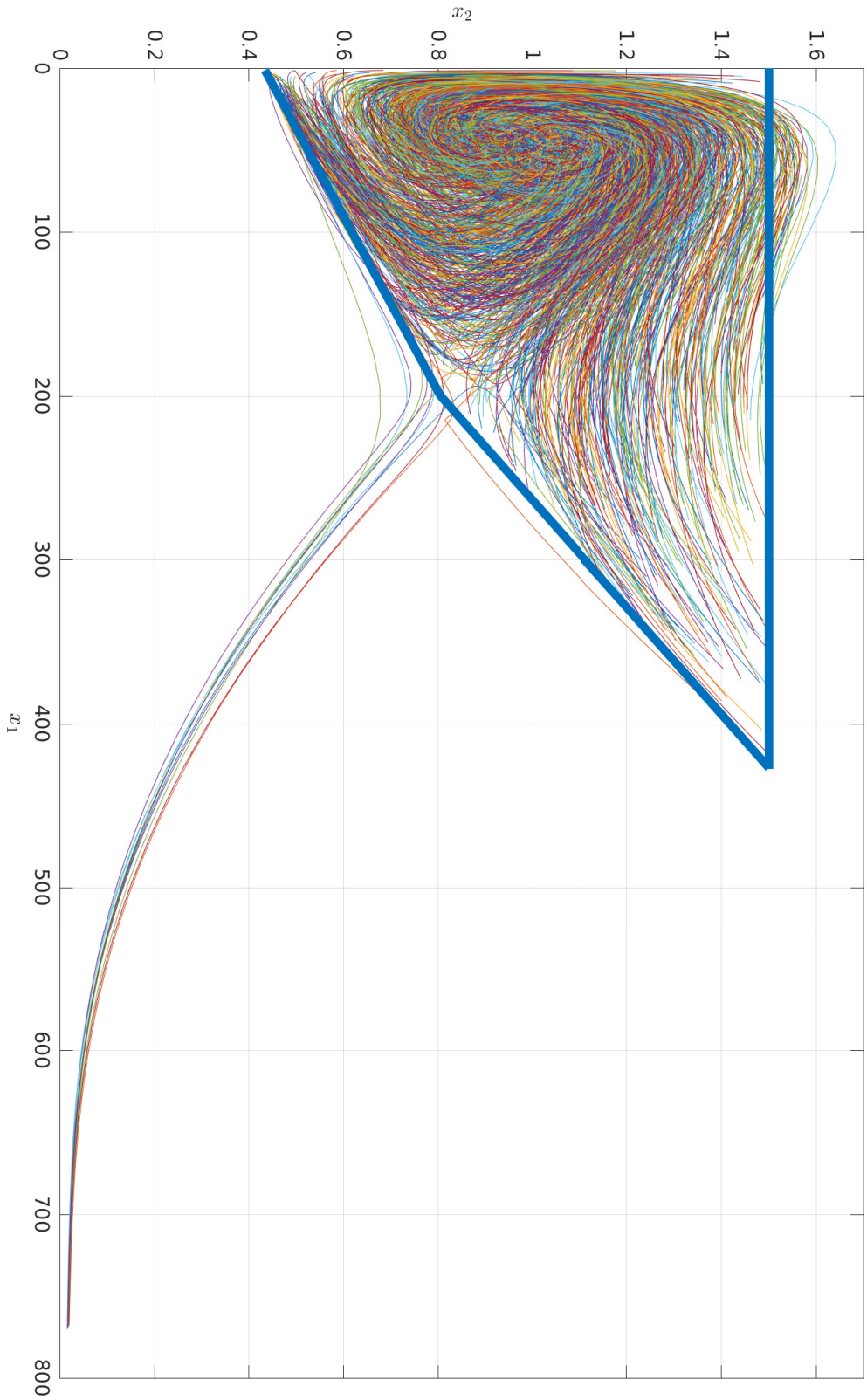

Figure 7.6: Monte-Carlo simulations to validate the certified target set Ω_0.

Therefore, 1 simulation requires around $621\mu s$ on an hp EliteBook 2.60GHz Intel Core i7.

Figure 7.7 shows the 3 certified cycles for $T = 5$ obtained using Algorithm 7.1, nominal and robust RoAs that have been estimated using the method presented in Chapter 6, where bang-bang control strategies were considered. We can see that, as the number of cycles increases, the certified RoA gets closer to the robust controlled one denoted Ω_R. Furthermore, it is interesting to notice that there is a small region of Ω_3, which is probabilistically certified but does not belong to the robust RoA, although the control structure in the robust case is less restrictive. This is potentially due to the fact that the probabilistic method is less conservative than the robust one.

7.4.4 Validation of the estimation of Ω_C

We approximated the probability of driving the states from Ω_3 to Ω_0 using 5000 Monte-Carlo simulations. We obtained that 99.6% of the trajectories of (7.1) having initial conditions in Ω_3 converge to Ω_0 using the probabilistic certified control strategies that we derived. Figure 7.8 shows the phase portrait of the 5000 Monte-Carlo trajectories. We can notice that only a small part of these trajectories violate the minimal constraint on immune cells density. The trajectories violating this constraints are presented in Figure 7.9.

7.5 Conclusion

In this chapter, we presented a framework of probabilistic certification for regions of attraction which is based on the randomized methods, allowing to overcome the conservatism of worst-case robust approaches by proposing a tractable problem with probabilistic constraints.

This framework has been used to derive a certified region of attraction for a cancer growth model. Furthermore, we provided a validation on the probability of driving the states to the certified safe target set with its corresponding control strategy.

The main advantages of this framework is that it is less conservative since it is more tolerant to constraints violations in the presence of uncertainties, in contrast to the robust design of RoAs. Furthermore, the methodology that we presented in this chapter provides the control strategy corresponding to each certified initial states set, which allowed us to validate the estimations using Monte-Carlo simulations.

The probabilistic certification of regions of attraction can be seen as a tool to tune the several parameters of the treatment protocols by properly choosing the model parameters and their distributions, the geometry of the regions of attraction to be certified and the control parametrization.

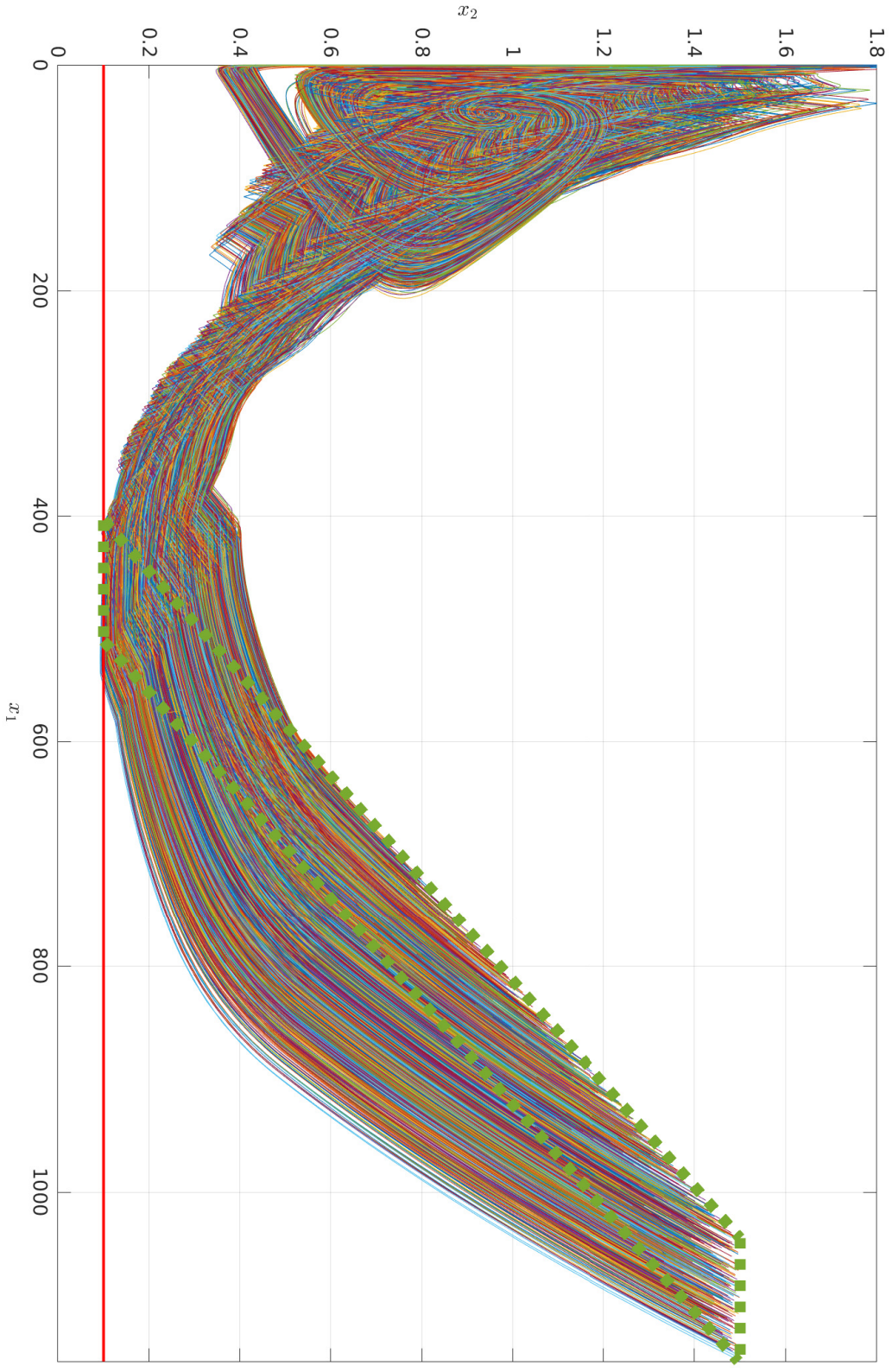

Figure 7.8: Monte-Carlo simulations to validate the certified sequence of controls with their respective sets, the green polytope in dashed line is the set Ω_3 where the initial states were selected.

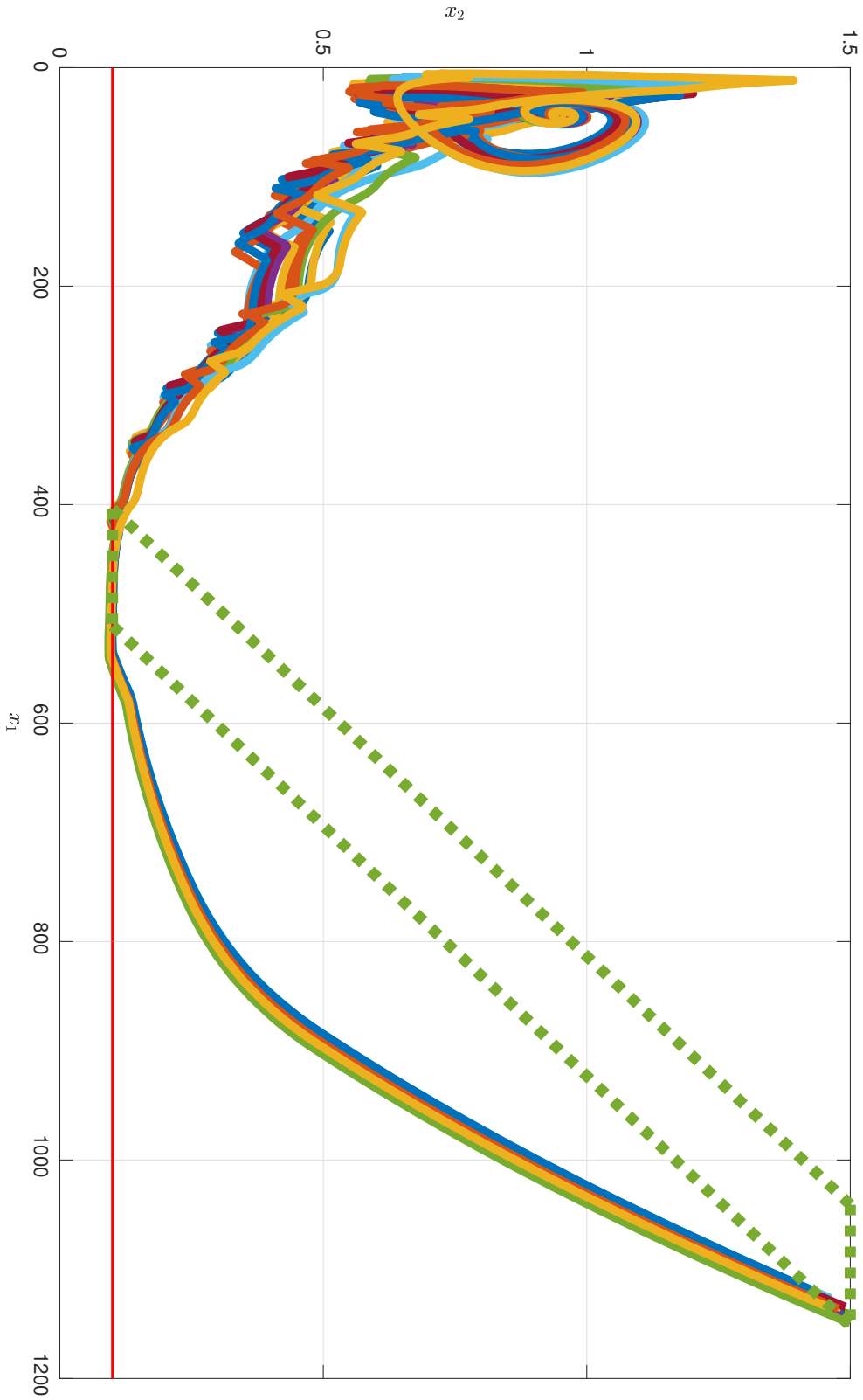

Figure 7.9: Monte-Carlo simulations, the trajectories that violate the minimal constraint on immune cells density, the green polytope in dashed line is the set Ω_3 where the initial states were selected.

Chapter 8

General conclusion

The main objective of this thesis was to propose frameworks and algorithms that are based on advanced control theory approaches, allowing to create systematic and generic numerical tools, in order to guide the design of cancer drugs scheduling.

Cancer dynamical systems are known to be highly uncertain by nature, and are often described by nonlinear complex dynamics that are not fully understood yet. These difficulties make the control of such systems a challenging task. Therefore, in this thesis, we focused in investigating control approaches allowing to take into consideration the uncertainties that can affect cancer dynamical systems. Furthermore, we aimed at pointing out the importance of considering stochastic parametric uncertainties in the drug schedules design.

In the context of cancer treatment scheduling, in addition to the complexities mentioned above, we have to take into consideration many constraints on the states as well as on the control inputs. An example is taking into account health constraints in order to prevent an eventual immune weakening of the human body, or drug toxicity constraints especially for chemotherapy, which is known to have many side effects. Moreover, we need to deal with optimality issues since we often want to reduce as fast as possible the tumor burden while avoiding an immune depletion.

One of the solutions proposed for this type of problems is optimal control design. Different approaches related to optimal control were designed in the literature, we reviewed some of them in Chapter 2. This category of approaches is interesting since it allows to deal with nonlinear systems, to consider hard constraints and to provide optimal guarantees. However, only few works dedicated to cancer treatment scheduling considered uncertainties on model parameters.

The first part of this thesis was dedicated to a literature review as well as to recall different theoretical concepts. In Chapter 2, we extensively explained the different dynamics related to the cancer growth phenomenon. We also presented the main therapies that are used for cancer treatment with a focus on immune dynamics and immunotherapy. Thereafter, we presented a brief review on the literature of cancer growth modeling

and introduced the problem of cancer therapies scheduling in terms of control design, as well as the main challenges that one has to face. We also proposed to use an optimal control approach allowing to take into consideration parametric uncertainties as well as uncertainties on the initial states, in the control design.

The approach that we proposed to use is based on the moment optimization framework, it consists in transforming a polynomial optimal control problem in the space of measures, and then rephrasing it in terms of moments. This method allows to consider a class of nonlinear systems that is widely used in many applications, which is polynomial dynamics. The appealing feature of this approach is that it is suitable for dealing with states and inputs as probability distributions, simply by managing the moments of the related probability distribution functions. This makes the explicit consideration of parametric uncertainties as well as initial state uncertainties straightforward in the optimal control problem formulation. In Chapter 3 we briefly recalled the main theoretical aspects of optimal control via moment optimization. We also explained in this chapter how to reformulate optimal control problems in terms of moments and gave some details about the reconstruction of input and state trajectories.

In the second part of this thesis, we used the moment optimization framework in order to schedule cancer treatment. We considered a widely used mathematical model, describing the interaction dynamics between a cancer, the immune systems as well as combined chemotherapy and immunotherapy. In Chapter 4, we first derived nominal optimal control profiles corresponding to drug schedules, where fixed model parameters were consider. Thereafter, we modeled the tumor growth rate and the natural influx of immune cells (which are model parameters) with probability distributions and designed robust optimal control profiles. Finally, we compared the efficiency of both profiles (nominal and robust) under parametric uncertainties, using Monte-Carlo simulations. The obtained results showed the importance of taking into account parametric uncertainties in the drug schedules design, since the nominal control profiles do not meet the control objectives under uncertainties.

In Chapter 5, we modified the well known Stepanova model used in Chapter 4 in oder to consider the detrimental effects that chemotherapy has on the immune system, by adding a term in the dynamical equation corresponding to the density of effector immune cells. Moreover, we added a new constraint, in the optimal control problem, in order to consider a minimal allowed density of immune cells in the optimal control problem. Furthermore, we considered the parameter standing for the detrimental effects of chemotherapy to be uncertain and described by a probability distribution. We designed nominal and robust control profiles and compared them, we noticed that the maximal concentration of chemotherapy has been considerably reduced, which highlights furthermore the importance of considering parametric uncertainties.

The moment optimization approach can be very promising for many applications, and it is worth applying it to other models describing cancer dynamics, in order to have an

idea on the appropriate drug injection schedules, when parametric uncertainties are considered. However, it is important to know that this approach has some limitations, which consist mainly in the restriction on polynomial dynamics and the limited dimension (state and control variables) that can be handled. Moreover, the required computational time might be relatively high in the case of solving a robust optimal control problem. However, in some applications, it remains crucial to guarantee robust performances.

On another hand, the estimation of domains of attraction for dynamical systems is a fundamental and important problem in control theory. This set provides all the possible initial states, for which there exists a control strategy, such that the state trajectories starting at these initial conditions can be driven to a stable equilibrium. Deriving an analytical expression for this type of sets is a challenging problem, especially for nonlinear dynamical systems. Therefore, there exist many works on numerical approaches, in the literature, to estimate the domain of attraction of dynamical systems. In Chapter 6, we provided a brief review on some widely applicable techniques to estimate the regions of attraction.

In the case of cancer dynamical systems, the domains of attraction represent the sets of initial health conditions (tumor volume and immune cells density for example), for which there exists a treatment strategy such that the patient is healed, without any health damage or immune depletion. Therefore, the characterization of this type of sets is very interesting for cancer dynamics. Furthermore, since this class of systems is known to be highly uncertain by nature, it is also important to estimate the RoA under uncertainties for such systems.

The third part of this thesis was dedicated to the estimation of domains of attraction for uncertain nonlinear systems describing cancer dynamics. In Chapter 6, we proposed a readily applicable approach to provide a characterization of the domain of attraction of the well know Stepanova's model for a given parameters vector. In this method that is in the same line as sliding mode control, we considered bang-bang control strategies. Moreover, we used this approach to derive an estimate of the robust domain of attraction, when the model parameters are considered to be uncertain.

Furthermore, in Chapter 6, we provided an extensive analysis on the effects of parametric uncertainties on the model equilibriums points, as well as on the region of attraction structure. We noticed that when considering parametric uncertainties, the size of the region of attraction is considerably reduced. Therefore the domain of attraction might be highly sensitive to parametric uncertainties, which is a crucial information in the context of cancer treatment, since such sets provide an information on the patients that can be healed, using appropriate treatments.

It is worth emphasizing that the methodology proposed in Chapter 6 does not provide a specific control strategy to apply, but, it rather gives an idea on the initial health conditions that can be healed or not. Furthermore, these results was used in Chapter 7 for

comparison purposes, in the latter chapter a methodology allowing to provide certified control strategies was presented.

The methodology that was proposed in Chapter 7 is based on the randomized algorithms and allows to estimate probabilistically certified regions of attraction. In this chapter, we used a modified Stepanova model, which was extended in order to consider the pharmacokinetics of chemotherapy explained in Chapter 2.

The framework of probabilistic certification of regions of attraction allows to certify in a probabilistic sense the existence of a control strategy that drives the states from an initial state to a certified target set. Unlike the robust classical design of regions of attraction that considers the worst-case scenario, the proposed framework avoids focusing on few unlikely very bad scenarios, allowing to overcome the conservatism of the robust RoA design by means of a probabilistic certification.

We used this approach in Chapter 7 in order to derive a certified region of attraction for a cancer growth model. Furthermore, this certified RoA was validated using Monte-Carlo simulations, by estimating the probability of driving the states to the certified safe target set, using the corresponding certified control strategies.

The results of Chapter 7 showed that the probabilistically certified region of attraction might be less conservative than the one based on the worst-case scenario, since there are some regions of the state space which belong to the probabilistically certified RoA and not to the robust one, even though the control inputs were more constrained in the probabilistic certification framework. An interesting perspective for the work of Chapter 7 would be to consider more flexible set structures, in order to provide a tighter approximation of the probabilistically certified RoAs.

Finally, the different frameworks presented in this thesis can be seen as tools allowing to tune the several parameters of cancer therapies protocols, in order to better achieve the treatment objectives. Furthermore, these tools help to build an awareness on the importance of considering parametric uncertainties in the control design.

Appendix A

Proof of Theorem 6.1

Let's consider the following polynomial:

$$a(x_2) = x_2^3 + \mu_C \left(\frac{\mu_I x_\infty \gamma_X - 2\mu_I \beta_Y x_\infty^2 \gamma_X}{\mu_I \beta_X x_\infty^2 \gamma_X^2} \right) x_2^2 + \mu_C^2 \left(\frac{\delta_Y + \mu_I \beta_Y x_\infty^2 - \mu_I x_\infty}{\mu_I \beta_Y x_\infty^2 \gamma_X^2} \right) x_2 - \frac{\mu_C^2 \alpha_Y}{\mu_I \beta_Y x_\infty^2 \gamma_X^2}. \tag{A.1}$$

Let a_2, a_1 and a_0 be the coefficients of the monic polynomial (A.1) such that:

$$\begin{cases} a_2 = \mu_C \left(\dfrac{\mu_I x_\infty \gamma_X - 2\mu_I \beta_Y x_\infty^2 \gamma_X}{\mu_I \beta_X x_\infty^2 \gamma_X^2} \right) \\ \\ a_1 = \mu_C^2 \left(\dfrac{\delta_Y + \mu_I \beta_Y x_\infty^2 - \mu_I x_\infty}{\mu_I \beta_Y x_\infty^2 \gamma_X^2} \right) \\ \\ a_0 = -\dfrac{\mu_C^2 \alpha_Y}{\mu_I \beta_Y x_\infty^2 \gamma_X^2} \end{cases}$$

Let $a_p = (a_2, a_1, a_0)^T$ be the coefficients vector corresponding to the polynomial $a(x_2)$. We can define the Hermite form corresponding to (A.1) as follows:

$$\mathcal{H}(a_p) = \begin{pmatrix} s_0 & s_1 & s_2 \\ s_1 & s_2 & s_3 \\ s_2 & s_3 & s_4 \end{pmatrix}$$

where s_0, s_1, s_2, s_3 and s_4 are defined as follows:

$$\begin{cases} s_0 = 3 \\ s_1 = -a_2 \\ s_2 = a_2^2 - 2a_1 \\ s_3 = -a_2^3 + 3a_1 a_2 - 3a_0 \\ s_4 = a_2^4 - 4a_1 a_2^2 + 2a_1^2 + 4a_0 a_2 \end{cases}$$

According to Theorem 1.1 in [75], the Hermit matrix $\mathcal{H}(a_p)$ is positive definite if and only if the roots of $a(x_2)$ are real and distinct.

List of Figures

List of Tables

Bibliography

[1] https://www.lungevity.org.

[2] Afenya, E. Acute leukemia and chemotherapy: A modeling viewpoint. *Mathematical Biosciences 138*, 2 (1996), 79–100.

[3] Alamir, M. Robust feedback design for combined therapy of cancer. *Optimal Control Applications and Methods 35*, 1 (2014), 77–88.

[4] Alamir, M. On probabilistic certification of combined cancer therapies using strongly uncertain models. *Journal of Theoretical Biology 384* (2015), 59–69.

[5] Alamo, T., Cepeda, A., Fiacchini, M., and Camacho, E. F. Convex invariant sets for discrete-time lur'e systems. *Automatica 45* (2009), 1066–1071.

[6] Alamo, T., Cepeda, A., and Limon, D. Improved computation of ellipsoidal invariant sets for saturated control systems. In *Proceedings of the 44th IEEE Conference on Decision and Control, and the European Control Conference* (Sevilla, Spain, December 2005).

[7] Alamo, T., Tempo, R., and Camacho, E. F. Randomized strategies for probabilistic solutions of uncertain feasibility and optimization problems. *IEEE Transactions on Automatic Control 54*, 11 (2009), 2545–2559.

[8] Alamo, T., Tempo, R., Luque, A., and Ramirez, D. R. Randomized methods for design of uncertain systems: Sample complexity and sequential algorithms. *Automatica 52* (2015), 160–172.

[9] Benzekry, S., Chapuisat, G., Ciccolini, J., Erlinger, A., and Hubert, F. A new mathematical model for optimizing the combination between antiangiogenic and cytotoxic drugs in oncology. *Comptes Rendus Mathematique* (2012).

[10] Blanchini, F. Ultimate boundedness control for discrete-time uncertain systems via set-induced Lyapunov functions. *IEEE Transactions on Automatic Control 39* (1994), 428–433.

[11] Blanchini, F. Set invariance in control. *Automatica 35*, 11 (1999), 1747 – 1767.

[12] Blanchini, F., and Miani, S. *Set-theoretic methods in control*. Springer, 2008.

[13] Bradford, E., and Imsland, L. Stochastic nonlinear model predictive control using gaussian processes. In *2018 European Control Conference (ECC)* (2018), pp. 1027–1034.

[14] Bratus, A., Samokhin, I., Yegorov, I., and Yurchenko, D. Maximization of viability time in a mathematical model of cancer therapy. *Mathematical Biosciences 294* (2017), 110–119.

[15] Bratus, A., Yegorov, I., and Yurchenko, D. Dynamic mathematical models of therapy processes against glioma and leukemia under stochastic uncertainties. *Meccanica dei Materiali e delle Strutture 6*, 1 (2016), 131–138.

[16] Cacace, F., Cusimano, V., Germani, A., Palumbo, P., and Papa, F. Closed-loop control of tumor growth by means of anti-angiogenic administration. *Mathematical Biosciences and Engineering 15*, 4 (2018), 827–839.

[17] Chareyron, S., and Alamir, M. Mixed immunotherapy and chemotherapy of tumors: Feedback design and model updating schemes. *Journal of Theoretical Biology 258*, 3 (2009), 444–454.

[18] Chesi, G. Estimating the domain of attraction for uncertain polynomial systems. *Automatica 40* (2004), 1981–1986.

[19] Claeys, M., S. R. Reconstructing trajectories from the moments of occupation measures. In 53^{rd} *IEEE Conference on Decision and Control* (Los Angeles, California, USA, December 2014), pp. 6677–6682.

[20] de Pillis, L. G., G. W. R. A. E. Mixed immunotherapy and chemotherapy of tumors: modeling, applications and biological Interpretations. *Journal of Theoretical Biology 238*, 4 (2006), 841–862.

[21] de Pillis, L., Gu, W., Fister, K., T., H., Maples, K., Neal, T., Murugan, A., and Yoshida, K. Chemotherapy for tumors: An analysis of the dynamics and a study of quadratic and linear optimal controls. *Mathematical Biosciences* (2006).

[22] de Pillis, L., and Radunskaya, A. A mathematical tumor model with immune resistance and drug therapy: an optimal control approach. *Journal of Theoretical Medicine 3*, 2 (2001), 79–100.

[23] de Pillis, L. G., Fister, K. R., Gu, W., Collins, C., Daub, M., Gross, D., Moore, J., and Preskill, B. Mathematical model creation for cancer chemo-immunotherapy. *Computational and Mathematical Methods in Medicine 10*, 3 (2009), 165–184.

[24] de Pillis, L. G., Fister, K. R., Gu, W., Head, T., Maples, K., Neal, T., Murugan, A., and Kozai, K. Optimal control of mixed immunotherapy and chemotherapy of tumors. *Journal of Biological Systems 16*, 1 (2008), 51–80.

[25] de Pillis, L. G., Gu, W., Fister, K. R., Head, T., Maples, K., Murugan, A., Neal, T., and Yoshida, K. Chemotherapy for tumors: An analysis of the dynamics and a study of quadratic and linear optimal controls. *Mathematical Biosciences 209*, 1 (2007), 292–315.

[26] de Pillis, L. G., and Radunskaya, A. A mathematical model of immune response to tumor invasion. In *Proceedings Second MIT Conference on Compurational Fluid and Solid Mechanics* (2003), pp. 1661–1668.

[27] de Pillis, L. G., and Radunskaya, A. The dynamics of an optimally controlled tumor model: A case study. *Mathematical and Computer Modelling 37*, 11 (2003), 1221–1244.

[28] Doban, A. I., and Lazar, M. Domain of attraction computation for tumor dynamics. In *53rd IEEE Conference on Decision and Control* (2014), pp. 6987–6992.

[29] d'Onofrio, A. Rapidly acting antitumoral antiangiogenic therapies. *Physical Review E - Statistical, Nonlinear, and Soft Matter Physics 76* (2007).

[30] d'Onofrio, A., and Cerrai, P. A bi-parametric model for the tumour angiogenesis and antiangiogenesis therapy. *Mathematical and Computer Modelling 49*, 5–6 (2009), 1156–1163.

[31] d'Onofrio, A., and Gandolfi, A. Tumour eradication by antiangiogenic therapy: Analysis and extensions of the model by Hahnfeldt et al. (1999). *Mathematical Biosciences 191*, 2 (2004), 159–184.

[32] d'Onofrio, A., Ledzewicz, U., and Schättler, H. *On the Dynamics of Tumor-Immune System Interactions and Combined Chemo- and Immunotherapy.* Springer Milan, 2012, pp. 249–266.

[33] Eftimie, R., Gillard, J. J., and Cantrell, D. A. Mathematical models for immunology: current state of the art and future research directions. *Bulletin of Mathematical Biology 78*, 10 (2016), 2091–2134.

[34] Ergun, A., Camphausen, K., and Wein, L. M. Optimal scheduling of radiotherapy and angiogenic inhibitors. *Bulletin of Mathematical Biology 65* (2003), 407–424.

[35] Farjami, S., Kirk, V., and Osinga, H. M. Computing the stable manifold of a saddle slow manifold. *SIAM Journal on Applied Dynamical Systems 17*, 1 (2018), 350–379.

[36] Feizabadi, M. Modeling multi-mutation and drug resistance: analysis of some case studies. *Theoretical Biology and Medical Modelling 14*, 6 (2017).

[37] Fiacchini, M. *Convex difference inclusions for systems analysis and design.* PhD thesis, Universidad de Sevilla, Spain, 2012.

[38] Fiacchini, M., Alamo, T., and Camacho, E. F. On the computation of convex robust control invariant sets for nonlinear systems. *Automatica 46*, 8 (2010), 1334–1338.

[39] Fiacchini, M., Alamo, T., and Camacho, E. F. Invariant sets computation for convex difference inclusions systems. *Systems & Control Letters 61*, 8 (2012), 819–826.

[40] Fiacchini, M., Tarbouriech, S., and Prieur, C. Polytopic control invariant sets for differential inclusion systems : a viability theory approach. In *Proceedings of the 2011 American Control Conference ACC* (2011), pp. 1218–1223.

[41] Francomano, E., Hilker, F. M., Paliaga, M., and Venturinoc, E. An efficient method to reconstruct invariant manifolds of saddle points. *Dolomities Research Notes on Apptoximation, Padova University Press 10* (2017), 25–30.

[42] Hahnfeldt, P., Panigrahy, D., Folkman, J., and Hlatky, L. Tumor Development under Angiogenic Signaling: A Dynamical Theory of Tumor Growth, Treatment Response, and Postvascular Dormancy 1. *Cancer Research 59* (1999), 4770–4775.

[43] Henrion, D. Optimization on linear matrix inequalities for polynomial systems control, 2014.

[44] Henrion, D., and Korda, M. Convex computation of the region of attraction of polynomial control systems. *IEEE Transactions on Automatic Control 59*, 2 (2014), 297–312.

[45] Henrion, D., Lasserre, J. B., and Löfberg, J. Gloptipoly 3: Moments, optimization and semidefinite programming. *Optim. Methods and Software*, 24(4-5 (2009), 761–779.

[46] Henrion, D., Lasserre, J. B., and Savorgnan, C. Nonlinear optimal control synthesis via occupation measures. In *Proceedings of the 47th IEEE Conference on Decision and Control* (Cancun, Mexico, December 2008), pp. 4749–4754.

[47] Henrion, D., and Pauwels, E. Linear conic optimization for nonlinear optimal control. *arXiv:1407.1650* (2018).

[48] Kassara, K., and Moustafid, A. Angiogenesis inhibition and tumor-immune interactions with chemotherapy by a control set-valued method. *Mathematical Biosciences 231*, 2 (2011), 135–143.

[49] Korda, M., Henrion, D., and Jones, C. N. Inner approximations of the region of attraction for polynomial dynamical systems. *IFAC Proceedings Volumes (IFAC-PapersOnline) 9*, 1 (2013), 534–539.

[50] Kovacs, L., Szeles, A., Sapi, J., Drexler, D. A., Rudas, I., Harmati, I., and Sapi, Z. Model-based angiogenic inhibition of tumor growth using modern robust control method. *Computer Methods and Programs in Biomedicine 114*, 3 (2014), e98–e110.

[51] Lasserre, J. B. Optimisation globale et théorie des moments. *Comptes rendus de l'Académie des Sciences Paris* (2000).

[52] Lasserre, J. B. Global optimization with polynomials and the problem of moments. *SIAM Journal on Optimization 11(3)*, 3 (2001), 796–817.

[53] Lasserre, J. B. Moments, positive polynomials and their applications. *Imperial College Press, London, UK* (2010).

[54] Lasserre, J. B., Henrion, D., Prieur, C., and Trélat, E. Nonlinear optimal control via occupation measures and LMI relaxations. *SIAM Journal on Control and Optimization 47*, 4 (2008), 1643–1666.

[55] Ledzewicz, U., and Faraji, M. On optimal protocols for combinations of chemo- and immunotherapy. In *51st IEEE Conference on Decision and Control* (Hawaii, USA, December 2015), pp. 7492–7497.

[56] Ledzewicz, U., and Schättler, H. Anti-angiogenic therapy in cancer treatment as an optimal control problem. *SIUE Summer Research Fellowship 46*, 3 (2006), 1052–1079.

[57] Ledzewicz, U., and Schättler, H. Optimal controls for a model with pharmacokinetics maximizing bone marrow in cancer chemotherapy. *Mathematical Biosciences 206*, 2 (2007), 320–342.

[58] Ledzewicz, U., and Schättler, H. Optimal and suboptimal protocols for a class of mathematical models of tumor anti-angiogenesis. *Journal of Theoretical Biology 252*, 2 (2008), 295–312.

[59] Ledzewicz Urszula, Naghnaeian Mohammad, S. H. Bifurcation of singular arcs in an optimal control problem for cancer immune system interactions under treatment. In *49th IEEE Conference on Decision and Control* (Atlanta, GA, USA, December 2010), pp. 7039–7044.

[60] Lesart, A. C. Modélisation théorique du développement tumoral sous fenêtre dorsale: Vers un outil clinique d'individualisation et d'optimisation de la thérapie. *Thèse, Université de Grenoble* (2013).

[61] Lobato, F. S., Machado, V. S., and Steffen, V. Determination of an optimal control strategy for drug administration in tumor treatment using multi-objective optimization differential evolution. *Computer Methods and Programs in Biomedicine 131* (2016), 51–61.

[62] Löfberg, J. Yalmip : A toolbox for modeling and optimization in matlab. In *Proceedings of the CACSD Conference* (Taipei, Taiwan, 2004).

[63] Louzoun, Y. The evolution of mathematical immunology. *Immunological Reviews 216*, 1 (2007), 9–20.

[64] Martin, R. Optimal control drug scheduling of cancer chemotherapy. *Automatica 28*, 6 (1992), 1113–1123.

[65] Marx, S., Pauwels, E., Weisser, T., Henrion, D., and Lasserre, J. Tractable semi-algebraic approximation using Christoffel-Darboux kernel. *http://homepages.laas.fr/henrion/papers/momgraph.pdf* (2019).

[66] Matveev, A. S., and Savkin, A. V. Application of optimal control theory to analysis of cancer chemotherapy regimens. *Systems & Control Letters 46*, 5 (2002), 311–321.

[67] Matveev, A. S., and Savkin, A. V. Influence of tumours on normal cells and optimal chemotherapy regimens: The case of several drugs and toxicity constraints. *Mathematical Medicine and Biology 22*, 2 (2005), 143–162.

[68] Mayne, D. Q. Competing methods for robust and stochastic MPC. In *6th IFAC Conference on Nonlinear Model Predictive Control* (Madison, WI, USA, August 2018), vol. 51, pp. 169–174.

[69] Merola, A., Cosentino, C., and Amato, F. An insight into tumor dormancy equilibrium via the analysis of its domain of attraction. *Biomedical Signal Processing and Control 3*, 3 (2008), 212 – 219.

[70] Mier, J., Aronson, F., Numerof, R., Vachino, G., and Atkins, M. Toxicity of immunotherapy with interleukin-2 and lymphokine-activated killer cells. *Pathology and Immunopathology Research* (1988).

[71] MOSEK ApS. *The MOSEK optimization toolbox for MATLAB manual. Version 9.0.*, 2019.

[72] Murray, J. M. Optimal control cancer growth. *Mathematical Biosciences 98* (1990), 273–287.

[73] Nath, N., Burg, T., Dawson, D. M., and Iyasere, E. Optimizing antiangiogenic therapy for tumor minimization. In *Proceedings of the 2010 American Control Conference* (2010), pp. 1242–1247.

[74] Navin, N. E. Tumor Evolution in Response to Chemotherapy: Phenotype versus Genotype. *Cell Reports 6*, 3 (2014), 417–419.

[75] Netzer, T., Plaumann, D., and Thom, A. Determinantal representations and the hermite matrix. *Michigan Math. J. 62* (2013), 407–420.

[76] Putinar, M. Positive polynomials on compact semi-algebraic sets. *Indiana University Mathematics Journal 42*, 3 (1993), 969–984.

[77] Riah, R. *Théorie des ensembles pour le contrôle robuste des systèmes non linéaires: Application à la chimiothérapie et les thérapies anti-angiogéniques.* PhD thesis, Communauté Université Grenoble Alpes, 2016.

[78] Riah, R., Fiacchini, M., and Alamir, M. Iterative method for estimating the robust domains of attraction of non-linear systems: Application to cancer chemotherapy model with parametric uncertainties. *European Journal of Control 47* (2019), 64–73.

[79] Rozova, V. S., and Bratus, A. S. Therapy strategy in tumour cells and immune system interaction mathematical model. *Applicable Analysis 95*, 7 (2016), 1548–1559.

[80] Savorgnan, C., Lasserre, J. B., and Diehl, M. Discrete-time stochastic optimal control via occupation measures and moment relaxations. In *Proceedings of the IEEE Conference on Decision and Control* (2009).

[81] Schättler, H., Ledzewicz, U., and Cardwell, B. Robustness of optimal controls for a class of mathematical models for tumor anti-angiogenesis. *Mathematical Biosciences & Engineering 8*, 2 (2011), 355–369.

[82] Sharifi, N., Ozgoli, S., and Ramezani, A. Multiple model predictive control for optimal drug administration of mixed immunotherapy and chemotherapy of tumours. *Computer Methods and Programs in Biomedicine 144* (2017), 13–19.

[83] Sharifi, N., Zhou, Y., and Holmes, G., C. Y. Overcoming channel uncertainties in touchable molecular communication for direct drug targeting assisted immunochemotherapy. *IEEE Transactions on NanoBioscience 19*, 2 (2020), 249–258.

[84] Stepanova, N. Course of the immune reaction during the development of a malignant tumour. *Biophysics* (1980).

[85] Streif, S., Henrion, D., and Findeisen, R. Probabilistic and set-based model invalidation and estimation using LMIs. In *Proceedings of the 19th World Congress, IFAC* (Cape Town, South Africa, August 2014), vol. 47, pp. 4110–4115.

[86] Sturm, J. F. Using sedumi 1.02, a Matlab toolbox for optimization over symmetric cones. *Optimimization Methods and Software 11*, 1–4 (1999), 625–653.

[87] Tempo, R., Calafiore, G., and Dabbene, F. *Randomized algorithms for analysis and control of uncertain systems, with applications (2nd ed.)*. London: Springer-Verlag, 2013.

[88] Topcu, U., Packard, A. K., Seiler, P., and Balas, G. J. Robust Region-of-Attraction Estimation. *IEEE Transaction on Automatic Control 55*, 1 (2010).

[89] Weiss, A., Ding, X., van Beijnum, J. R., Wong, I., Wong, T. J., Berndsen, R. H., Dormond, O., Dallinga, M., Shen, L., Schlingemann, R. O., Pili, R., Ho, C. M., Dyson, P. J., van den Bergh, H., Griffioen, A. W., and Nowak-Sliwinska, P. Rapid optimization of drug combinations for the optimal angiostatic treatment of cancer. *Angiogenesis 18*, 3 (2015), 233–244.

[90] Wodarz, D., and Komarova, N. *Computational Biology of Cancer: Lecture Notes and Mathematical Modeling*. World Scientific, 2005.

[91] Zarei, M., Javadi, K., and Kalhor, A. Perturbed tumor immunotherapy domain of attraction estimation via the arc-length function. In *2018 25th National and 3rd International Iranian Conference on Biomedical Engineering (ICBME)* (2018), pp. 1–6.

[92] Zhou, B., Duan, G., and Lin, Z. Approximation and monotonicity of the maximal invariant ellipsoid for discrete-time systems by bounded controls. *IEEE Transactions on Automatic Control 55*, 2 (2010).